Study of Radio Frequency Inductively Coupled Thermal Plasma Torch (RF ICPT) for Radioactive Waste Treatment: Thermoplastics - Polyethylene and Polyvinyl Chloride (PVC)

By

Isaac Hassen

A thesis submitted to the
School of Graduate and Postdoctoral Studies in partial
fulfillment of the requirements for the degree of

Master of Applied Science in Nuclear Engineering

Faculty of Energy and Nuclear Science

University of Ontario Institute of Technology (Ontario Tech University)

Oshawa, Ontario, Canada

June 2021

THESIS EXAMINATION INFORMATION

Submitted by: **Isaac Hassen**

Master of Applied Science in Nuclear Engineering

Thesis title: Study of Inductively Coupled Thermal Plasma Torch (ICPT) for Radioactive Waste Treatment: Thermoplastics - Polyethylene and Polyvinyl Chloride (PVC)

An oral defense of this thesis took place on June, 2021 in front of the following examining committee:

Examining Committee:

Chair of Examining Committee	NAME Dr. Jennifer McKellar
Research Supervisor	NAME Dr. Hossam Gaber
Examining Committee Member	NAME Dr. Filippo Genco
Thesis Examiner	NAME, Dr. Franco Gaspari, Faculty of Science

The above committee determined that the thesis is acceptable in form and content and that a satisfactory knowledge of the field covered by the thesis was demonstrated by the candidate during an oral examination. A signed copy of the Certificate of Approval is available from the School of Graduate and Postdoctoral Studies.

ABSTRACT

Despite advancements in technology and many progresses made in effort for radioactive waste (RW) treatment and overall management, there is still no final and ever lasting solution. Among the many RW materials originating from nuclear power plants (NPPs), thermoplastics such as polyvinyl chloride (PVC) and polyethylene (PE) contribute significant amount to the overall volume of RW. The presence of radioactive nuclides in PVC and PE waste originating from NPPs and their plastic nature (non-bio-degradable characteristics) present two challenges at once. To solve the challenges presented by such plastic RW, a thermal plasma waste treatment approach was considered. A radiofrequency (RF) inductively coupled plasma torch (ICPT) was designed in SOLIDWORKS and simulated using COMSOL Multiphysics software, and its thermal behavior was studied. Its applicability including advantages and shortcomings for such use was studied.

Keywords: Inductively coupled plasma torch (ICPT); Radioactive waste (RW); COMSOL Multiphysics Simulation; ICPT design; Polyvinyl chloride (PVC) and Polyethylene (PE).

AUTHOR'S DECLARATION

I hereby declare that this thesis consists of original work of which I have authored. This is a true copy of the thesis, including any required final revisions, as accepted by my examiners.

I authorize the University of Ontario Institute of Technology (Ontario Tech University) to lend this thesis to other institutions or individuals for the purpose of scholarly research. I further authorize University of Ontario Institute of Technology (Ontario Tech University) to reproduce this thesis by photocopying or by other means, in total or in part, at the request of other institutions or individuals for the purpose of scholarly research. I understand that my thesis will be made electronically available to the public.

The research work in this thesis that was performed in compliance with the regulations of Research Ethics Board/Animal Care Committee under **REB Certificate number/Animal care certificate file number**.

Isaac Hassen

YOUR NAME

STATEMENT OF CONTRIBUTIONS

The detailed mechanical design described in chapter 4 was performed at Advanced Plasma Engineering Lab (APEL) at UOIT (Ontario Tech University) operated by Dr. Hossam Gaber. I was responsible for designing an RF plasma torch, compute mathematical modelling and physical simulation of the torch

Innovation summary:

- Development of an atmospheric pressure RF induced thermal plasma system for plastic radioactive waste and solid waste treatment.
- RF-ICPT detailed engineering design and simulation.

ACKNOWLEDGEMENTS

First, I want to express my immense gratitude and appreciation to my excellent supervisor Professor Dr. Hossam Gaber. Professor Gaber, in addition to providing excellent supervision and guidance, has believed in me and has given me all the necessary help and support I needed to complete this thesis work. I want to thank also all the lab members who make the lab an enjoyable place to be.

A special thanks goes to Dr. Vahid Damideh as well. Dr. Damideh taught me how to conduct a thorough scientific research, how to make advanced assembly in SolidWorks, how to measure the frequency of RF power supply and many more. Since they are many, for the sake of space, I will not mention all the lessons I learnt from him. I want to thank him for challenging me to improve my simulations, my schematics and designs. I will forever be grateful for teaching all these things, I will honor you by generously teaching whatever I learned to the next person and help the society.

Among the many friends and family who help and support me the most I want to mention the most important ones. I will begin by thanking the most beautiful and smartest girl I know - Mirt Mehany. I owe you a great gratitude: for all your understanding and support, for not giving up on me in difficult times, for understanding and accepting my choices and decisions even when you disagreed with them. I am blessed for having you; I want to be there for you in your life journey as you were there for me A special thanks goes to my mom and my uncle Tinkish. Although they have no idea what I am doing, they were cheering when they saw me happy, and suffering when they saw me sad. I could never have done it without your encouragements and support.

Finally, I want to thank all my family and friends for all their support.

Contents

LIST OF TABLES

LIST OF FIGURES

CHAPTER 1

CHAPTER 2

CHAPTER 3

CHAPTER 4

CHAPTER 5

CHAPTER 6

CHAPTER 7

LIST OF ABBREVIATIONS AND SYMBOLS

AC	Alternative current
CAD	Computer assisted design
DC	Direct current
EMC	Electromagnetic compatibility
EW	Exempt waste
HLW	High level waste
I.D.	Inner diameter
IAEA	International Atomic Energy Agency
ICPT	Inductively coupled plasma torch
ILW	Intermediate level waste
LLW	Low level waste
LTE	Local thermodynamic equilibrium
NPP	Nuclear power plant
O.D.	Outer diameter
PE	Polyethylene
PPE	Personal protective equipment
PTFE	Polytetrafluoroethylene
PVC	Polyvinyl chloride
RF	Radio frequency
RW	Radioactive waste

Chapter 1: Introduction

1.1 Background

Currently, Ontario, Quebec and Saskatchewan in Canada and other 30 countries around the world operate nuclear power plants. Many more other new plants are being build or are in plans. There are around 440 power reactors in the world and they provide about 10% of the world's energy demand [1] [2]. Competitive electricity production price, higher energy density per fuel volume and low amount of greenhouse gas emission are among the advantages of nuclear energy. However, nuclear industries, like any other, produces waste. Significant portion of waste produced from nuclear power plants is radioactive waste (RW) [3].

Nuclear power plant's daily operations and their decommissioning generate RW. This type of waste, because of its long lasting effects, requires special handling and management above and beyond other hazardous waste [4]. Thus, its treatment needs rigorous attention and focus to prevent the public and the environment to be exposed to radiation hazards. Although there is no one common strategy for management of radioactive waste, each nuclear energy producing countries have developed their own national strategies. Radioactive waste is commonly categorized according to form, physical state (solid/liquid), activity (specific activity), source and radionuclides half-life. In broader terms, RW are classified in high level waste (HLW) which accounts to only 1 % of overall radioactive waste by volume. The remaining 99 % do not produce significant

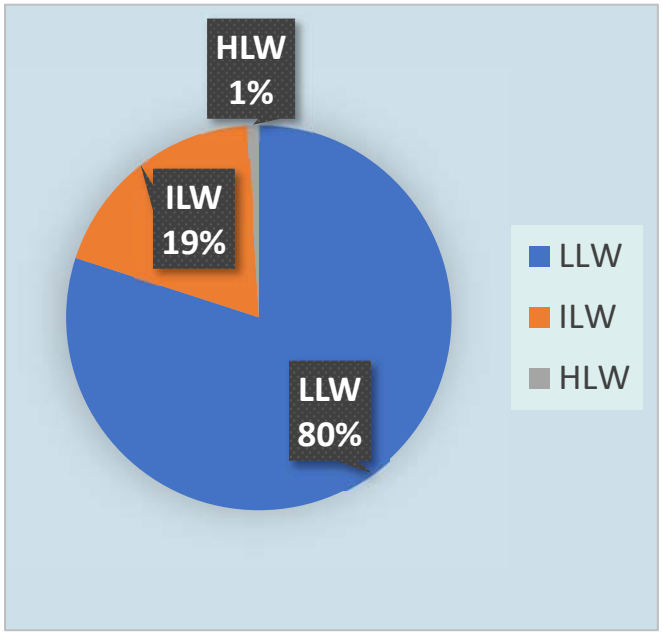

Figure 1.1 Radioactive Waste Volume

decay heat, they are classified as intermediate level waste (ILW) which accounts for 19 % in volume; example of it includes resins, spent ion exchange resins used for radioactive stream filtration. Lastly, low-level waste (LLW) which accounts for 80 % of the volume; LLW includes many of the mixed waste like: PPE equipment such as gloves and protective shoes and clothing, plastics, cleaning rags, mops et cetera [5].

1.1.1 Thermoplastics in NPPs

Due to ease of handling, costs and material properties, thermoplastics are widely used in nuclear power plants. In NPPs, materials for piping systems, electrical conduit and storage tanks are made of thermoplastics, especially polyethylene (PE) and polyvinyl chloride (PVC). PE and PVC compared to their metal counter parts, have lower installation costs. In addition to that, they are lighter in weight, easier to bend and install, and are less impacted by corrosion. PE and PVC can be processed into products that have long-life time and can be used for variety of applications such as pipes, window frames, cable insulation, floors coverings, roofing sheets, et cetera [6].

The usage of PE and PVC in NPPs are increasing, at the same time their usage and production for other applications that are indirectly linked to nuclear power production is also increasing every year. Consequently, the volume of thermoplastics in the waste stream has also increased. Although PE and PVC have relatively long life prior to being considered as waste, sooner or later they will be part of LLW. With aging and decommissioning of NPPs, such thermoplastics are also reaching the end of their utility and are being discarded as waste. In fact, recently, the fast growth of such thermoplastic waste has raised some concerns and has gained attention in the public discussion. For these reasons, many researches are being devoted to finding environmentally and economically acceptable lasting solutions for treatment and disposal of such waste [7].

One method to reduce the volume of waste from such thermoplastics is thermal treatment. PE and PVC have onset decomposition temperature of 500 $°C$ and 300 $°C$ respectively [8] . The

equilibrium melting temperature of polyethylene and PVC ranges from 160 – 245 $°C$ and at temperatures 350 – 500 $°C$ up to 70 % of their composition gasifies [9], [10].

1.2 Motivation

The issue of RW treatment and disposal has taken an ever-growing importance in countries with nuclear power plants. The lack of a permanent solution for final disposal of RW and their continuous increase in volume of these waste, coupled with the ever-decreasing availability of temporary storage space is proving to be very concerning. The concerns caused by RW cannot be mitigated by traditional technologies. Improvement of the existing technologies or invention of new ones must be part of the solutions. Current and traditional methods of RW treatment and disposal can be improved and made efficient. Improved and efficient RW treatment can contribute to addressing some of the general public's concerns on nuclear industry, as RW management is one of the concerns that the industry faces from the public opinion.

As such, the main motivation that inspired this research is the desire to contribute to finding solution for RW treatment.

1.3 Challenges

The main targets of RW treatment process involves in the volume reduction and homogenization of the waste. The method, among many others, widely used to achieve these targets in solid RW is a thermal process called incineration. However, incineration through oxidation (combustion) has undesirable by-products; this process releases CO_2, H_2O, SO_2, NO, and HCl gases. Emission of these gases has an emission cost, in addition to impacting the environment negatively.

In order to avoid the release of such gases, a plasma thermal source can be used. There are several plasma-based waste treatment facilities that utilize plasma for waste processing applications such

as: pyrolysis and gasification of municipal solid waste and vitrification of ash waste. However, there is no reported use of ICPTs for waste treatment in industrial scale [11].

Waste treatment facility that utilizes thermal plasma for waste treatment application use a type of plasma known as DC thermal plasma. For waste treatment application, DC plasmas are widely utilized compared to other types of plasma due to their higher efficiency and lower capital cost of the technology. However, because of routine electrode maintenance, inactivity period and cost can be considerable. Other limitations of a DC thermal plasma torch include higher consumption of plasma working gases and limitation to the type of gases to be used; reactive gases are not applicable to such plasmas [12]. Otherwise, these gases can contaminate, corrode or activate the electrodes. In case of ICPTs, however, there are no electrode, thus, any type of gas can be used. ICPT can be used in wide range of operation condition including reducing, oxidizing or inert conditions. One important advantage of ICPT is the fact that materials to be treated can be injected and can be made to pass through the core of the plasma (the hottest region). For the reasons mentioned, ICPTs can complement other technologies or be an alternative technology for RW treatment.

1.4 Problem Definition

At the core of inductively coupled plasma system is ICPT. Since 1961, when Thomas Reed published an article “Induction-coupled plasma torch”, the basic model and working principle of ICPT did not undergo a huge transformation. However, there exist various ICPT designs ranging from 2 – 8 turn coils, with up-to 3 gas flow system. In order to apply an ICPT in RW treatment application, ICPT that fits in to a reactor chamber must be designed. However, design of an ICPT have some challenges.

The main challenges of designing tangential (vertical, plasma jet same direction as gravitational acceleration) ICPT that is imbedded in a reactor chamber consists of mainly:

- Plasma discharge ignition.

This is because inductively coupled RF discharges at atmospheric pressure are effective in sustaining plasma, however due to their low value of electric field, they cannot achieve ignition on their own.

- Gas flow system
- RF power matching efficiency

1.5 Research Objectives

The main objective of this thesis is to design an enhanced RF inductively coupled atmospheric thermal plasma torch (ICPT) for RW treatment application with emphasis on the volume reduction. In order to achieve the project's objective, list of tasks to be performed are as follows:

1. Design of a novel RF atmospheric pressure ICPT with key features.

Inductively coupled plasma torches use the magnetic field induced by a current flowing through a helical coil with N turns. However, this magnetic field is not strong enough to achieve ignition, hence introducing an electrode or achieving gas breakdown from high voltage source is necessary. From the first ICPT design to the latest, one of the biggest challenges of ICPTs have been to RF matching. In this thesis, an optimized RF matching (energy/power coupling from power supply to the coil) will be one of the key features of the design. In addition to that, a RF/EMC shielding base that provides mechanical support to the torch will be featured.

2. Evaluation of the designed ICPT through Multiphysics modelling and simulation

Any new design needs to be tested and optimized to further improve the output. For this reason, a simulation of the designed torch needs to be conducted and validated with an experimental run. The data from the simulation and experiment need to be analyzed, specifically the effect of the graphite on the temperature of the plasma will be studied.

3. Modification of reactor chamber, ICPT integration in the chamber and simulation of fluid heat transfer in the chamber.

1.6 Thesis Structure

The thesis is structured in 6 chapters as follows. In the first chapter, introduction, a simple background (1.1) on RW and its origin is found. Following the background, the reason for doing this thesis is explained in the motivation (1.2). Consequent to the motivation, challenges (1.3) faced by some of current RW treatment methods and RW volume increment has been discussed. The questions that this thesis tried to answer are found in the problem statement (1.4) section. Tasks that need to be computed in order to answer the questions from the problem statements section are found in the objectives (1.5) section.

In the second chapter, literature reviews of important topics for the thesis are explained. It starts with an introductory review on radioactivity and types of radioactive decays (2.1), followed by in depth description of RW and its broad classifications (2.2). RW thermal treatment technologies and their applicability is briefly reviewed in (2.3). In (2.3.1) Plasma torch application in RW treatment in with specific examples is explained. The main types of plasma torches and their characteristics is briefly reviewed followed by an in-depth review of ICPT designs in (2.4-2.5).

Methodologies to carry out the project is found in chapter 3. It includes the necessary tasks to be performed in order to achieve the objectives outlined in chapter 1, in addition to providing the logical flow of the tasks.

Conceptual design and detailed 3D engineering design of ICPT with all the necessary parts, materials and dimensions are described in chapter 4.

In chapter 5 mathematical modelling and physical simulation of the ICPT design is computed and the results are explained in this chapter

A preliminary experiment of ICPT is conducted and result are shown in chapter 6. The material used, the experimental setup and procedures are described in depth.

In chapter 7 Conclusions are made based on the simulation results. Recommendation on the designed torch is suggested, description of future works, testing the designed torch in future experiments with experimental setup.

Chapter 2: Literature Review

2.1 Radioactivity

Many elements, in nature, exist in different forms of isotopes. Isotopes are chemically identical elements that differ in the number of neutrons in the nuclei. On Earth, most isotopes are stable. However, some elements such as uranium (^{238} U) have radioisotopes that are unstable; they spontaneously decay till they become stable. This spontaneous decay is referred as radioactivity [13]. These unstable isotopes, while decaying, release energy in form of electromagnetic waves or sub-atomic particles. The energy released during radio decay is known as radiation. The natural spontaneous decay of unstable radio-isotopes to stable radio-isotopes occur commonly in three processes: alpha (α), beta (β) and gamma (γ) decays [14].

- α decay: This process, usually, occurs only in heavy particles and these heavy particles release an alpha particle (2 protons and 2 neutrons) and decays to element with 4 less nuclides. Alpha particles are highly ionizing; however, they cannot penetrate human skin, a sheet of paper or even a few centimeters of air.
- β decay: This process is a result of a neutron decaying to a proton and fast-moving (high kinetic energy) electron; many radioisotopes decay in this form. Beta particles can penetrate more than alpha particle; they can penetrate the skin. A thin plastic or wood can shield beta particles.
- γ decay: An element with an excited electron releases a gamma ray when the electron de-excites. Gammas are rays, i.e., electromagnetic waves with wavelength like that of x-rays. They can penetrate very deep into most objects, therefore heavy materials like steel, concrete or lead with a substantial thickness is needed to shield against them.

One other important form decay in nuclear power plants is neutron decay/emission. In this process neutrons are emitted from fission reactions in the core of nuclear reactors. They are very penetrating and difficult to stop. To slow them down moderators made of graphite or polyethylene are used; they can also be slow down by water or wood [15].

2.2 Radioactive Waste

Many industries, research institutes,, hospitals and university labs use radiation and radioactive materials for various application such as: nuclear power generation, nuclear medicine, agriculture, and many more [16]. The refuse from these applications can be RW. According to IAEA, RW is defined as:

> "material that contains, or is contaminated with, radionuclides at concentrations or activities greater than clearance levels as established by regulatory body, and for which no use is foreseen" [17].

RW needs particular attention in its handling and management to protect public health and the environment; usually RW is managed in three broad stages: A Treatment (includes segregation, volume reduction and conditioning), B Storage and C Final Disposal [18]. Treatment of RW with an emphasis on volume reduction is the focus of this thesis.

Concentration and half-life of radionuclides vary widely depending on the origin of RW. In addition, RW having same origin can have different physical form (solid liquid and gaseous form) [19] . In order to better treat and manage RW, it is important to differentiate and segregate them based on some common characteristics. Numerous classification schemes are developed to categorize RW. Generally, RW are classified based on their physical state, radiological properties (half-life and radioactivity content) and source [6][7]. In terms of radiological properties, more broadly, RW is classified as low-level waste (LLW), intermediate-level waste (ILW) and high-level waste (HLW). These classifications are based on exempt waste (EW, RW that can be disposed or recycled without provision for radiation protection.) [20]. RW clearance level is $< 10\,\mu Sv/y$ of effective dose per individual material and/or $< 1\,person\,Sv/y$ for collective effective dose [19][20]. Based on EW and clearance level, LLW, ILW and HLW are defined as the following [18][21]:

LLW: - Activity level above clearance level and thermal power below $2\ kW/m^3$.

LLW does not meet clearance level due to the presence of radionuclides, that have either short half-lives at high activity level, or long half-life at low activity level. Thus, it must be separated

and confined for few decades. Current disposal method for this class is to store it in engineered near surface facility.

ILW: - Activity level above clearance level and thermal power below 2 kW/m^3.

The difference between LLW and ILW is in their content of radionuclides with long half-life – ILW has more of them. ILW may contain relatively high level of activity radionuclides with long half-life, such as radionuclides with alpha particles emission. These radionuclides are long lived; the duration of time they require to decay to an activity level tolerable is very long. For these reasons, this class of waste cannot be disposed at near surface facility; it needs higher degree of separation and confinement and is disposed tens to hundreds of meters deep below the surface.

HLW: - Activity level above clearance level and thermal power above 2 kW/m^3.

HLW has a great amount of radionuclide with long half-life, the decay of which produces a considerable amount of heat. In general, such class of waste is disposed in hundreds of meters deep into the surface of a stable geological formation.

2.3 Plasma and Thermal Treatment of Radioactive Waste

There are many thermal technologies used in radioactive waste pre-treatment, treatment and conditioning processes. Among those thermal technologies, the ones that are currently deployed and routinely applied in radioactive waste facilities, nuclear power plants, and nuclear fuel cycle facilities around the world are the followings [22].

- Calcination
- Wet combustion
- Incineration
- Molten salt oxidation
- Pyrolysis
- Thermochemical treatment
- Metal melting

- Synroc
- Vitrification
- Plasma

Which thermal technology to apply for a particular site depends on some factors like the capability of the thermal technology to treat a certain type of waste, economic consideration, social consideration and environmental consideration. There is no one thermal technology that is accepted universally to treat all radioactive wastes, there are advantages, disadvantages and restrictions for each method [23] . In order to help us compare among these thermal technologies, table 2.1 shows the types of RW that each thermal technology can be utilized to treat [22].

Table 2.1 Thermal Technologies and Their Applicability to Common Waste

Technology	Waste type						
	Organic liquids	Inorganic liquids	Organic solids	Inorganic solids	Mixed organic-inorganic solids	Mixed organic-inorganic liquids	Spent resins
Calcination	NA	A	NA	NA	NA	NA	NA
Incineration	A	A	A	NA*	A*	A	A
Melting	NA	NA	NA	A	NA	NA	NA
Molten salt oxidation	A	NA	A	LA	LA	LA	A
Pyrolysis	A	NA	A**	A**	A	A	A
Synroc	NA	NA	A	A	A	NA	NA
Thermo-chemical treatment	NA	NA	A	A	A	NA	A
Vitrification	NA	A	A**	A**	A**	NA	A
Wet combustion	A	NA	A	NA	NA	NA	A***
Plasma	A	A	A	A	A	A	A

Legend:

A	Technology is applicable to this waste type
NA	Technology is not applicable to this waste type
LA	Technology has limited applicability to this waste type
*	Small pieces of inorganic are acceptable without causing damage or plugging of the system.
**	Applicable only for the granular or powder form of this waste type
***	Applicable only to organic spent resins

From table 2.1, it can be noted that plasma technology is the only thermal technology that is applicable to all types of waste. Beyond the applicability of thermal plasma technology to all type of waste, it also has other advantages due to its unique characteristics. Thermal plasma has high energy density and can reach a maximum temperature of more than 10000 K and its power source is supplied from electricity [24]. These characteristics of plasma makes it advantageous to other thermal technologies because plasmas:

- can achieve temperature of tens of thousands Kelvin, which is well above the melting points of many waste materials and ashes [25]. This allows for high reactant transfer rates.
- While incineration and pyrolysis are oxidizing processes, in which their end products, due to the presence of oxygen, result in increased CO_2 and generation of NO_x SO_x, plasma inhibits NO_x SO_x generation because it is a reducing process [26][27][28].

2.3.1 RW Treatment Using Thermal Plasma Torches

Although there are many waste treatment facilities that use thermal plasma technology for their operations, the same cannot be said for RW treatment facilities. Facilities that use thermal plasma for RW treatment are not that many; the first site to apply thermal plasma for RW treatment was ZWILAG facility in Switzerland; it went in operation in 2004 [22][29]. ZWILAG treats Switzerland's entire LLRW output originating from medicine, research, industry and Swiss NPP. It uses DC thermal plasma of 1.2 MW and processes 1000 waste drums annually (1 drum = 200 l) [30]. Due to logistical and organizational reasons, ZWILAG goes in operation twice a year for ten weeks process time, with maximum capacity of 200 kg/h and 300 kg/h for combustible and melting waste respectively [22] [23].

As recently as 2018, another thermal plasma RW treatment facility, KOZLODUY was commissioned and started operations in Bulgaria. Its heat source is 500 kW non-transferred DC thermal plasma torch with a capacity of treating 250 tons of RW annually [31]. Implementation of thermal plasma treatment in these facilities is reported to be advantages, because it fulfills all the high standard environmental requirements [11][12].

The advantages of plasma technologies in RW treatment for volume reduction, waste homogenization, conditioning and so on has been reported in many scientific publications. *Prado et al* reported using plasma torch to treat RW sample materials and achieving volume reduction factor of 1:90 – 1:100 [32]. *Cheng et al* claimed to have treated incinerated ash with a plasma torch and to obtain a volume and weight reduction of the sample 6.4 and 1.7 times, respectively. In addition, *Cheng et al* reported conditioning and vitrification of heavy metals in the incinerated ash resulting in reduced leaching [33]. Thermal plasma treatment of RW meets ALARA principles in a process that is environmentally friendly all in one process; without the need to have a facility for sorting and condition according to a study conducted by Decker [29].

2.4 Thermal Plasma Torches

Thermal plasmas are partially ionized gases characterized by their local thermodynamic equilibrium (LTE) condition. In this condition, electrons, ions, heavy particles and/or molecules all have the same temperature [34]. There are three ways of generating thermal plasmas: direct current (DC), radio frequency inductively coupled plasma (RF-ICP) and microwave sources[35]. DC and RF plasmas are well established methods in both laboratory, and commercial and industrial scale of generating thermal plasmas.

2.4.1 DC Thermal Plasma Torches

DC plasma torches usually consist of two electrodes (cathode and anode); electric arc is formed between the cathode tip and the anode surface due to the voltage difference between the electrodes.

Plasma is formed when gas flows through the electrodes and the voltage difference between the electrodes starts a gas breakdown. Gases, which are good insulator at room temperature, are ionized and made electrically conducting. When current passes through the ionized gases, a phenomenon common with generating plasmas known as gas discharge is achieved.

There are two types of DC thermal plasma torches; they are called transferred and non-transferred plasmas. Both types of DC plasma torches consist of two electrodes (cathode and anode) through which plasma gases, typically argon, nitrogen, oxygen, helium, hydrogen and air, are passed to sweep the arc formed by the electrodes and create a plasma jet in the case of non-transferred and main arc in case of transferred plasma. Figure 2.1 shows the DC transferred and non-transferred arc schematics.

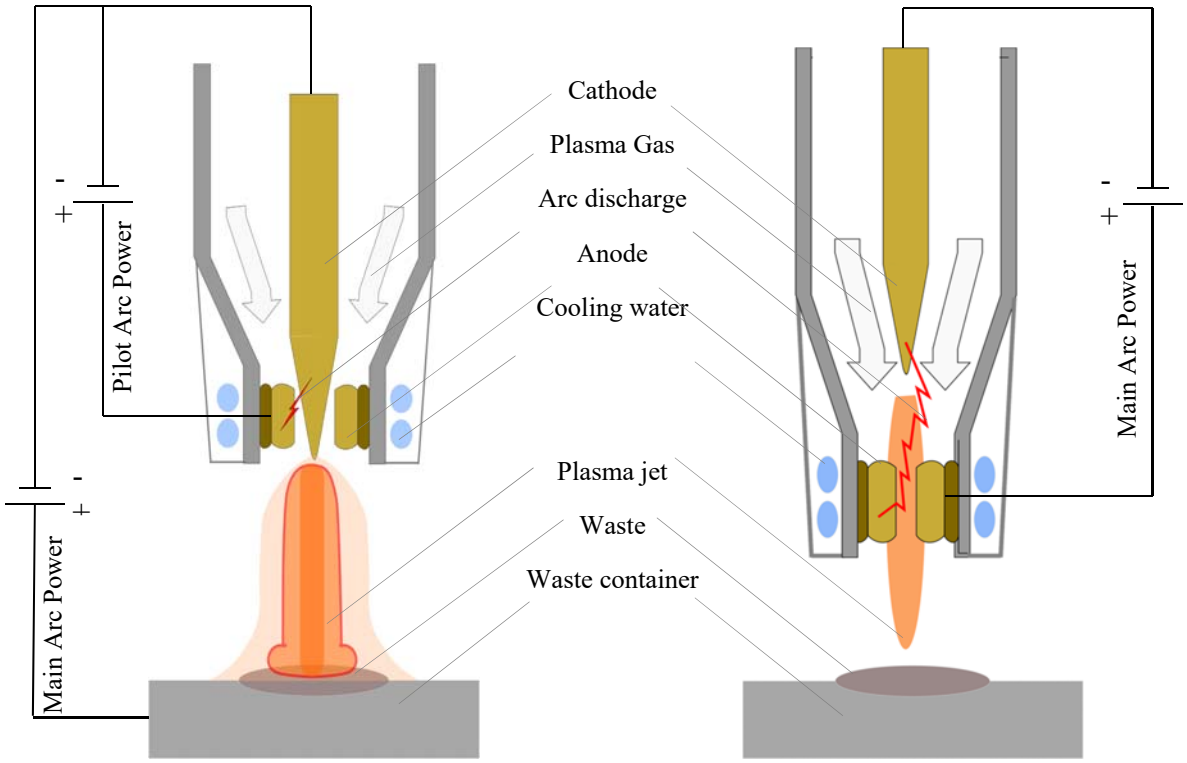

Figure 2.1 Schematic of DC transferred arc (left) and non-transferred arc (right) plasma torches.

The application of DC plasmas in waste treatment is well established; many facilities around the world operate DC plasma technology to treat many types of waste. The top ten companies for such operation are listed in table 2.2 [34].

Table 2.2 Top 10 Companies utilizing thermal plasma for waste treatment.

#	COMPANY	PRODUCTION MW	COUNTRY
1	Advance plasma power	100	Belgium
2	CHO-Power	37.5	UK
3	Green power system	35	USA
4	Sunbay energy Corp.	26	Canada
5	EnviroParks Limited	20	UK
6	Advanced plasma power	17	UK
7	Advanced plasma power	16.3	UK
8	Maharastra Env.Power	1.6	India
9	Maharastra Env.Power	1.6	India
10	Plasco Energy Group	1 (per ton)	Canada

2.4.2 RF-ICPTS

RF- Inductively-coupled plasma operation is like that of the induction heating of metals. With difference being, the load, with plasma, is a conducting plasma gas with considerably lower electric conductivity than most metals. As shown in figure 2, typically a RF-ICPT consist of three cylindrical dielectric tubes, water cooled solenoid copper coil of n-turns around the outer dielectric tube and three-line gas flow system: carrier gas, central gas and sheath gas.

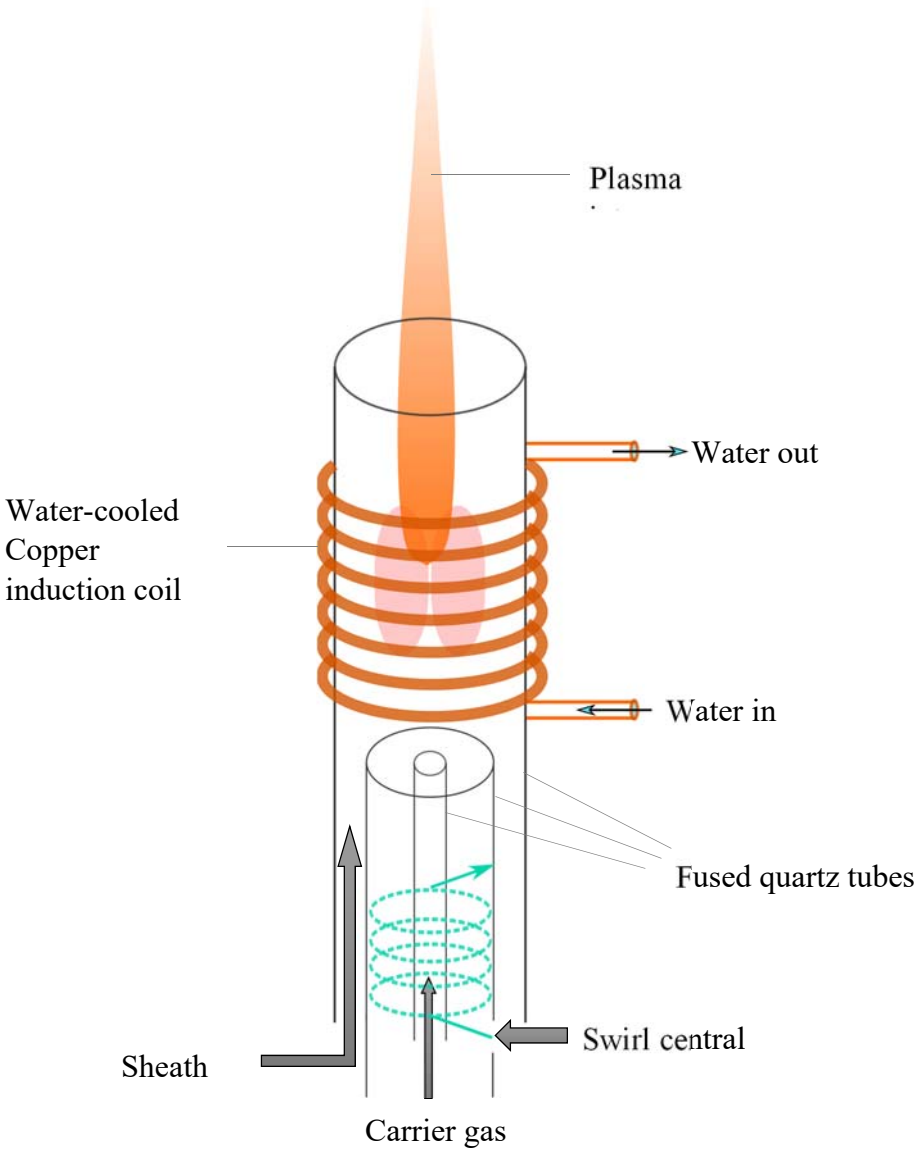

Figure 2.2 Schematics of RF inductively coupled plasma torch.

Metal or fused quartz are common materials for the carrier gas tube. The main purpose of the carrier gas line is to introduced liquid or powder of sample materials to be treated for processing. The central gas line is where the plasma forming gas is introduced. Usually, an argon gas is used as plasma forming gas due to its lower breakdown voltage. The purpose of the sheath gas, on the other hand, is to cool down the wall of the torch and prevent it from melting [36].

2.5 RF-ICPT

In 1947, Babat was the first to report inductively coupled plasma generation experiments at atmospheric pressure and lower at up to 100 kW power level. He could observe at atmospheric pressure (with increase in pressure) and 100 kW power level a thermal plasma transition [37]. His experiments were conducted in static system; no flowing gas was introduced to the system to get a self-sustaining plasma jet. Reed was the first to report development of ICPT; his ICPT worked at atmospheric pressure with argon as flowing gas in a 26 mm outer diameter quartz tube surrounded by 5 turns of solenoid copper coil, with excitation frequency of 4 MHz, 1.5 kW power level [38]. 1965 Wendt and Fassel reported an ICPT with three dielectric tube (coolant, plasma and aerosol tubes) with inner diameter 22 mm, 16 mm, 5 mm, outer diameter 24 mm, 18 mm, 7 mm, respectively. Coolant, plasma and aerosol tube have length of 22 cm (11 cm above coil), 12.5 cm (ending 1.7 cm below coil) and 15 cm (ending below plasma tube by 4 mm) respectively [39]. Many researchers, following Reed and, Wendt and Fassel, have worked considerably to improve the design of ICPT for various applications. *Hollabaugh et al*. reported ICPT design with water cooled copper fingers inside the outer tube. The fingers were used to keep the outer tube wall cool, and to transfer energy from induction coil to the plasma [40]. *Mostaghimi et al*. has developed a model of ICPT with outer tube made of porous ceramic (permeable ceramic tube), this would trap 80 % of radiative losses of the plasma, however losses due to conduction increases [41]. *Van der Plas et al*. constructed an ICPT cooled radiatively by using boron nitride (ceramic) as a segment of the outer tube. This torch, however, due to evaporation of boron nitride, caused clouding of the torch. *Kameyama et al*. reported a design dual RF torch system (main RF and igniter RF) [42]. *Yabuta et al*. designed and constructed a dual inlet ICPT in order to stabilize the plasma jet and reduce gas consumption, their torch was also modified to operate with helium as working gas [43]. *Alavi et al*. designed and constructed a conical ICPT for spectrochemical analysis, and they reported an increase gas velocity, reduced gas and power consumption [44]. However, this torch is small for waste treatment application.

From reviewing the design of ICPT, it can be said there is a lot of effort and progress made to improve the design of the torch. However, there is still room for design improvement in terms of

cooling the outer tube, starting and sustaining plasma easily and with as little power as possible, to reduce the operational cost of the torch and energy coupling. Improvement in cooling will lead to reduced ICPT operational cost, which in turn can make ICPTs competitive against other plasma torches for various applications, including for RW treatment. This thesis work tries to contribute to improvement of ICPT design and its application in RW treatment.

Chapter 3: Methodology

To treat and achieve high volume reduction of RW materials, a high thermal source from simple and efficient ICPT was proposed. Then, an ICPT was to be designed and implemented in an experiment. To achieve this goal, some objectives (chapter 1.5) were put forward. The objectives were realized through some scientific investigation which will be mentioned in this chapter. Three major tasks were identified and computed as shown in the flow diagram given in figure 3.1.

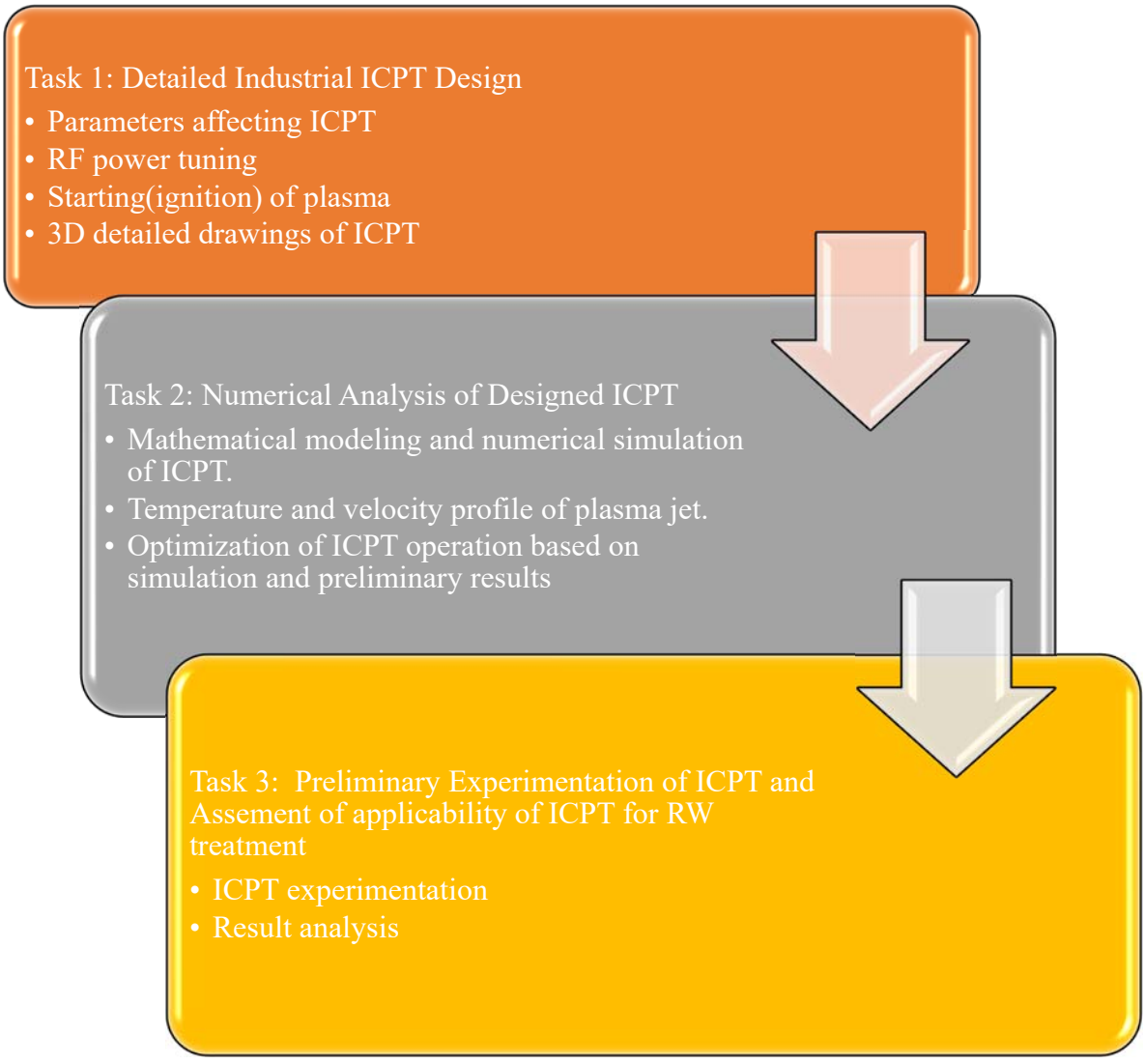

Figure 3.1 Flow diagram of thesis project

Task 1 tried to achieve a detailed industrial design of ICPT through evaluation and optimization of influencing parameters, such as: coil design, RF power tuning, gas flow rates and properties of material that make part of the torch. Based on that a detailed 3D ICPT was drawn using ONSHAPE (free CAD online cloud software) and SOLIDWORKS. ONSHAPE was used as a preliminary design because it does not have all the features that SOLIDWORKS has. It is also public, once your design is on ONSHAPE, it becomes public. For privacy and intellectual property protection, ONSHAPE is not adequate. That said, ONSHAPE can be accessed through phone, tablet and laptops or any other devices if there is internet connection. SOLIDWORKS, on the other hand, is a commercial software that can be pricy for students if it is not provided by the institution. Unfortunately, for students in the Faculty of Energy Systems and Nuclear Sciences at Ontario Tech University SOLIDWORKS license is not provided. Our lab server at APEL (Advance Plasma Engineering Lab) has a basic SOLIDWORKS license for one desktop. The design presented in this thesis is designed in SOLIDWORKS on the desktop at APEL. This way the design remains APEL's property and any future APEL member can edit or improve it.

For the completion of task 1, qualitative observations from preliminary RF plasma torch experiments were taken as input for the torch design. Few preliminary experiments were conducted as explained in Chapter 6. The observation from these experiments, added with literature reviews, were used as input to design an ICPT with key features in power/energy coupling, cooling and RF/EMC shielding. To move on to the following tasks (task 2 and 3), completing task 1 was necessary.

Understanding the thermodynamic property with great focus on temperature and velocity of the plasma jet was the main goal of task 2. To achieve that a computational fluid flow (CFD) model of plasma jet was created, and simulation was performed using COMSOL MULTIPHYSICS commercial software. Boundary conditions and operation parameters, and input parameters for the modelling and simulation were obtained from the torch characteristics from task 1. This includes dimensions of dielectric barrier, gas (mass) flow rate, type of gas and initial temperature. Some assumption in the physical and mathematical modelling of the torch was put forward in order to get a converging solution. These assumptions helped to reduce the cost, time and space needed to solve the Multiphysics problems of ICPT. The results of the simulation were validated from some benchmark models from literature reviews. The output of the simulation discussed includes plasma

jet axial, radial plasma temperature profile, plasma maximum temperature and heat source from joule heating. Based on the simulation results and validation, further optimization and improvement of the task 1 were conducted. Consequently, the designed ICPT was improved and optimized, to be constructed.

Task 3 has the aim of investigating the capability of the designed ICPT in RW treatment application. From simulation results from task 2, plasma jet temperature and velocity profiles are plotted in MATLAB. The graphs include plasma jet temperature and velocity profile at the exit nozzle of the torch (at z=180 mm) and in the symmetry line (r=0). Data for the plots are imported to MATLAB from COMSOL. From the plots of plasma jet temperature and velocity profiles, the capability of the designed ICPT is studied. The designed torch's temperature profile inside a reactor chamber is also taken into consideration in order to make a conclusion in its thermal capability for thermoplastic waste treatment. The required temperature to degrade thermoplastics like PE and PVC are discussed in chapter 1.1.1. Task 3 is concluded with discussion of the advantages and disadvantages of ICPTs for thermoplastic waste application and with some recommendations regarding the applicability of the ICPT.

After completing the 3 tasks mentioned above, recommendations on future works are briefly presented. Schematics on how to operate the torch, collect experimental data and waste treatment are shown in Chapter 7. Spectroscopic data to be able to estimate density and temperature of plasma jet, enthalpy measurement (graphite) to be able to estimate the efficiency of the torch are recommended and the possible experimental setup shown in figure 7.2 and 7.3.

3.1 ICPT Design Methodology

The final design presented in this thesis followed the necessary design process steps. These steps can be summarized as design input, design process and design output. The design input includes:

- Requirements
- Safety measures
- Assumptions
- ICPT operating experience
- Design basis (conditions that the ICPT must be able to cope with)
- Conceptual design

After establishing clear design input parameters, the design process stage followed. In this stage, project scope was established as in chapter 1.5. After that, based on the constraints (budgetary, space, input power source limitations are some of the constraints) and requirements, design options were generated. Subsequently, based on constraints and requirements, ICPT operating experience and procurement best possible option was selected.

The design output is provided in detail in the next chapter (chapter 4). A detailed engineering document, with all the ICPT components including dimensions and materials, has resulted from the engineering process.

3.2 Summary of ICPT Modelling and Simulation Methodology

The output from the design process has been modelled and simulated using a Multiphysics software. An ICPT with similar geometry and characteristics was modelled and simulated in COMSOL. A plasma module with heat transfer and fluid flow tree was used from COMSOL to compute the simulation. Due to computational limitation, some assumptions were made to model and simulate the torch. Continuity, momentum and energy equations were applied to solve the ICPT model. In chapter 5, an in-depth explanation on ICPT modelling, simulation and its data analysis can be found.

Chapter 4: Proposed Plasma Torch Design

The first step of any design is to understand all the necessary design considerations and requirements. Establishment of design consideration and requirements are made at conceptual design phase. In this chapter a conceptual design of plasma torch, its safe operation and a detailed 3D CAD drawing of an ICPT will be demonstrated.

4.1 Conceptual Design

The concept of ICPT is like that of the induction heating of metals; the main difference being the load. While the working load in metal induction is a metal, in ICPT the load is a conducting plasma gas with considerably lower electric conductivity than most metals. This has a great influence on size, power and optimal frequency combination necessary to sustain a stable discharge. Freeman and Chase tried to explain the physics concepts of ICP through well-known and developed concept of metal induction heating by creating a model called channel model. In this model, as shown in figure 1, the plasma is represented by an equivalent cylindrical workload of radius r_n, with uniform temperature and electric conductivity. Outside of the cylindrical region, the gas is assumed to be non-conductive with temperature spanning between that of the plasma and inner wall of the dielectric tube [45]. The application of an oscillating electromagnetic field through the coil generates eddy currents in the external shell of the cylindrical load. The thickness of the shell, known as skin depth δ , then can be given as a function of the oscillator frequency and the electrical conductivity of the load σ. It so can be estimated as:

$$\delta = \left(\frac{1}{\pi \mu_0 \sigma f}\right)^{\frac{1}{2}} \qquad (1)$$

Where μ_0, permeability of the load (in case of plasma, that of free space can be taken) has the value of $4\pi \times 10^{-7}$ H/m. An ICP torch with average temperature of 8000 K operating with argon at atmospheric pressure, $\sigma = 1000 \frac{S}{m}$, and $f = 13.56\ MHz$, the skin depth would be at about 4.32

mm. When comparing the skin depth value of plasma and cylindrical metal loads, it is found that the later have skin depth as small as up-to 100 times [46]. This is the reason why a high frequency (MHz) power supply is needed for excitation of ICPT compared to metal induction. The inner radius of the dielectric barrier must be at least twice the skin depth in order to confine the plasma within.

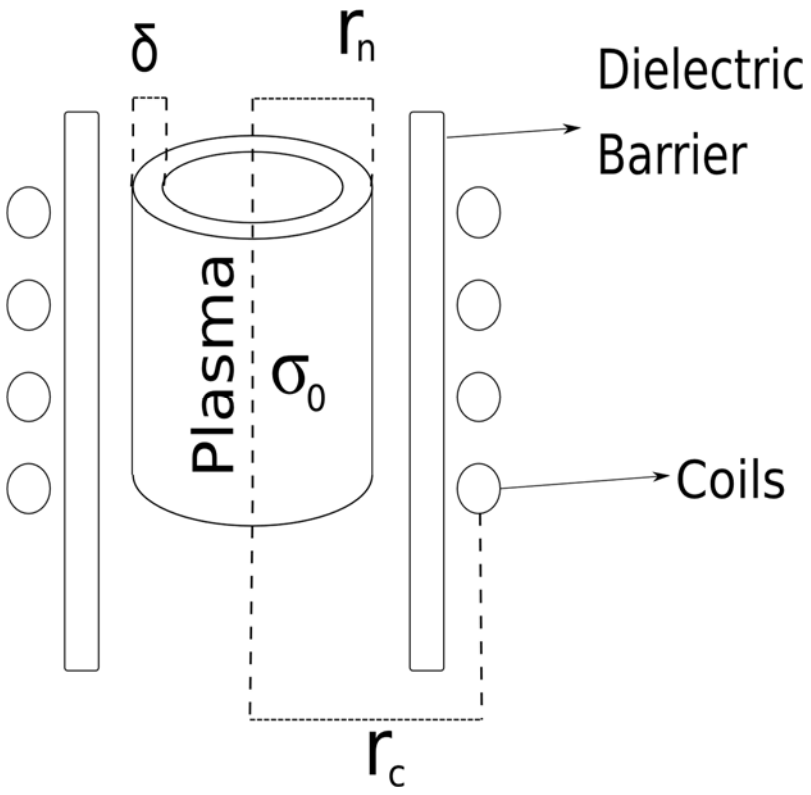

Figure 4.1 Channel Model first developed by Freeman and Chase.

4.1.1 Energy Efficiency

Energy efficiency of RF plasma system is affected by proper matching of the various electric circuits and coupling parameters and geometry of the torch. In ICPTs, electrical energy is provided by RF power supply at high frequency. To transmit the input power from the RF power supply to the plasma with great efficacy, matching/tuning the impedances of the power supply and the torch (plasma load) is necessary. To protect the power supply from fluctuation in impedance due to

plasma and ensure maximum transfer of energy, low power ICPTs (<10 kW) use an impedance matcher that tune the power supply to a fixed impedance of 50 Ω.

Not all the power from the RF power supply (P_E) transfer to the gas discharge, some part of the energy is lost in the matching circuit and some due to coil resistance. The rest of the power after the various losses is then coupled to the plasma. Power coupled to the plasma (P_p) is proportional to the coupling efficiency (η_c) and their relation can be calculated as:

$$\eta_c = \frac{P_p}{P_E} \tag{2}$$

Coupling efficiency is directly proportional to coupling parameter k, which in turn is affected by radius of the plasma load (r_n) and skin depth. A NASA investigation in RF plasma prepared by Mensing and Boedeker showed this relation as shown in equation 4 [47].

$$k = \frac{1}{\sqrt{2}} \times 2\frac{r_n}{\delta} \tag{3}$$

Equation 4 can be simplified as:

$$k = \sqrt{2} \times \frac{r_n}{\delta} \tag{4}$$

The study found that maximum coupling efficiency is obtained at $2.5 \leq k \leq 4$, which corresponds to $1.8 \leq \frac{r_n}{\delta} \leq 2.5$. The coupling efficiency depend on the ratio of plasma radius and induction coil radius as well; the optimum ratio for $\frac{r_n}{r_c} = 1$ [46], [48]. However, due to the need to have a dielectric tube for gas introduction, it is mechanically impossible to achieve unity in plasma to coil radii. Thus, values close unity (0.7 – 0.8) are acceptable.

4.1.2 Induction Coil

Energy efficiency/coupling to the plasma is also affected by the coil. The RF power supply induces high frequency alternating current to the coil generating a strong time-varying magnetic field.

When a gas is passed through a dielectric tube circumscribed by the solenoid coil, the strong magnetic field ionize the gas and form plasma. In ICPT, the last component of the electrical system is induction coil and the energy efficiency from the coil to the plasma is affected by the following factors:

- Material – although silver is the most electric conductive metal, it is expensive compared to copper. For this reason, copper, which is the second most electric conductive metal is used as a coil material. More specifically a hollow copper coil is used to keep it cool by passing water through it. Keeping the coil cool is important for efficient energy coupling and life span of the copper.

- Dimension – Length and number of turns of the coil affect the inductance as given by the formula:

$$L = \frac{\mu_0 N^2 A}{l} \qquad (5)$$

  Where μ_0, N, A and l represent free space permeability, number of coil-turns, area inscribed in the coil and length of the solenoid coil, respectively. Once the optimum values for N, A and l is found through calculation and experiment, they should be kept constant to achieve good matching, especially if the matching network is manual and not digital. Slight change on these dimensions can cause issues with matching.

- Position – placement of the coil around the dielectric tube is very important; it is usually placed near the end of the dielectric tube so not to expose long part of the tube to high temperature due to radiation of plasma jet.

4.1.3 Requirements

As discussed in 4.1, to have a RF ICPT system, an RF power supply with frequency level in range of MHz is needed. An impedance matching to tune the RF power supply to the RF induction coil are also needed to complement the electric part of a RF ICPT system.

The ICPT discussed in this thesis is aimed to use argon and nitrogen as central (plasma forming) gas and sheath gas respectively. A flow meter is needed to regulate the flow of argon and nitrogen gas through the dielectric (quartz) tube.

The ICPT is designed with long hours of operation in consideration, therefore, a RF radiaton shielding is a very important requirement. This is to protect personnel safety.

A discription of RF power supply, impedance matching and gas cylinders the ICPT is designed for are as follows:

RF power supply

RF power supply is supplied by RF VII Inc, model # RF-10-XII, serial #: RF 1K-0228 1000 W at 13.56 MHz power generator. The RF generator is connected to an automatic matching network; and it has a maximum output power of 1110 W. At maximum power, the RF has 13.56 MHz frequency. This RF generator has a reflected power limit of 69 W, when this reflected power is reached, forward power cannot be increased anymore. At this reflected power, the RF generator must be turned off immediately to avoid any damage to it. To reach the maximum power of the generator and have as less reflected power as possible, a good impedance matching is essential.

RF Tuning/ Matching Network

The RF generator is connected to the matching network procured from Advanced Energy M/N 3155405-300 S/N 1370363 by a coaxial N-N 8 ft cable. This matching network has an impedance/ inductive reactance of 50 ohms.

Induction Coils

A refrigeration copper tubing of 4 mm and 3 mm outer and inner diameter respectively was procured. Based on the optimal value of the inductance, a certain length of the coil was cut to form N-turn (N = 7). As shown in figure (4.4), the induction coil is connected to the matching network, which in turn is connected to the RF power generator.

Gas Cylinder Tanks

Two stainless steel gas cylinder tanks, one with argon and the other with nitrogen gas were procured from Air Liquide.

The argon gas cylinder tank has a volume of 9.3 m^3, a pressure of 17820 KPa, with purity of argon gas > 99.999% O_2 < 2 part per million (ppm), H_2O < 3 ppm and THC < 0.5 ppm.

The nitrogen gas (N_2) cylinder tank has a volume of 8.45 m^3, a pressure of 17820 KPa, with purity of argon gas > 99.999% O_2 < 2 part per million (ppm), H_2O < 3 ppm and THC < 0.5 ppm.

Argon is used as plasma forming gas because it has lower breakdown voltage compared to most gases [49].

Nitrogen is used as sheath gas. The choice to use nitrogen gas (N_2) comes from safety and financial reasonings. Nitrogen is an inert and abundant gas; this makes it cheap. In addition, thermal conductivity of nitrogen is higher than argon [50]. Thus, nitrogen can carry the plasma jet further in the axial direction than argon.

Flowmeters

Dwyer VFA-10-SSV and VFA-25-SSV air flowmeters for argon and nitrogen respectively were procured.

4.2 Atmospheric Pressure ICPT Detailed Mechanical Industrial Design

In this section 3 D CAD of ICPT will be demonstrated component by component with their dimension and type of material. A brief explanation why a certain material is chosen will be also provided.

The torch is designed to have water cooling capability for the dieletric barrier, if there should be the need. Water can be flown if/when necessary beteen the outer dielectric tube (quartz) and RF/EMC shielding cylinder to add external cooling for the wall. This is a novelty in ICPT design. The RF/EMC shielding cylinder, in addition to providing a base for a copper/aluminum tape for RF/EMC shielding, can also act as a tube for cooloing water. The design of the torch is based on preeliminary experimental results discussed in chapter 6. One other novelty of the design of torch is energy coupling effiecency of 100%. The power supplied from the RF power source is 100% coupled to the induction coil. 100% energy coupling is achieved though inductance calculation as in eq (5) chapter 4.1.2, and preliminary experiments.

The mechanical part of the ICPT is designed using SolidWorks and a detailed part by part engineering document is provided as follows:

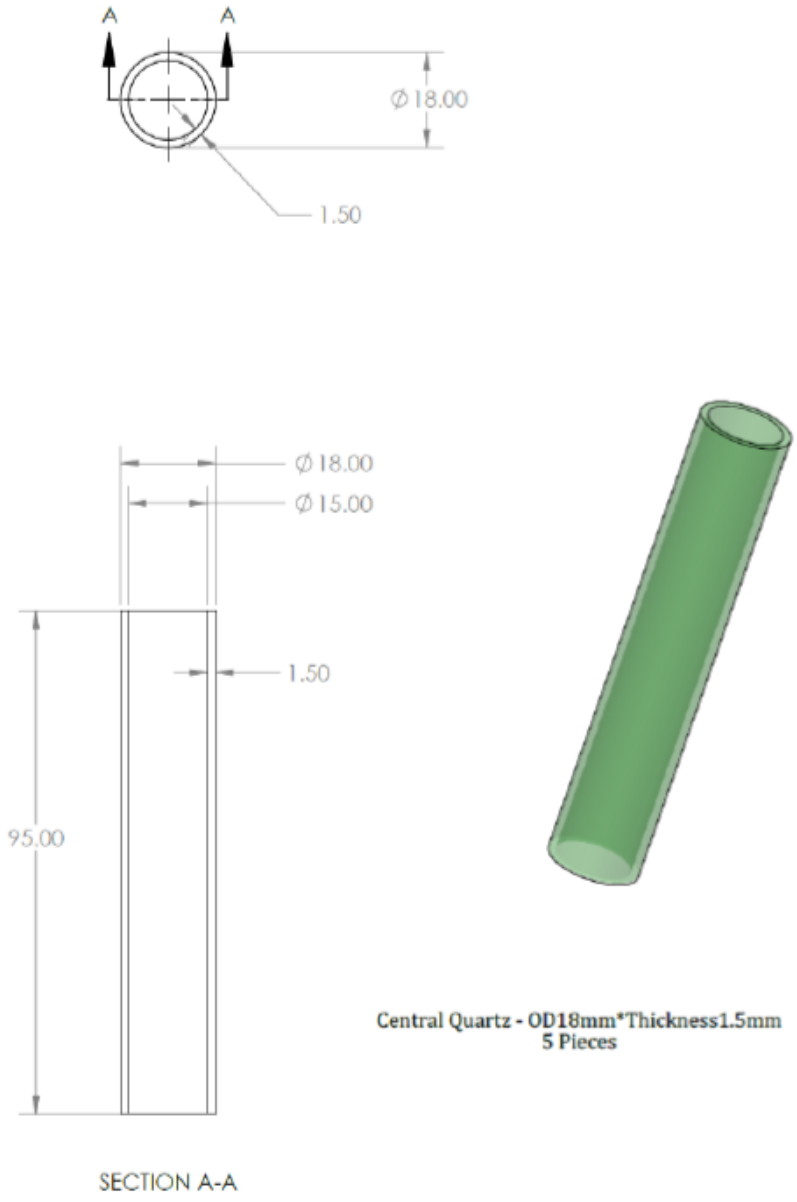

Figure 4.2 Central quartz tube

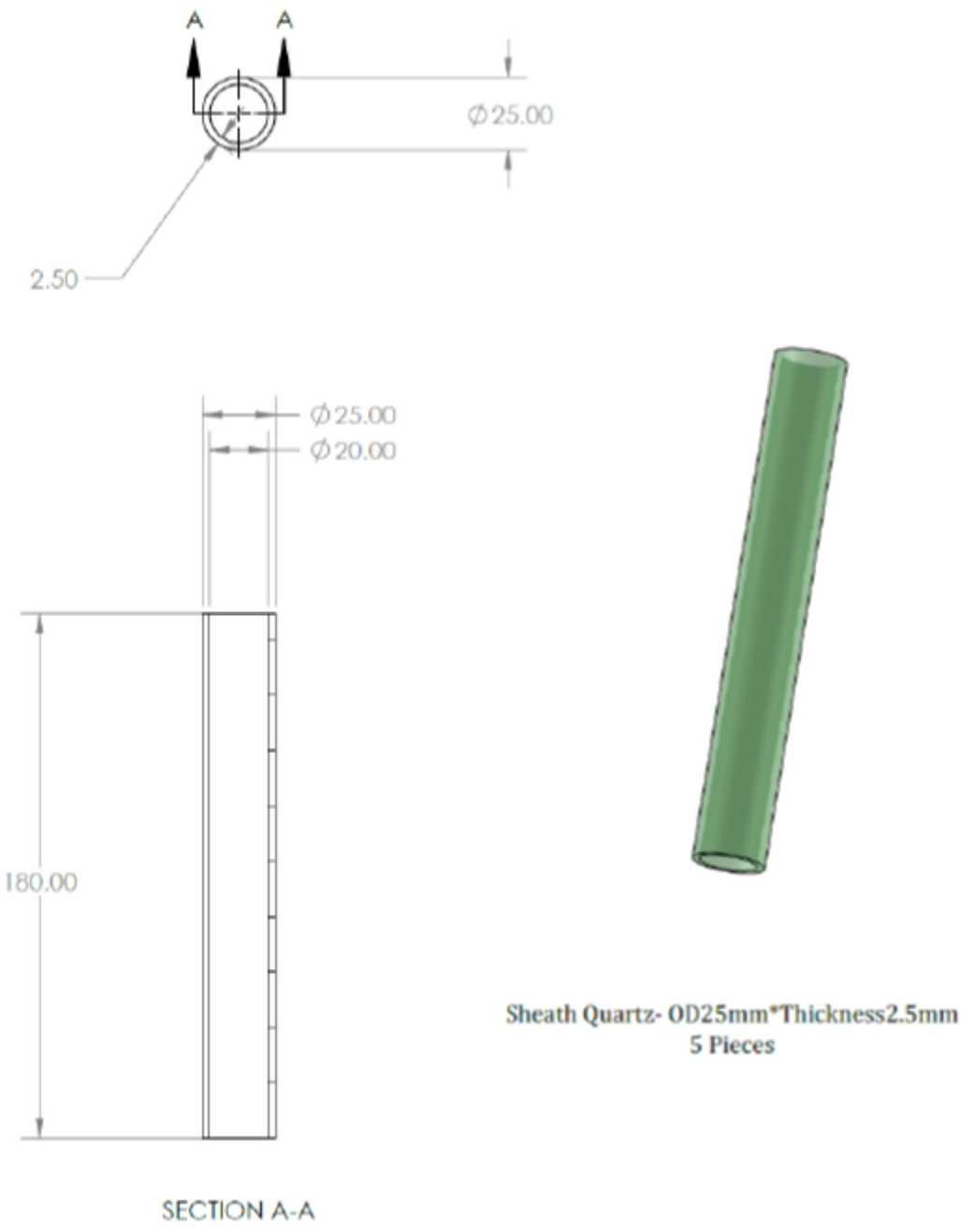

Figure 4.3 Sheath (outer) quartz tube

Figure 4.4 Copper induction coil

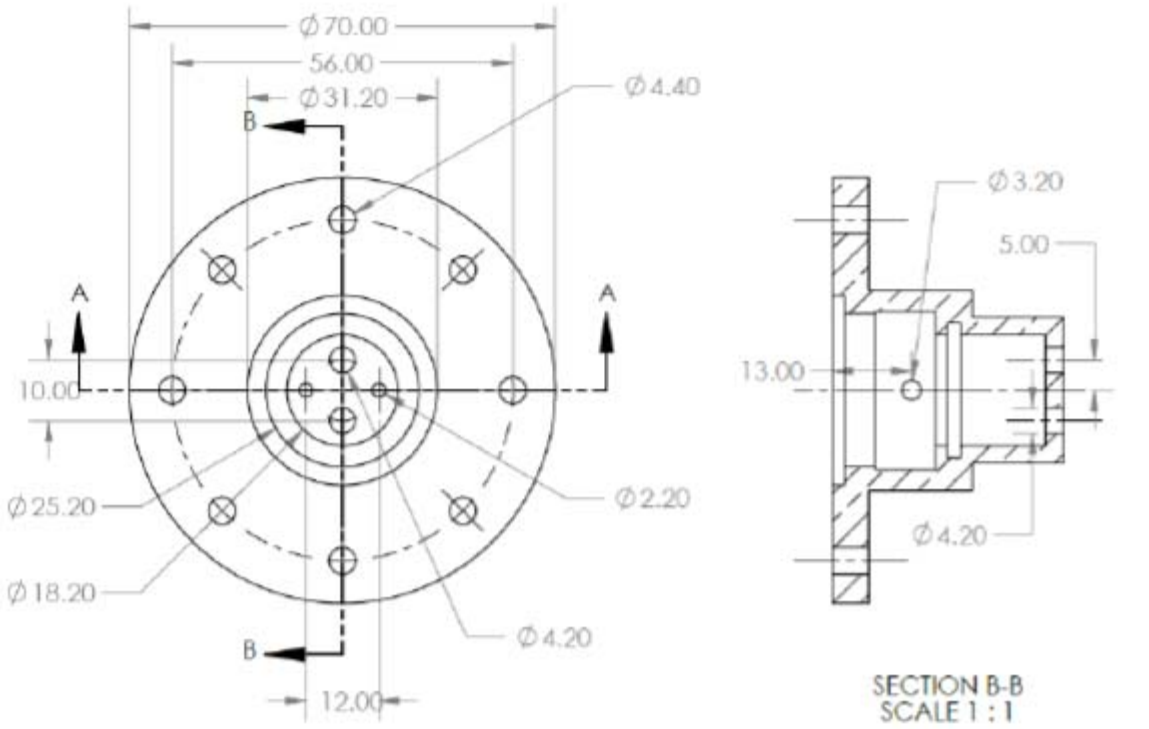

Gas Distributor Head - Copper
1 Piece

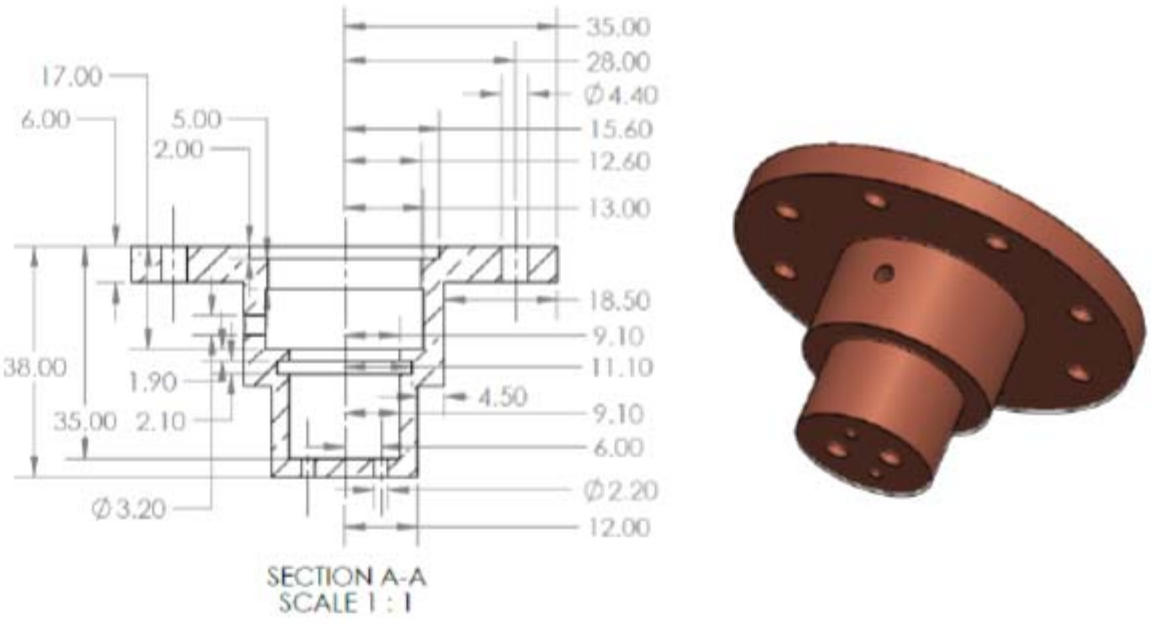

Figure 4.5 Copper gas distributer head

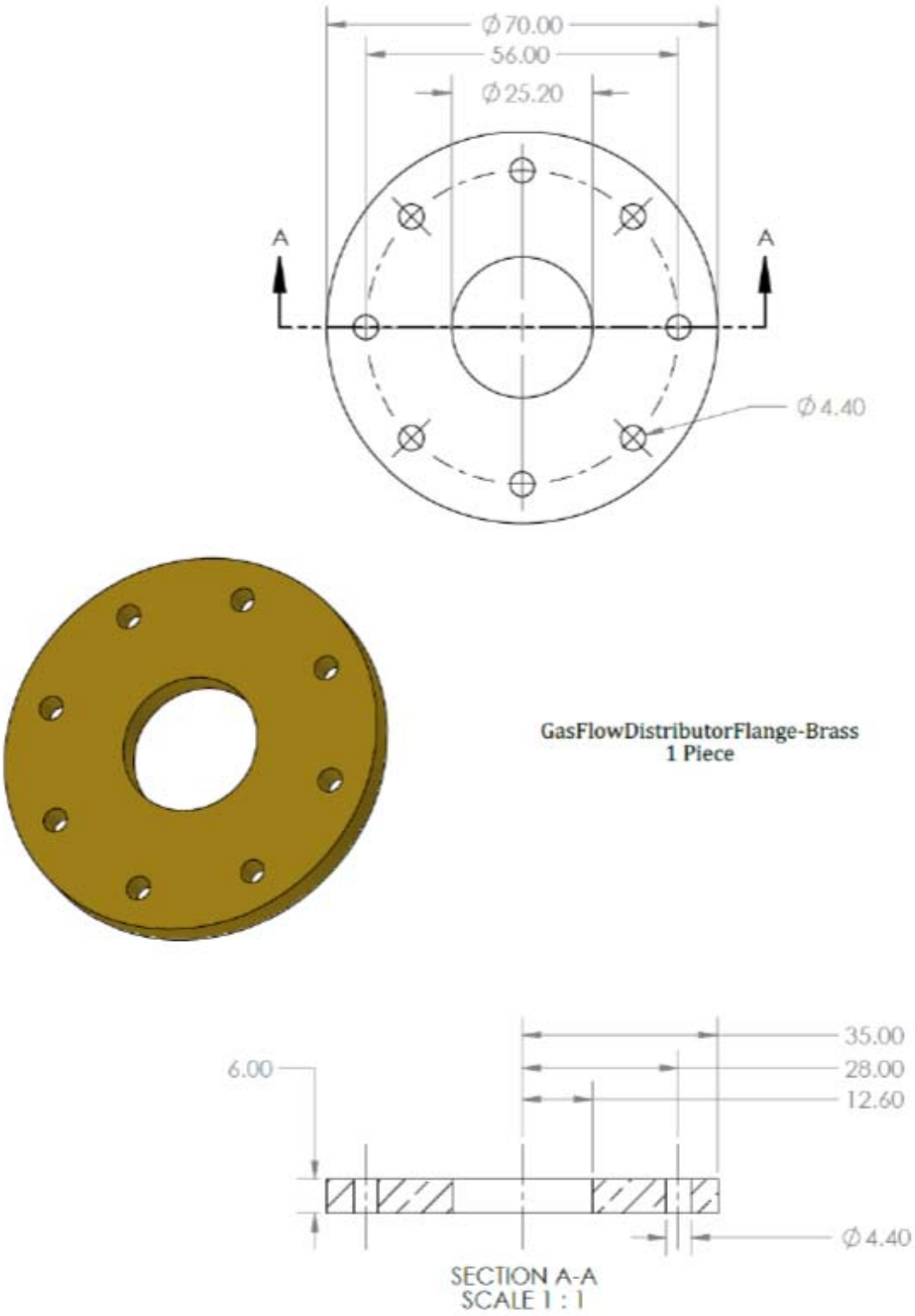

Figure 4.6 Flange for gas flow distributor

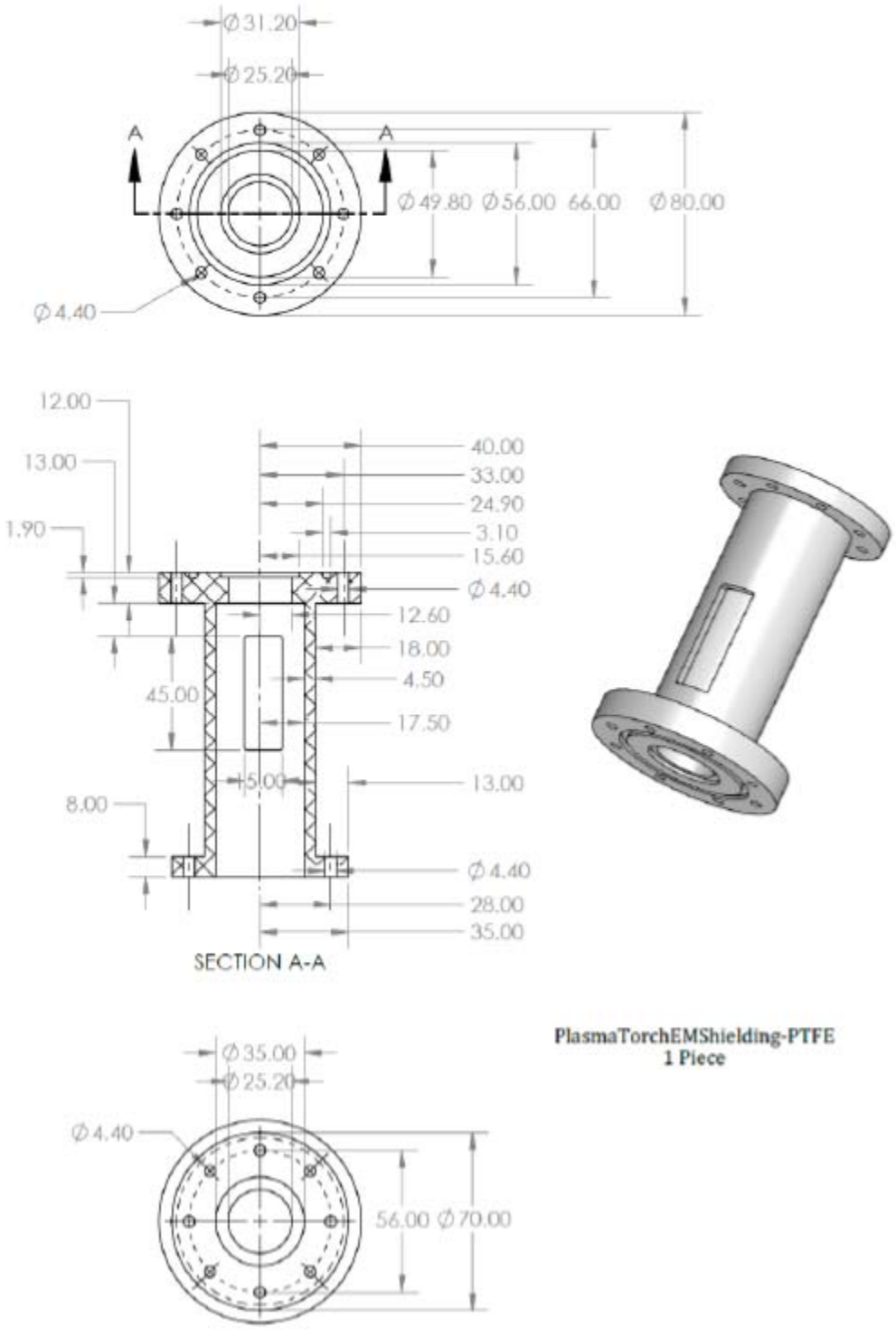

Figure 4.7 Plasma torch support and RF shielding base.

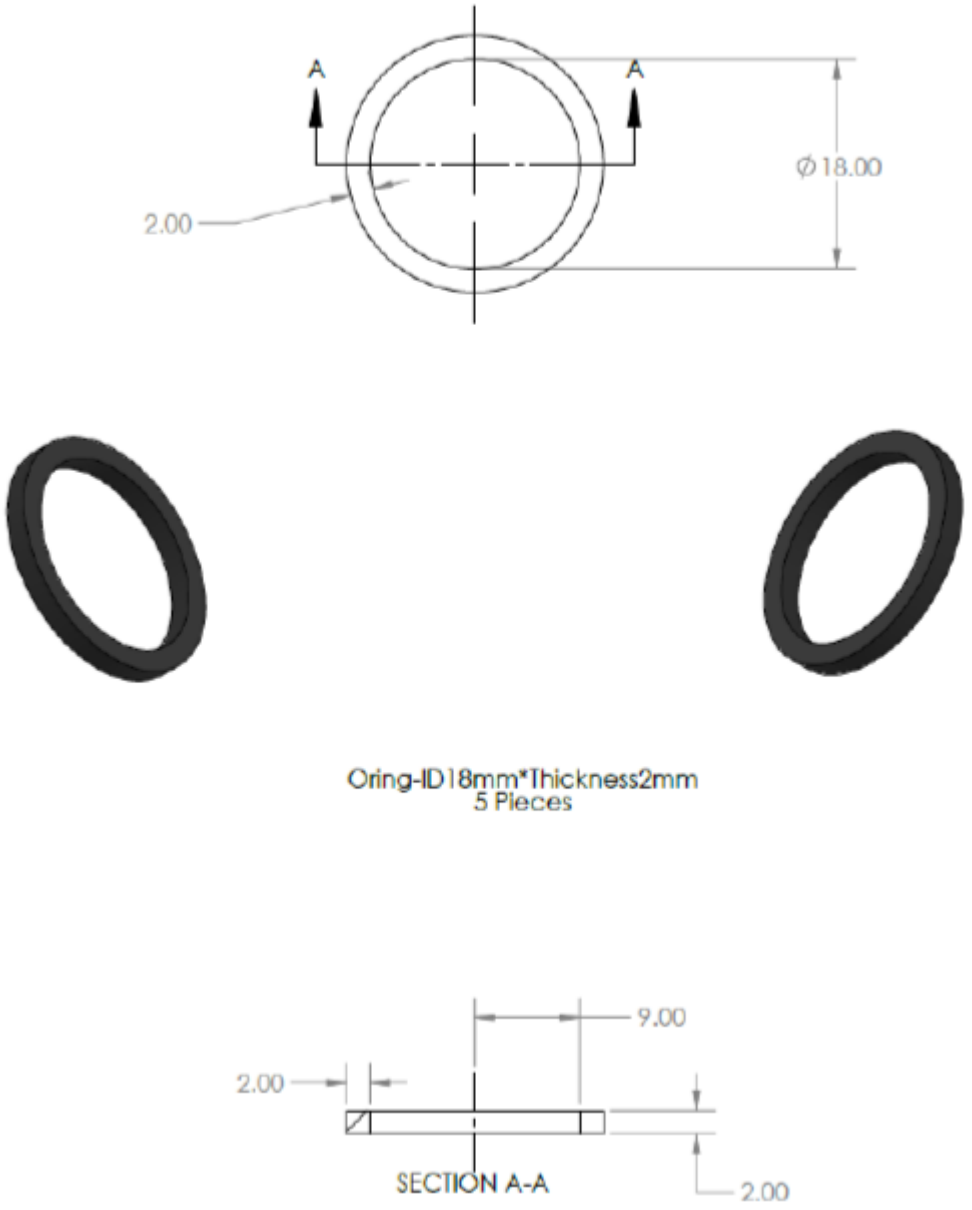

Figure 4.8 O-ring for central quartz tube

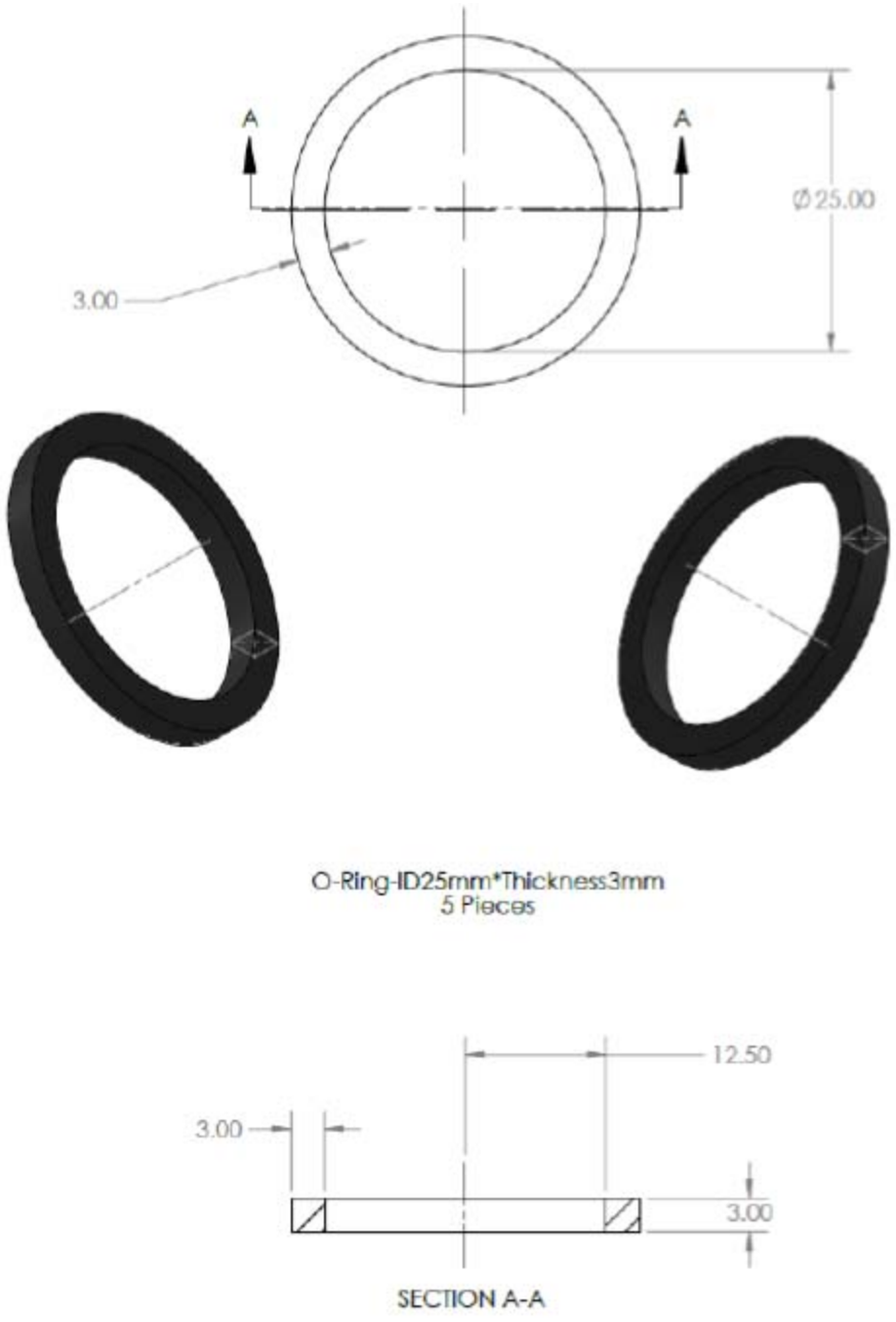

Figure 4.9 O-rings for sheath quartz tube

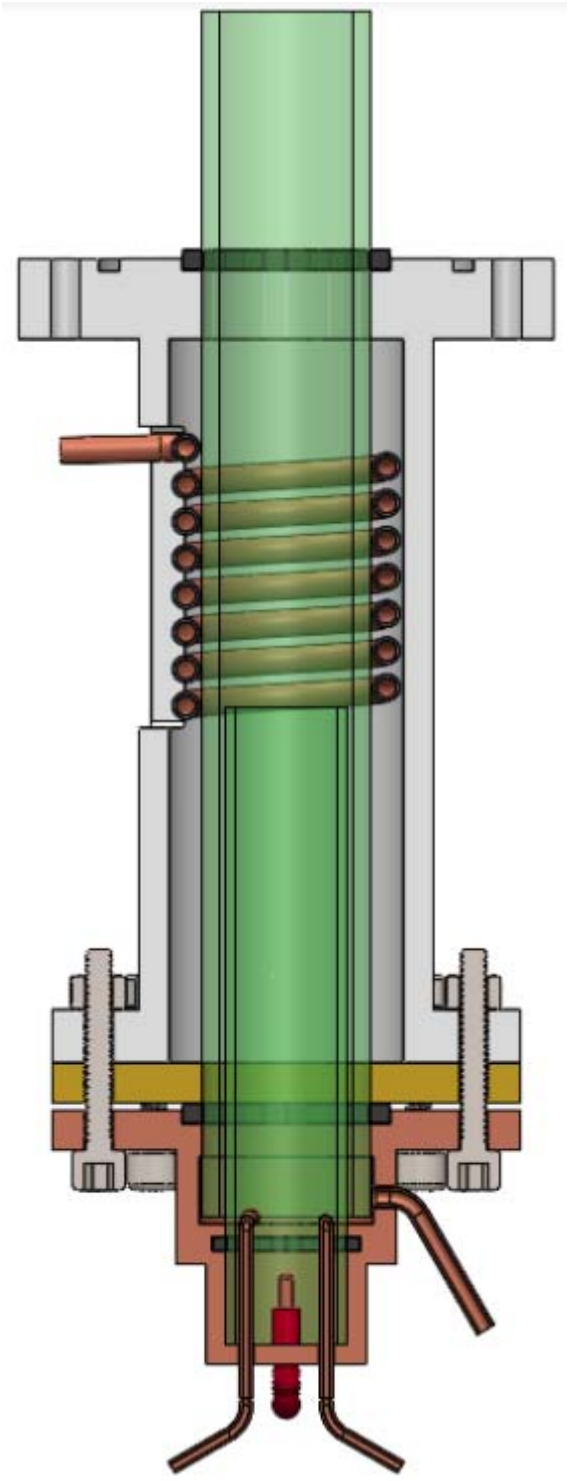

Figure 4.10 Frontal section view of RF plasma torch assembly.

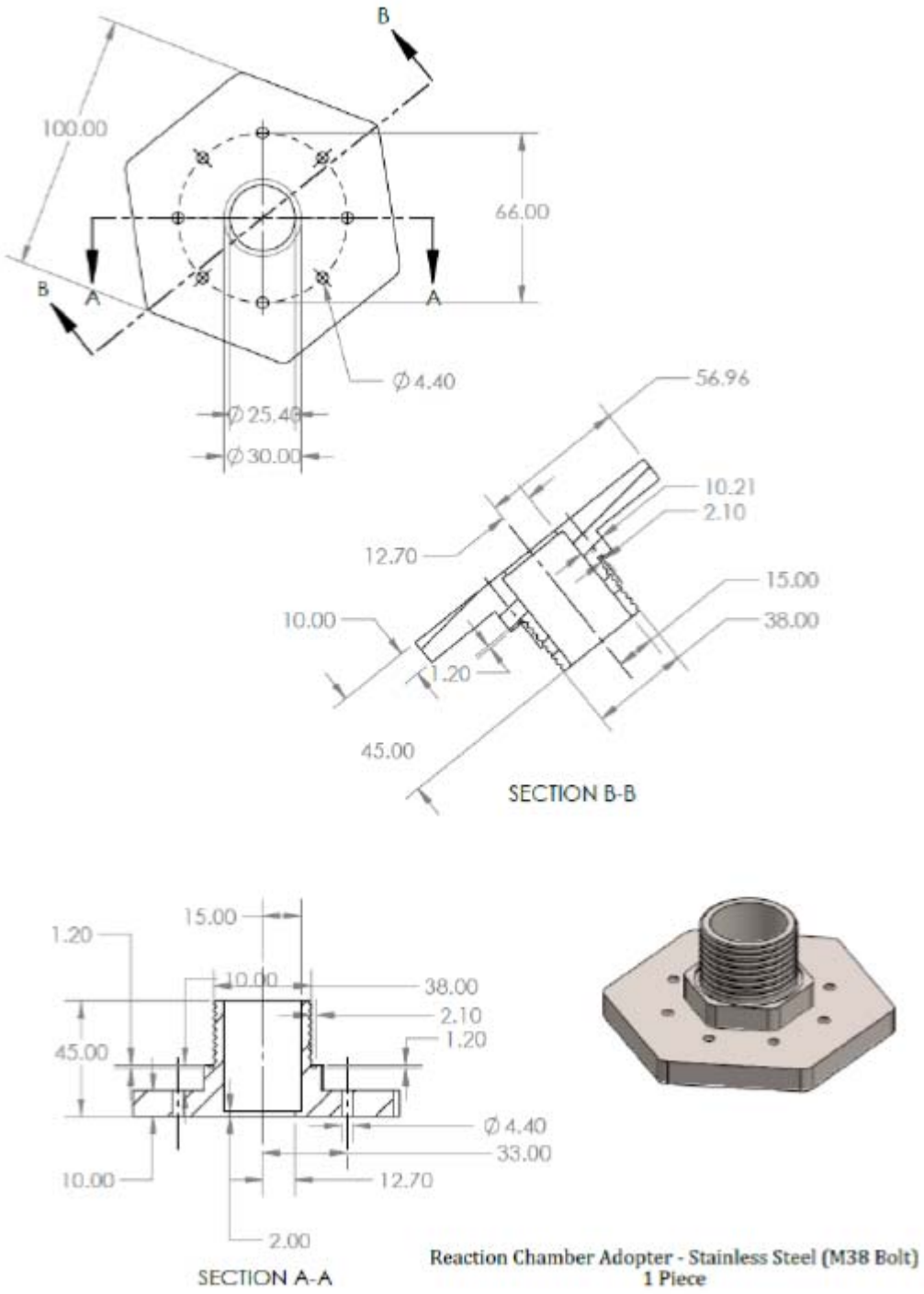

Figure 4.11 ICPT and reactor chamber adaptor/connector

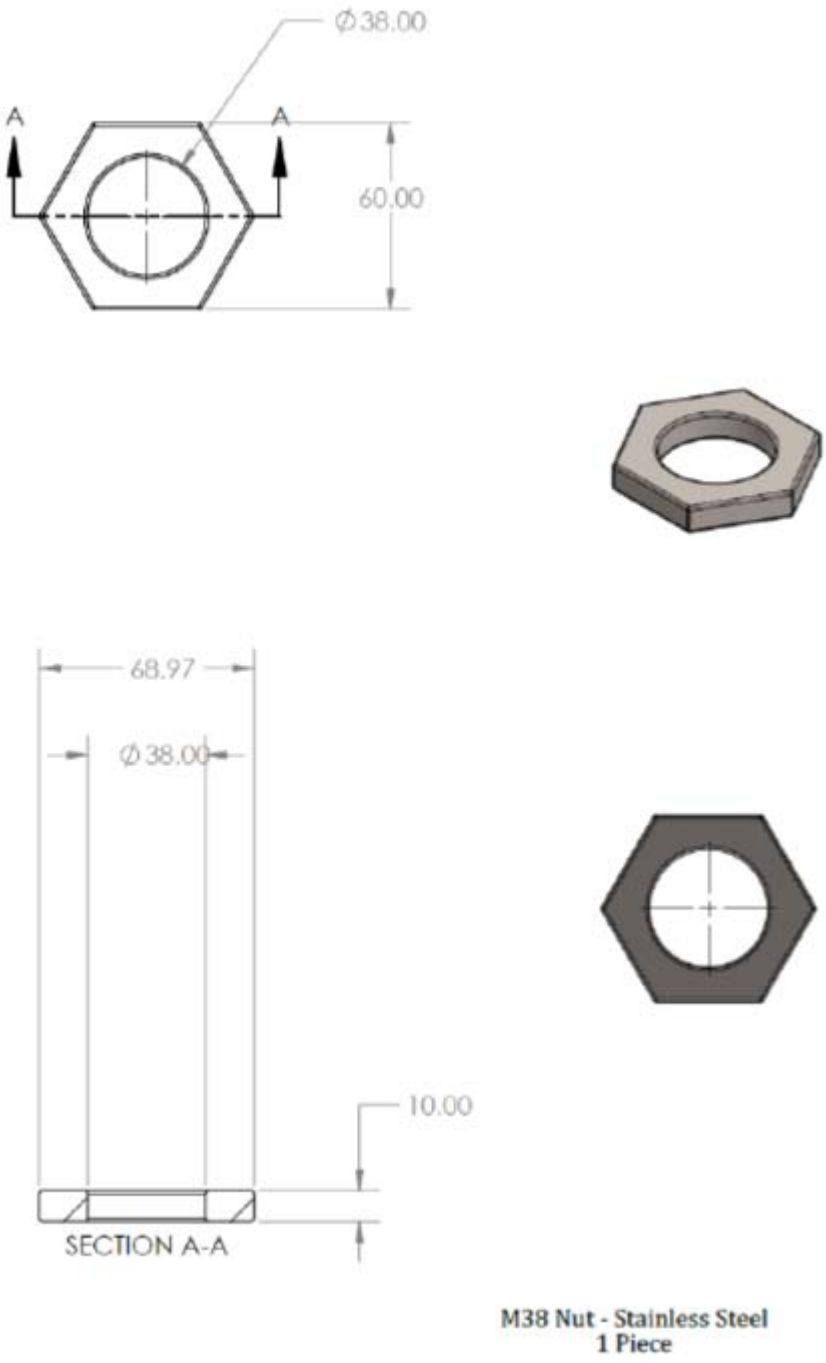

Figure 4.12 Nut for ICPT and reactor chamber adaptor/connector

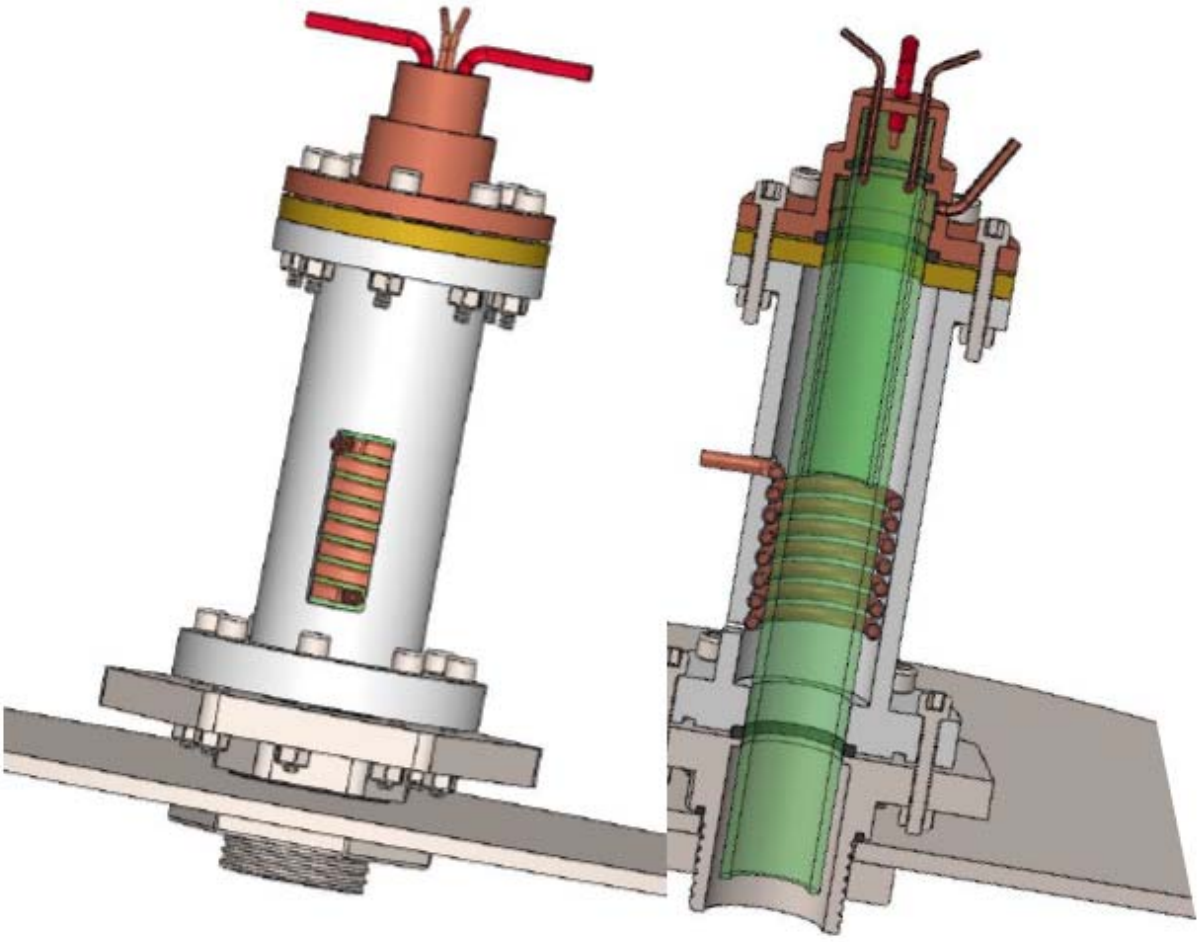

Figure 4.13 Assembly of ICPT integrated to chamber

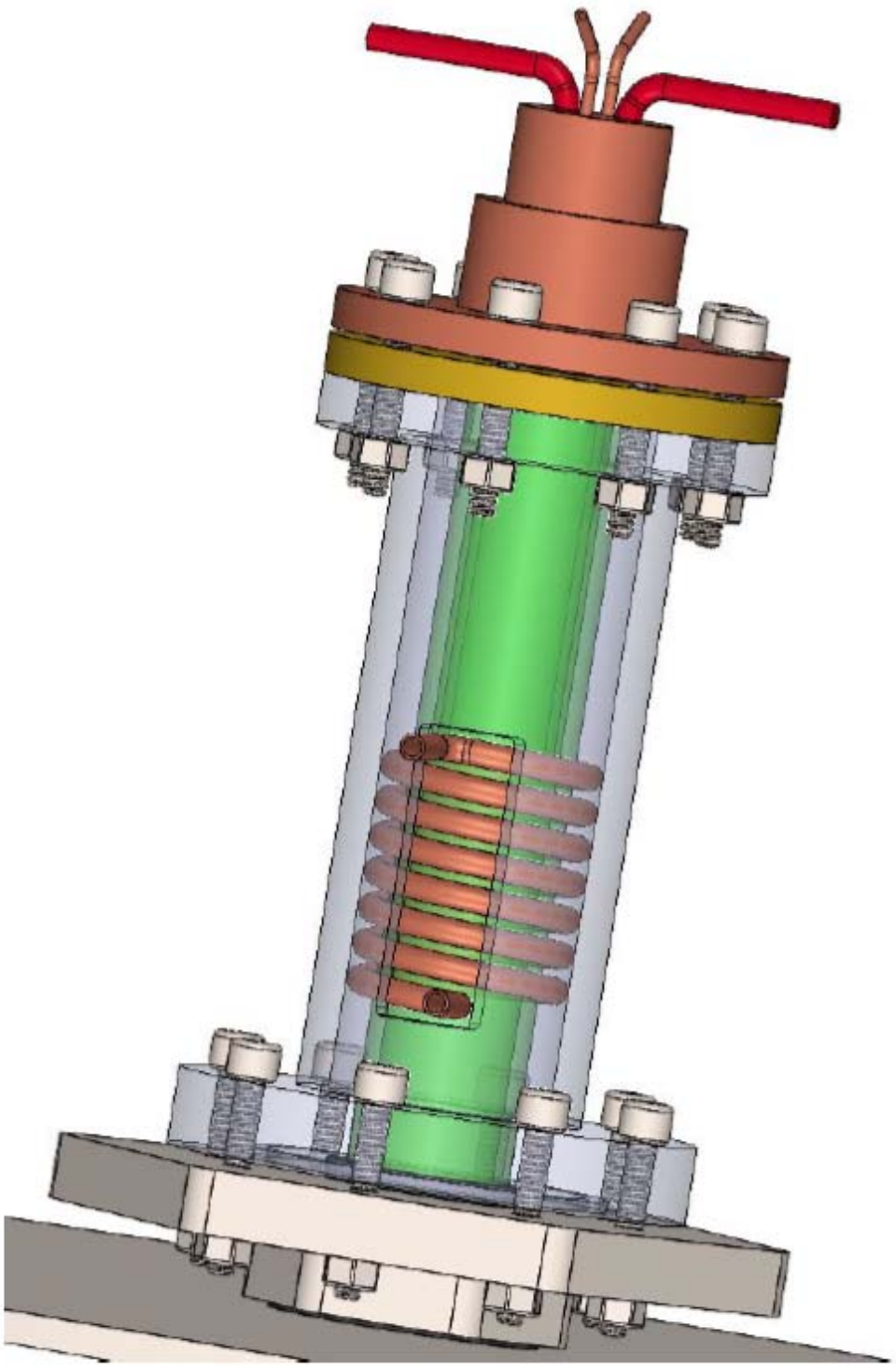

Figure 4.14 Final assembly of ICPT integrated to chamber

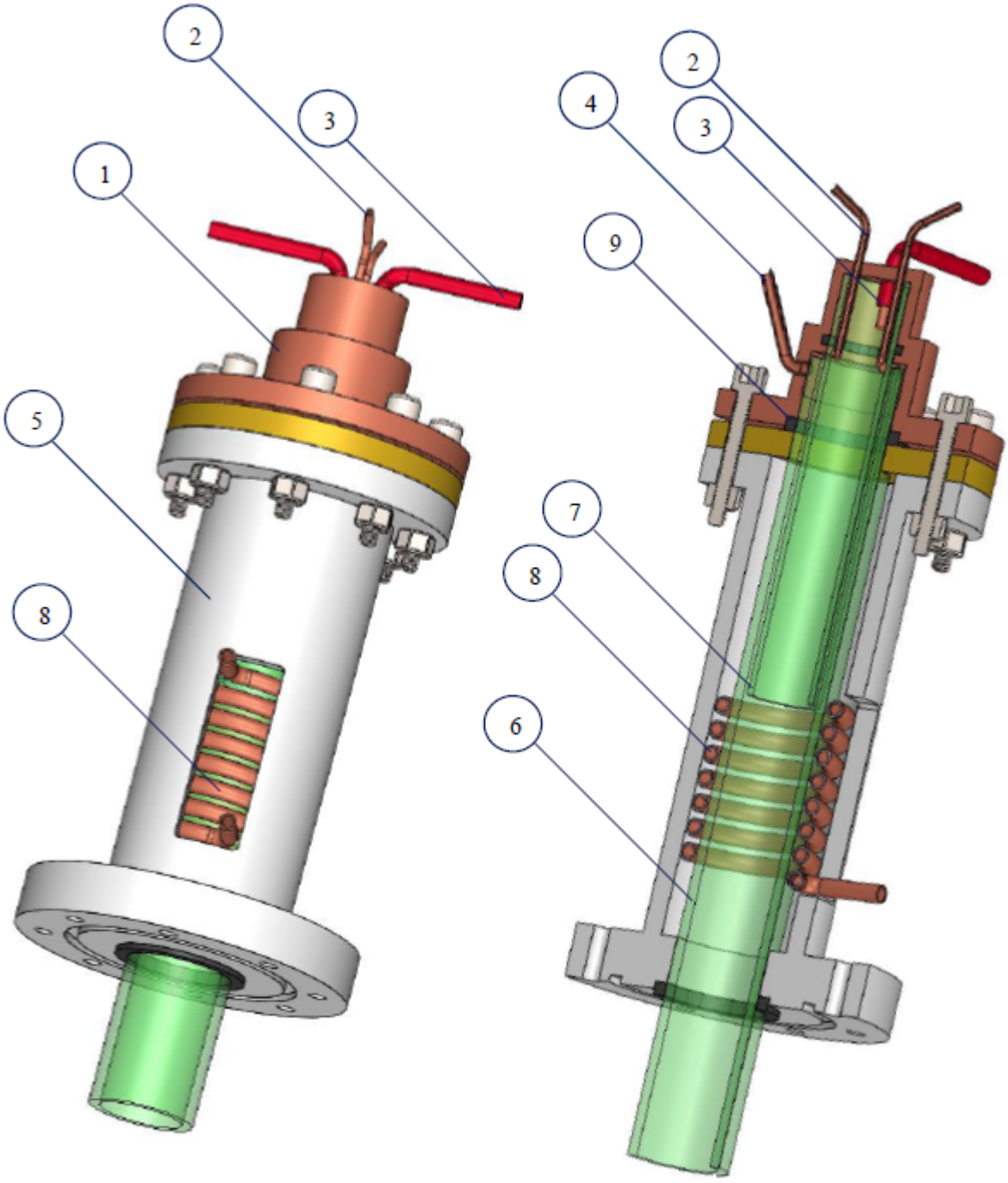

Figure 4.15 ICPT assembly and its components

Figure 4.15 shows ICPT part components with numbers. The numbers represent the following part components:

1. Plasma Gas Flow Distributor Head (Copper)

The material choice for this part must be a non-magnetic one. In case of metals, the options are reduced to aluminum, gold, silver, stainless steel and copper. Although stainless steel is a cheaper metal then copper, it is harder to machine than copper. For this reason, copper was chosen.

2. Swirl Central Gas Flow Inlet (Copper Tube)

Copper pipes were also chosen as gas flow line materials. The reason to this is copper pipe of these dimensions are easy to find, cheaper to purchase and if need be, they can be soldered to the plasma gas flow distributor head.

3. Plasma Igniter Pins (High Voltage Feedthrough)

According to Paschen curve to achieve a gas breakdown at atmospheric pressure in air, an electric potential difference in kV between the pins is needed [51]. To be able to carry such a high voltage, high voltage wires must be procured.

4. High Flow Sheath Gas Inlet (Copper Tube)

The same reasoning as in #2

5. RF/EMC Shielding Cylinder (PTFE, Covered by Metal Tape)

In order to operate the torch for long period of time while protecting personnel who are near the torch, a safety measure regarding the RF radiation must be taken. A shielding base made of polytetrafluoroethylene (PTFE) was chosen to wrap a metal tape around it. PTFE is a plastic thus

– nonmagnetic; it is relatively light, cheap and easy to machine, at the same time, it also has relatively good strength to resist bending.

6. Sheath Quartz (O.D. 25mm×Thickness 2.5mm)

7. Central Quartz (O.D. 18mm×Thickness 1.5mm)

#6 and 7 have the same reason for the choice of material. The reason to choose quartz as a dielectric material is due to its lightness and cost compared to ceramic.

8. 7-Turn RF Coil (Copper Tube, O.D. 4mm)

See chapter 4.1.2

9. O-Ring (Viton)

Viton is chosen as O-ring material because it has one of the higher melting temperatures compared to other simple rubber O-rings.

Chapter 5: Atmospheric Pressure ICPT Modelling and Simulation

RF inductively thermal plasma torches have gained a wide range of industrial application over the past several decades. Their application ranges from surface treatment such as: powder spheroidization, nano-sized powders synthesis, surface coating, to waste treatment, mass and optical spectrometric analysis and many more. This is because the plasma jet produced from RF ICPTs can be pure and of high enthalpy content [52]. To continue and expand the success of RF ICPTs application to more industries and field studies, further investigation of various phenomena that can impact the output of RF torch needs to be conducted. In recent decades, there has been great effort dedicated to modelling and simulation of RF ICPTs initiated by Boulos, Proulx and Mostaghimi, their researches mainly focused on understanding the heat transfer, fluid from of the plasma jet, electromagnetic field effect, particle injections and in flight particles effect on plasma jet – in 2D [53][54][55][56]. Successively, Bernardi and Colombo have developed a 3D ICPT model using FLUENT commercial software and introducing user defined function (UDF) to complement the software [57] [58][59] . Many other researchers – not mentioned here- are also devoting incredible effort to studying different phenomenon of plasma jet, ICPT modeling and simulation to add to existing knowledge and understanding.

In this chapter a modeling and simulation of plasma torch and, a plasma torch inside a chamber will be presented. The model and simulation results that are in the interest of this thesis will be discussed.

5.1 Model Description

A model that closely describe the designed ICPT was developed using commercial Multiphysics software called COMSOL Multi-physics, version 5.5 of this software released in 2019 was used. To perform this simulation in COMSOL the following modules are necessary: plasma module and AC/DC module. Plasma module contains various type of plasma physics "trees" among them the one applicable for this thesis is equilibrium discharge. In equilibrium discharge there are branches as well, from there, equilibrium inductively coupled plasma is the one applicable for this thesis. As such, this branch was selected. The study was computed in the frequency-transient study as temperature change in time and distribution of electromagnetic field needed to be calculated.

In this model, as in the design, the ICPT has two gas flow inlet lines, central gas line and sheath gas line. For simplicity of the model, argon gas was introduced in both inlet lines with flow rate as indicated in table 4.1, inside the quartz tube, as we move farther away from the wall of the torch, the Reynolds number decreases, this allows as to assume the flow to be laminar [60].

As a 2D asymmetric geometry, the induction coils are not presented in helical solenoid, but rather as parallel to one another and perpendicular to the torch. As the design shows in figure 4.4, the coil in real ICPT winds around the outer quartz tube in a solenoid. However, for simplicity of the model, a 2D coil with 4 mm diameter, and 5 mm distance from the center point of one coil to the center point of adjacent coil, was set. The distance from the center of the coil to the symmetry line and to r=0 (i.e., L_c and r_c) can be found in table 4.1. The fact that the coils are not in 3D helical shape as in the designed torch have an impact on the simulation results, a 3D modelling could give a more accurate solution and the result of temperature will not be fully symmetric. However, with increase in frequency from 3 – 13.56 MHz, the effect of coil orientation on the symmetry of the plasma jet temperature decreases. Therefore, in high frequency a 2D coil geometry as can be in figure 4.11 can be a close enough approximation. In this case, as frequency of coil excitation is 13.56 MHz is used, a symmetric temperature profile result can be predicted.

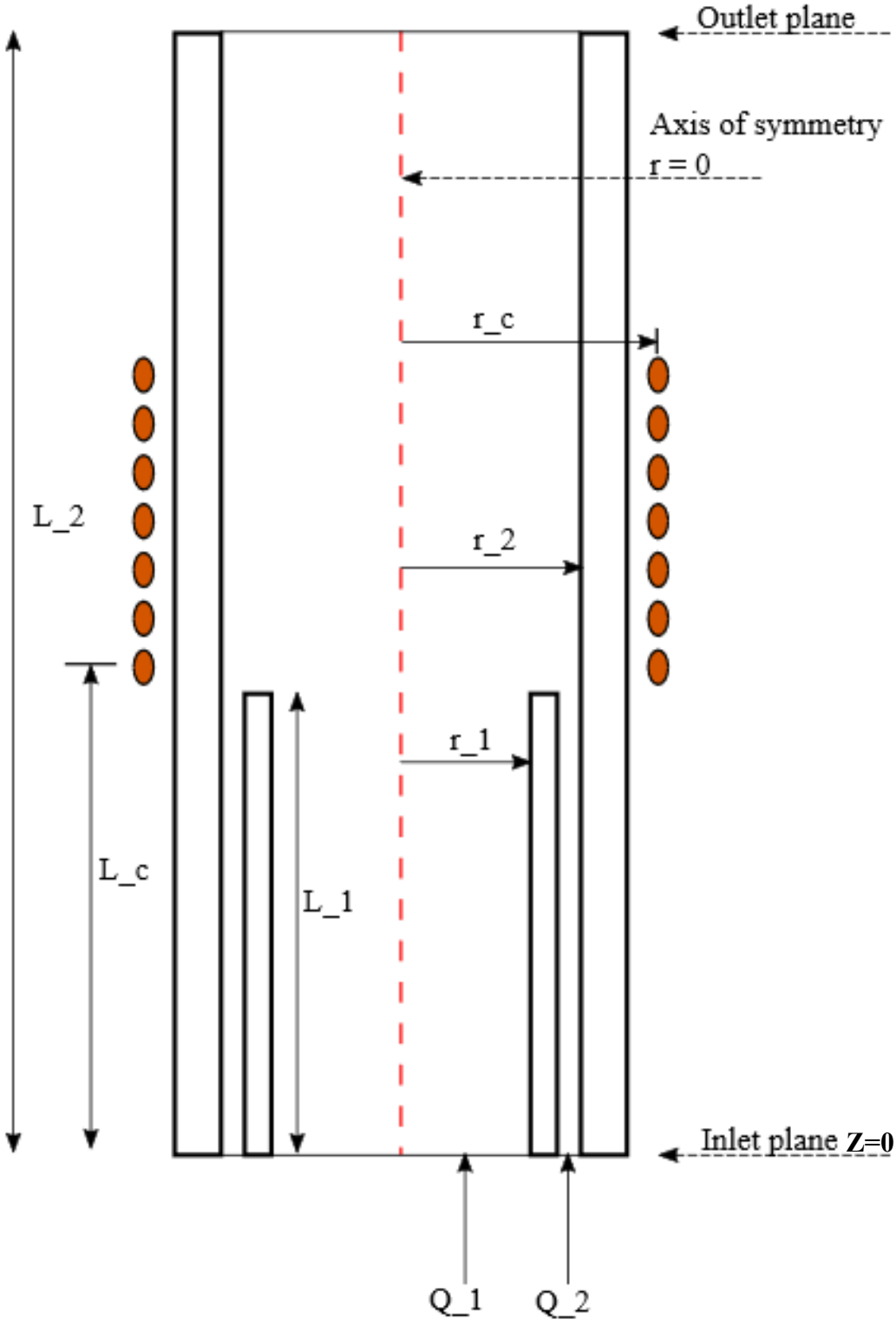

Figure 5.1 Schematic of a 2D asymmetric ICPT model.

Table 5.1 Plasma Torch Simulation Parameter

Name	Expression	Value	Description
T0	293.15 [K]	293.15 K	Room Temperature
Pex	1 [kW]	1000 W	Coil excitation power
Freq	13.56 [MHz]	1.356E7 Hz	Coil excitation frequency
r_1	7.5 [mm]	0.0075 m	Inner radius of central tube
L_1	95 [mm]	0.095 m	Height of central tube
d_1	1.5 [mm]	0.0015 m	Thickness of central tube
r_2	10 [mm]	0.01 m	Inner radius of sheath tube
L_2	180 [mm]	0.18 m	Height of sheath tube
d_2	2.5 [mm]	0.0025 m	Thickness of central tube
d_c	4 [mm]	0.004 m	Coil diameter
r_c	15 [mm]	0.015 m	Radial distance to the center of the coil
L_c	100 [mm]	0.1 m	Height to the center of the coil
Q_1	4 [l/min]	6.6667E-5 m^3/s	Central gas flow rate
Q_2	15 [l/min]	2.5E-4 m^3/s	Sheath gas flow rate
M	0.04 [kg/mol]	0.04 kg/mol	Molar mass - Argon
mv_stp	22.4 [l/mol]	0.0224 m^3/mol	molar volume at STP - Argon
$\dot{m}1$	M*Q_1/mv_stp	1.1905E-4 kg/s	Central tube mass flow rate
$\dot{m}2$	M*Q_2/mv_stp	4.4643E-4 kg/s	Sheath tube mass flow rate
ρ_stp	1.91 [kg/m^3]	1.91 kg/m^3	Density at STP - Argon
A1	pi*(r_1) ^2	1.7671E-4 m^2	Cross section - central tube
A2	pi*(r_2^2-(r_1+d_1) ^2)	5.969E-5 m^2	Cross section - sheath tube
v1	(mdot1/rho_stp)/A1	0.35271 m/s	Central gas flow velocity
v2	(mdot2/rho_stp)/A2	3.9158 m/s	Sheath gas flow velocity

This model, as in many models in literature review, assumes a local thermodynamic equilibrium (LTE) condition. This assumption is a close approximation, although not fully correct. At atmospheric pressure and higher, the collision speed of atoms or molecules increases, and their collision time decreases. The collision time in atmospheric RF plasma jets is in the order of $1 \times 10^{-11} s$ [61], while in our case of 13.56 MHz, it takes approximately 74 ns for the RF electromagnetic field to complete one period. This means for every oscillation, the collision of a single electron with atoms is in the order of thousands. The frequent and many collisions of an electrons with atoms lets us to be able to consider LTE condition. *P. Yang et al*. reported that using two-temperature model as supposed to LTE condition, in atmospheric pressure, does not produce a significant difference in ion and electron temperature [62]. For this reason, LTE condition can provide a very good approximation of non-LTE condition in close to atmospheric or higher pressures. In addition to that, LTE condition has a consistent formulation and there is no need to calculate, formulate or make assumption on energy transfer or/and power coupling between electrons and ions.

Assumptions made to perform the modeling of ICPT design can be summarized as follows [63]:

1. The ICPT has a geometry of a full azimuthal symmetry.
2. The axial component of the coil current is ignored, so the coil is approximated to arrays of current carrying parallel copper rings with 4 mm O.D.
3. The plasma is formulated in a steady state, since Reynolds number is below 1000, a laminar flow is used to model the plasma [60].
4. The plasma is assumed to be optically thin under LTE conditions.
5. Since the flow is non-turbulent, from the energy equation, viscous dissipation and pressure work are ignored.

5.2 Domain and Material

To perform the modelling of the ICPT in COMSOL, after completing the geometry, the domains and materials must be defined. The domains for this modelling are explicitly named as plasma, quartz, coil and air as shown figure 4.12. Domains in COMSOL 2D geometry are surfaces. The next step after naming the domains is to specify the material physical and chemical behavior. In this simulation, all material properties used are obtained directly from COMSOL library, add material section.

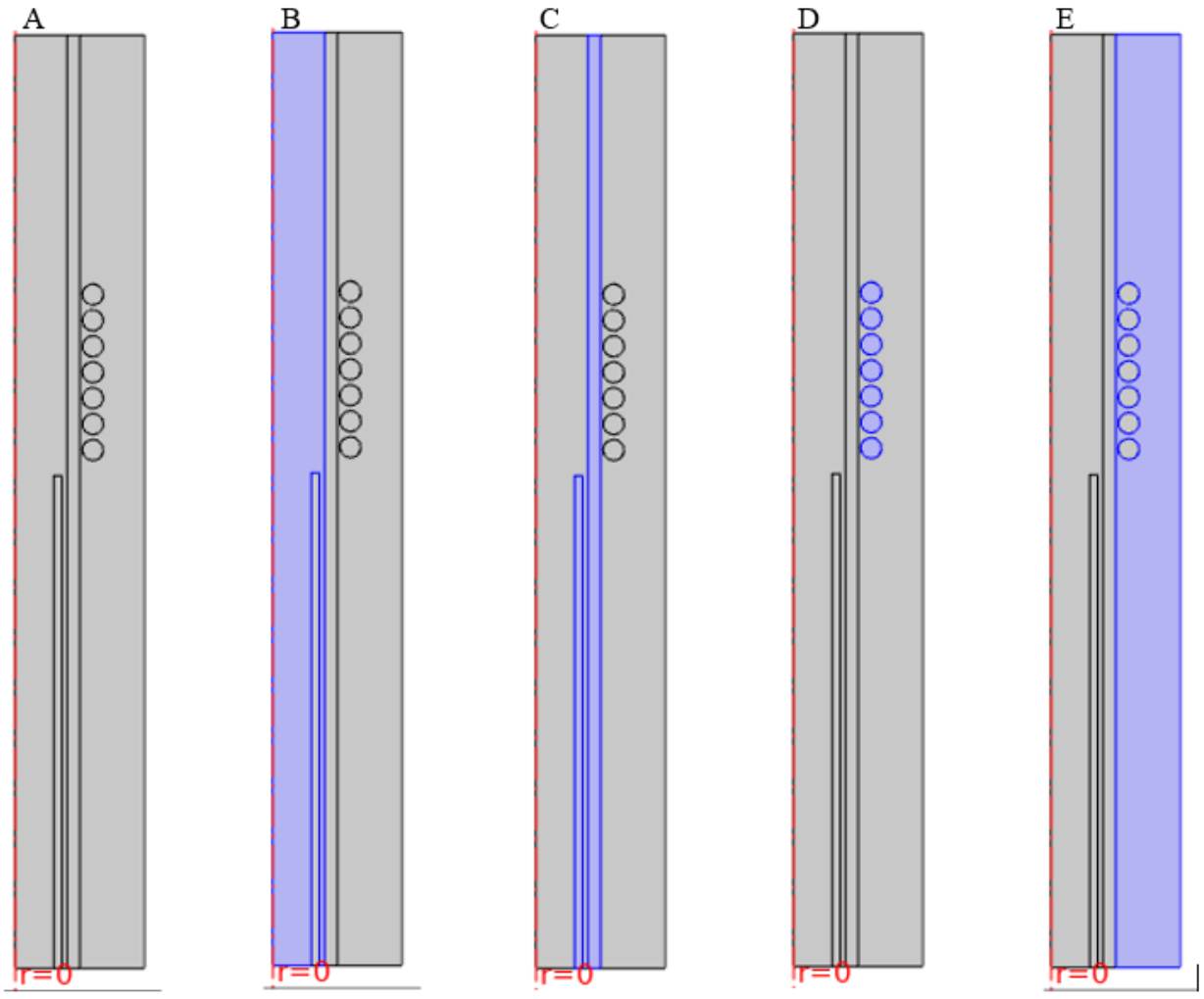

Figure 5.2 Domains in COMSOL for modeling ICPT. B shows plasma domain, C shows central and sheath quartz tube domains, D shows coil domains and E shows ambient air domain.

The material chosen are argon for the plasma domain, quartz for the quartz domains, copper for the coil domains and air for the ambient air domain. The physical and chemical properties and values of the materials are shown in the tables below. The values of the materials from the table can be obtained from the COMSOL library or be adjusted based on literature reviews or NIST data. The values used in the domain materials to compute the simulation are listed in the tables 5.2 – 5.5.

Table 5.2 Physical properties and values of Argon [64], [65]

Property	variable	value	unit	Property group
Density	rho	rho(T)	kg/m³	Basic
Heat capacity at constant pressure	Cp	cp(T)	J/(kg·K)	Basic
Thermal conductivity	k_iso; kii = k_iso, kij = 0	k(T)	W/(m·K)	Basic
Relative permeability	mur_iso; murii = mur_iso, murij = 0	1	1	Basic
Relative permittivity	epsilonr_iso; epsilonrii = epsilonr_iso, epsilonrij = 0	1	1	Basic
Dynamic viscosity	mu	mu(T)	Pa·s	Basic
Electrical conductivity	sigma_iso; sigmaii = sigma_iso, sigmaij = 0	if(sigma(T)<sigma_min, sigma_min, sigma(T))	S/m	Basic
Ratio of specific heats	gamma	1.66	1	Basic
Total volumetric emission coefficient	Qrad	Qrad(T)	W/m³	Radiation heat transfer
Local property sigma_min	sigma_min	1[S/m]	S/m	Local properties
Density	rho	rho(T)	kg/m³	Basic
Heat capacity at constant pressure	Cp	cp(T)	J/(kg·K)	Basic
Thermal conductivity	k_iso; kii = k_iso, kij = 0	k(T)	W/(m·K)	Basic
Relative permeability	mur_iso; murii = mur_iso, murij = 0	1	1	Basic
Relative permittivity	epsilonr_iso; epsilonrii = epsilonr_iso, epsilonrij = 0	1	1	Basic
Dynamic viscosity	mu	mu(T)	Pa·s	Basic

Electrical conductivity	sigma_iso; sigmaii = sigma_iso, sigmaij = 0	if(sigma(T)<sigma_min, sigma_min, sigma(T))	S/m	Basic
Ratio of specific heats	gamma	1.66	1	Basic
Total volumetric emission coefficient	Qrad	Qrad(T)	W/m³	Radiation heat transfer
Local property sigma_min	sigma_min	1[S/m]	S/m	Local properties

Table 5.3 Physical properties and values of Quartz [64], [65]

Property	variable	value	unit	Property group
Relative permeability	mur_iso; murii = mur_iso, murij = 0	1	1	Basic
Electrical conductivity	sigma_iso; sigmaii = sigma_iso, sigmaij = 0	1e-12[S/m]	S/m	Basic
Heat capacity at constant pressure	Cp	820[J/(kg*K)]	J/(kg·K)	Basic
Relative permittivity	epsilonr_iso; epsilonrii = epsilonr_iso, epsilonrij = 0	4.2	1	Basic
Density	rho	2600[kg/m^3]	kg/m³	Basic
Thermal conductivity	k_iso; kii = k_iso, kij = 0	3[W/(m*K)]	W/(m·K)	Basic
Surface emissivity	epsilon_rad	0.7	1	Basic
Relative permeability	mur_iso; murii = mur_iso, murij = 0	1	1	Basic

Table 5.4 Physical properties and values of Copper [64], [65]

Property	variable	value	unit	Property group
Relative permeability	mur_iso; murii = mur_iso, murij = 0	1	1	Basic
Electrical conductivity	sigma_iso; sigmaii = sigma_iso, sigmaij = 0	5.998e7[S/m]	S/m	Basic

Relative permittivity	epsilonr_iso; epsilonrii = epsilonr_iso, epsilonrij = 0	1	1	Basic
Heat capacity at constant pressure	Cp	385[J/(kg*K)]	J/(kg·K)	Basic
Surface emissivity	epsilon_rad	0.5	1	Basic
Density	rho	8940[kg/m^3]	kg/m³	Basic
Thermal conductivity	k_iso; kii = k_iso, kij = 0	400[W/(m*K)]	W/(m·K)	Basic
Young's modulus	E	126e9[Pa]	Pa	Young's modulus and Poisson's ratio
Poisson's ratio	nu	0.34	1	Young's modulus and Poisson's ratio
Reference resistivity	rho0	1.667e-8[ohm*m]	Ω·m	Linearized resistivity
Resistivity temperature coefficient	alpha	3.862e-3[1/K]	1/K	Linearized resistivity
Relative permeability	mur_iso; murii = mur_iso, murij = 0	1	1	Basic
Electrical conductivity	sigma_iso; sigmaii = sigma_iso, sigmaij = 0	5.998e7[S/m]	S/m	Basic
Relative permittivity	epsilonr_iso; epsilonrii = epsilonr_iso, epsilonrij = 0	1	1	Basic
Heat capacity at constant pressure	Cp	385[J/(kg*K)]	J/(kg·K)	Basic

Table 5.5 Physical properties and values of Air [64], [65]

Property	variable	value	unit	Property group
Relative permeability	mur_iso; murii = mur_iso, murij = 0	1	1	Basic
Relative permittivity	epsilonr_iso; epsilonrii = epsilonr_iso, epsilonrij = 0	1	1	Basic
Electrical conductivity	sigma_iso; sigmaii = sigma_iso, sigmaij = 0	if(sigma(T)<sigma_min, sigma_min, sigma(T))	S/m	Basic
Density	rho	rho(T)	kg/m³	Basic

Heat capacity at constant pressure	Cp	cp(T)	J/(kg·K)	Basic
Thermal conductivity	k_iso; kii = k_iso, kij = 0	k(T)	W/(m·K)	Basic
Dynamic viscosity	mu	mu(T)	Pa·s	Basic
Ratio of specific heats	gamma	1.40	1	Basic
Local property sigma_min	sigma_min	1[S/m]	S/m	Local properties
Total volumetric emission coefficient	Qrad	Qrad(T)	W/m³	Radiation heat transfer

5.3 Mathematical and Physical Model

In inductively equilibrium discharge from plasma module in COMSOL, three physics are applied. These are physics of electromagnetic field (EMF), heat transfer in fluid and laminar flow. Energy, momentum and continuity equation will be discussed with brief description.

EMF

The high frequency RF currents from the coil drive a high magnetic field gradient as discussed in chapter 2 and 3. This phenomenon is responsible for the elevated temperature in atmospheric RF ICPTs. The electromagnetic phenomena in plasma can be solved according to Maxwell's equation and Ampere's law as follows:

$$\vec{\nabla} \cdot \vec{\boldsymbol{E}} = \frac{\rho}{\boldsymbol{\varepsilon_0}} \tag{6}$$

$$\vec{\nabla} \cdot \vec{\boldsymbol{B}} = 0 \tag{7}$$

$$\vec{\nabla} \times \vec{\boldsymbol{E}} = -\frac{\partial \vec{\boldsymbol{B}}}{\partial t} \tag{8}$$

$$\vec{\nabla} \times \vec{\boldsymbol{B}} = \mu_0 \varepsilon_0 \frac{\partial \vec{\boldsymbol{E}}}{\partial t} + \mu_0 \vec{\boldsymbol{J}} \cong \mu_0 \vec{\boldsymbol{J}} \tag{9}$$

$$\vec{\boldsymbol{J}} = \sigma \vec{\boldsymbol{E}} \tag{10}$$

$\vec{\boldsymbol{E}}, \vec{\boldsymbol{B}}$ and $\vec{\boldsymbol{J}}$ are time varying electric field, magnetic field and current density respectively, ρ is the electric charge density and μ_0, ε_0 are permeability and permittivity of free space. Faraday's equation (8) can be simplified as $E \sim Bl/t$, l being the plasma diameter (characteristic length and t is time. Considering fluid velocity (plasma jet velocity) $v = l/t$ and speed of light in vacuum, for 13.56 MHz and $l \approx 0.01\ m$ contribution from the current is:

$$\frac{\mu_0 \varepsilon_0 \frac{\partial \vec{\boldsymbol{E}}}{\partial t}}{\vec{\nabla} \times \vec{\boldsymbol{B}}} \sim \frac{E/t}{c^2 B/l} \sim \left(\frac{v}{c}\right)^2 \sim 10^{-7} \tag{11}$$

This implies, in conducting plasma, the electric field, at any moment in time, does not have enough strength to cause high charge distribution velocity in comparison with c. That is the reason why equation (9) is simplified as such [36].

EMF contribution to the energy equation is given by excitation power $\boldsymbol{P}$ to the coil and joule heating.

$$\boldsymbol{P} = \frac{1}{2}\sigma \vec{\boldsymbol{E}} \tag{12}$$

Heat transfer in fluid and laminar flow are solved through continuity, momentum and energy equation as follows:

Continuity

$$\frac{\partial(\rho u)}{\partial z} + \frac{1}{r}\frac{\partial(\rho r v)}{\partial r} = 0 \tag{13}$$

Momentum

$$\rho u \frac{\partial u}{\partial z} + \rho v \frac{\partial u}{\partial r} = -\frac{\partial p}{\partial z} + 2\frac{\partial}{\partial z}\left(\mu \frac{\partial u}{\partial z}\right) + \frac{1}{r}\frac{\partial}{\partial r}\left[\left(\mu r \frac{\partial u}{\partial r} + \frac{\partial v}{\partial z}\right)\right] + F_z \tag{14}$$

Energy

$$\rho u\frac{\partial h}{\partial z}+\rho v\frac{\partial h}{\partial r}=\frac{\partial}{\partial z}\left(\frac{\lambda}{C_p}\frac{\partial h}{\partial z}\right)+\frac{1}{r}\frac{\partial}{\partial z}\left[r\left(\frac{\lambda}{C_p}\frac{\partial u}{\partial r}\right)\right]+P-R \tag{15}$$

Heat transfer equation

$$\rho C_p\frac{\partial T}{\partial t}+\rho C_p u\nabla T=\nabla(k\nabla T)+\boldsymbol{P}-Q_c \tag{16}$$

Where:

r, z	Two axes, radial and axial
u, v	Velocity components in radial and axial direction respectively
ρ	density
λ	Thermal Conductivity
μ	Viscosity
C_p	Specific heat at constant pressure
h	enthalpy
p	Pressure
P	Heating power
R	Heat loss due to radiation
T	Temperature
Q_c	Collision heating

In this model, excitation to a seven turns Copper coil is provided at a frequency of 13.56 MHz Joule heating is then used to ionize the gas flowing in the sheath tube (plasma confinement tube). A frequency-transient study with coil featuring a fixed power set at 1000 W (1 kW) is used.

5.4 Results and Discussion

Modeling and simulation results for the ICPT design and ICPT inside a reactor chamber will be discussed in this section. The characteristic of the ICPT can be found in figure and table 5.1, as a reminder, the operating condition can be briefly summarized as the following:

- 95 and 180 mm central and sheath gas tube with 15 mm i.d., 18 mm o.d. and 20 i.d., 25 o.d. respectively.
- 7 turn, 4 mm o.d. copper coil with excitation power and frequency of 1000 W and 13.56 MHz, respectively.
- Central and sheath argon gas flow rate of 4 and 15 slpm, respectively.

5.4.1 Case 1. ICPT Simulation

An ICPT simulation with characteristic and operation condition described in chapter 5.2 and 5.3 and briefly summarized in chapter 5.4 was simulated using COMSOL Multiphysics in transient state. As shown in figure 5.3, an instantaneous increase in heat source from joule heating can be observed. The increase in joule heating is around the coil region and drops exponentially to 0 away from the coil region. Although, the joule heating provides high and instantaneous power to the gas, it alone is not enough to start (ignite) the discharge in experimental setup. To overcome this, recall the assumption setting the conductivity of argon at 1 S/m at the start to reach the ignition of the plasma. The plasma temperature as seen in figure 5.4 rises from 0 – 0.5 s and drops slightly from 0.5 – 0.15 s. There is a sudden jump from 0.15 to 0.2 s before stabilizing at t=0.25 s. From t=0.25

– 0.5 s, the plasma is stabilized and the increment in plasma temperature is small, the stabilization of the plasma in time is shown in figure 5.5.

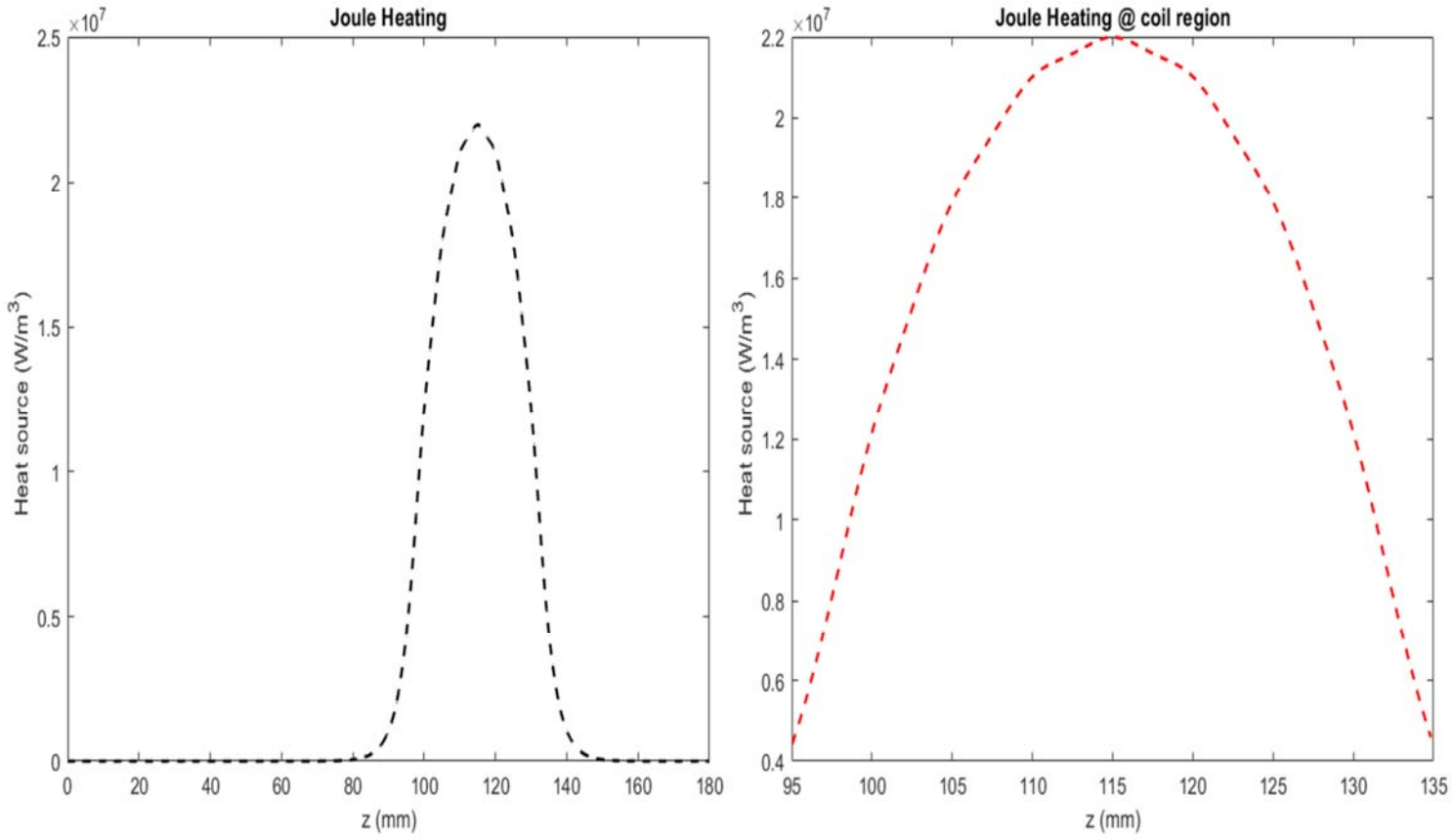

Figure 5.3 a. Joule heating vs z, axial length of the plasma torch. b) Joule heating vs z, coil region (i.e., 98 < z < 132 mm)

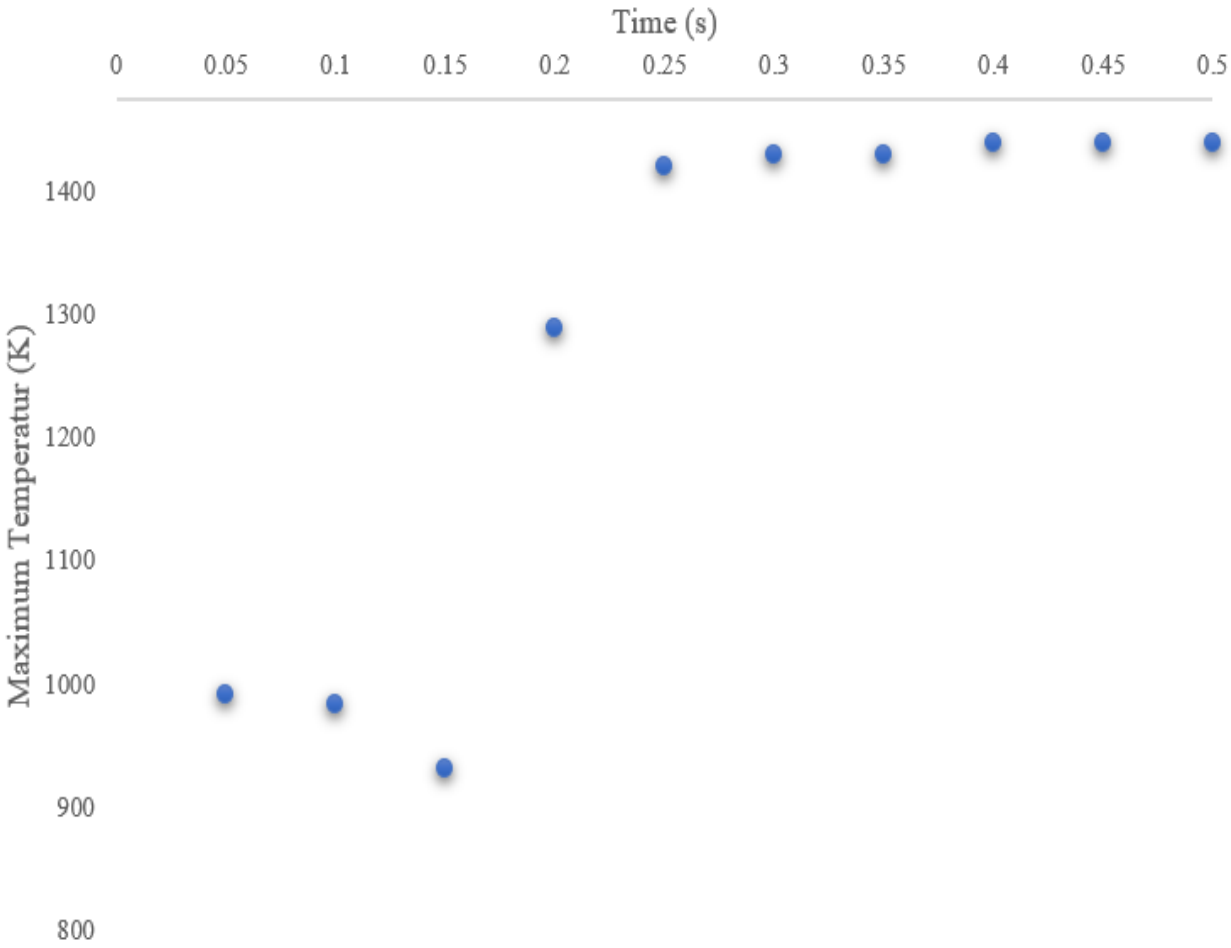

Figure 5.4 Maximum plasma jet temperature vs time.

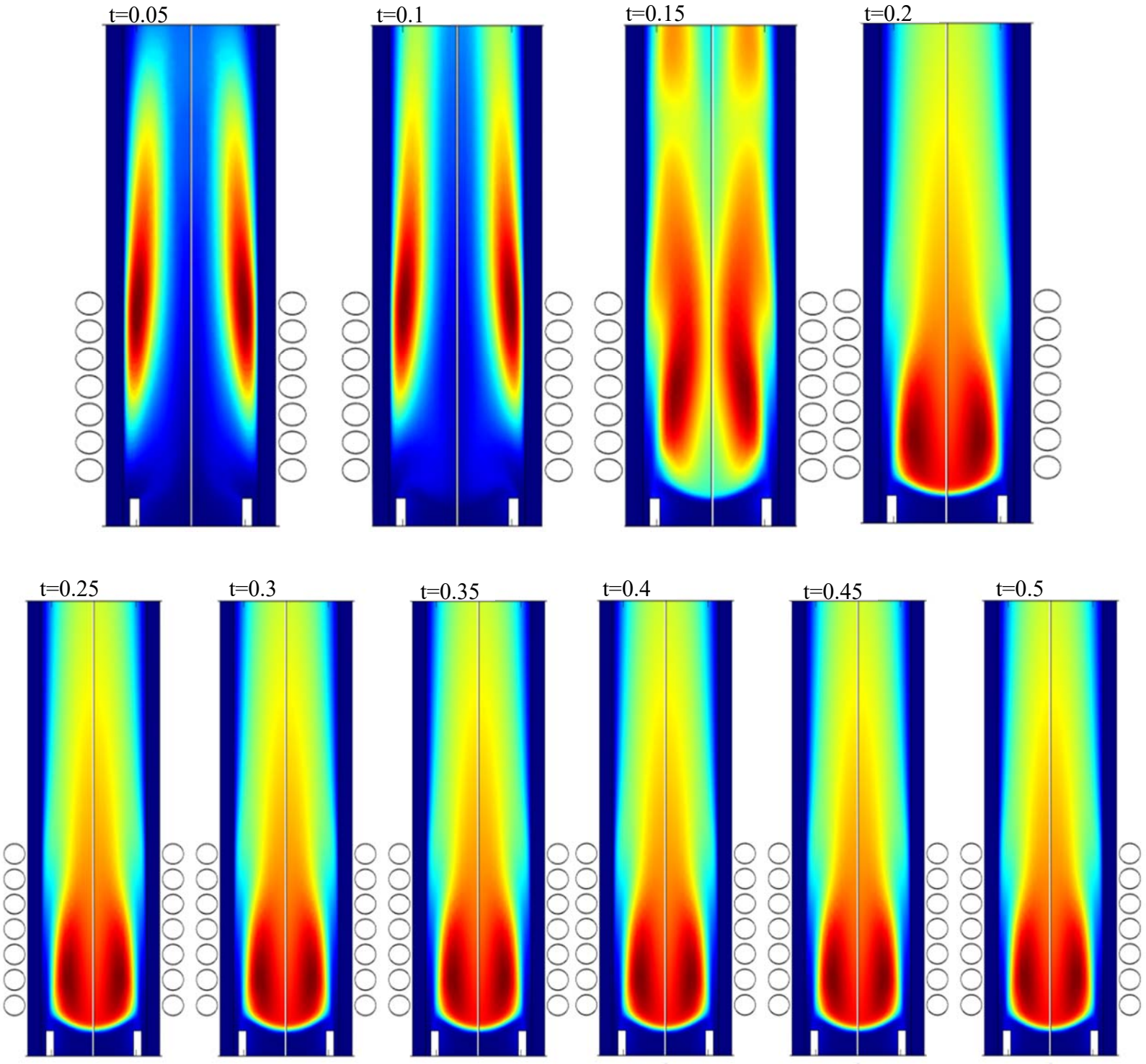

Figure 5.5 Ignition and stabilization of plasma jet in time

5.4.1.1 Plasma jet temperature and velocity profile

Temperature

The temperature profile of the plasma jet in the center line and the temperature profile contour in the axial direction is shown in figure 5.6. It can be noted that near the dielectric wall the plasma temperature is close to room temperature. For this reason, in this condition there is no need for additional cooling of the dielectric wall. It also means thermal loss due to conduction to the wall is low. On the other hand, thermal loss due to convection is high. Maximum plasma temperature

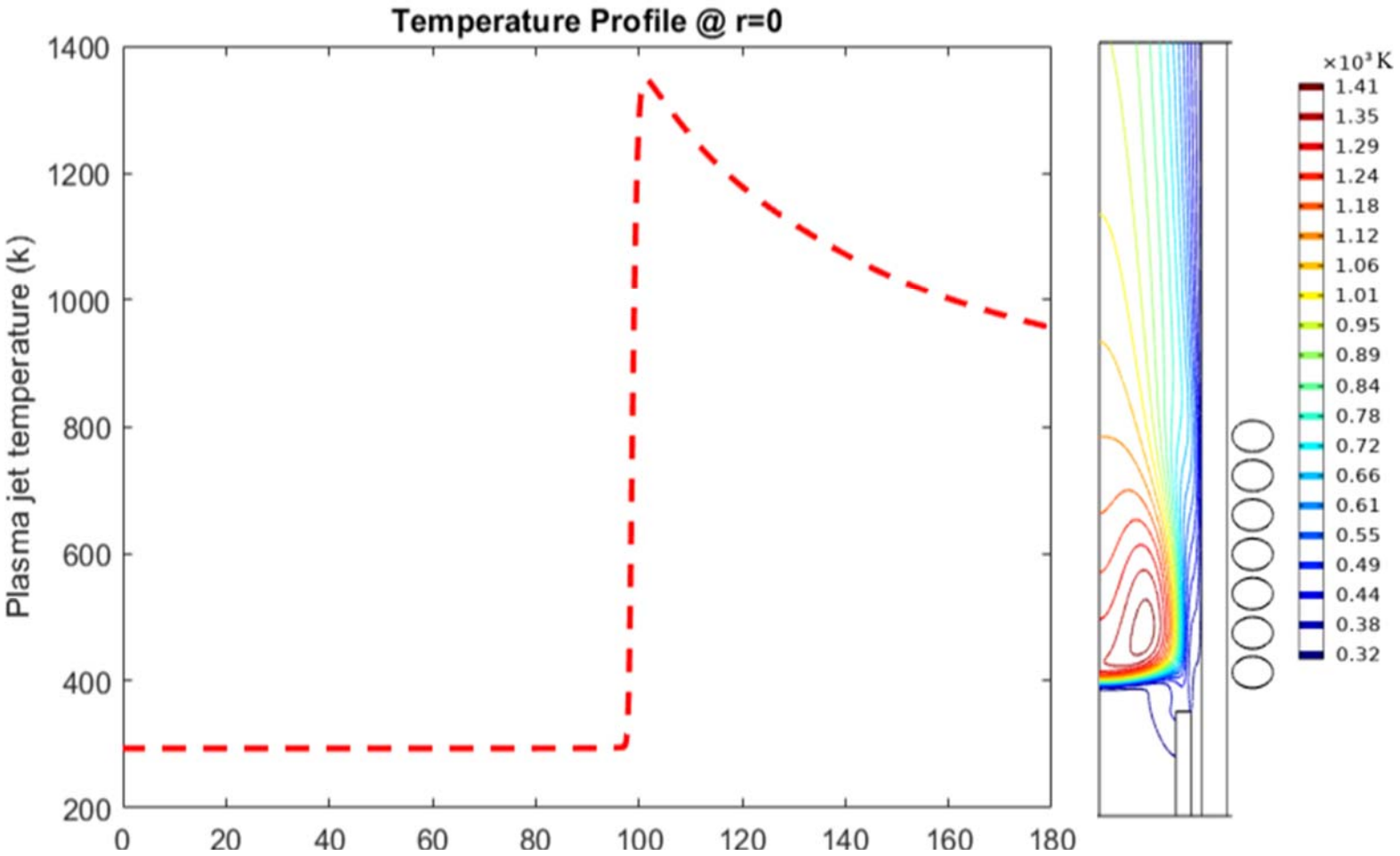

Figure 5.6 Temperature profile of plasma jet at center line r = 0 to the left, and temperature profile contour to the left

of 1407 K is found at r, z coordinate of (3.5, 107) mm, which is far enough from the wall not to cause damage to it through thermal shock.

From figure 5.6, the drop in radial temperature can also be observed. In figure 5.7, a radial temperature profile at the end of the torch nozzle i.e., z = 180 mm is shown. The graph in 5.7 shows a parabola like drop in plasma jet temperature moving away from centerline r = 0. A local maximum temperature of 955.88 K is reached at r = 0. It is important to note that maximum plasma jet temperature is found at r = 3.5 mm at z = 107 mm (same z as the top edge of the second coil), the local maximum at the nozzle exit (z = 180) is at the center line. This is consistent with other works done by researchers in the field. The absolute maximum temperature of plasma jet is not at the center line; it is around the skin depth.

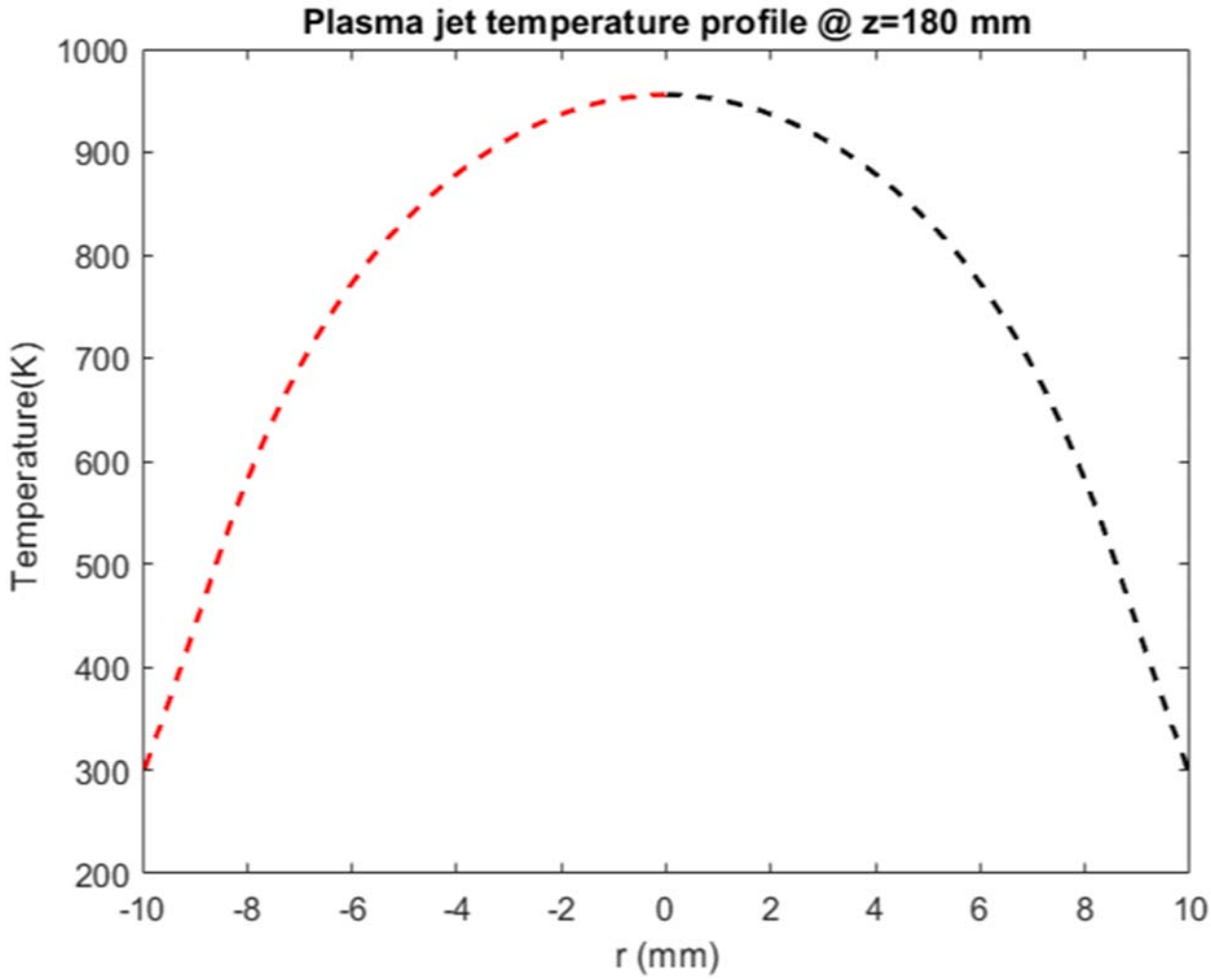

Figure 5.7 Radial temperature profile of plasma jet at the end of torch nozzle (i.e., z = 180)

Velocity

Figure 5.8 shows the plasma jet velocity profile magnitude and contour. It can be observed that the higher gas flow coming from the sheath line pushes the plasma jet axially. This push increases the plasma volume. Many researches on the impact of sheath flow line as reported from *S.B. Punjabi et al, J. Mostaghimi et al* and *M. Boulos et al* indicate that increasing the sheath gas flow rate while keeping the overall flow rate constant results [66]:

- Longer plasma jet in the z direction
- Cooling of the dielectric (quartz in this case) tube wall

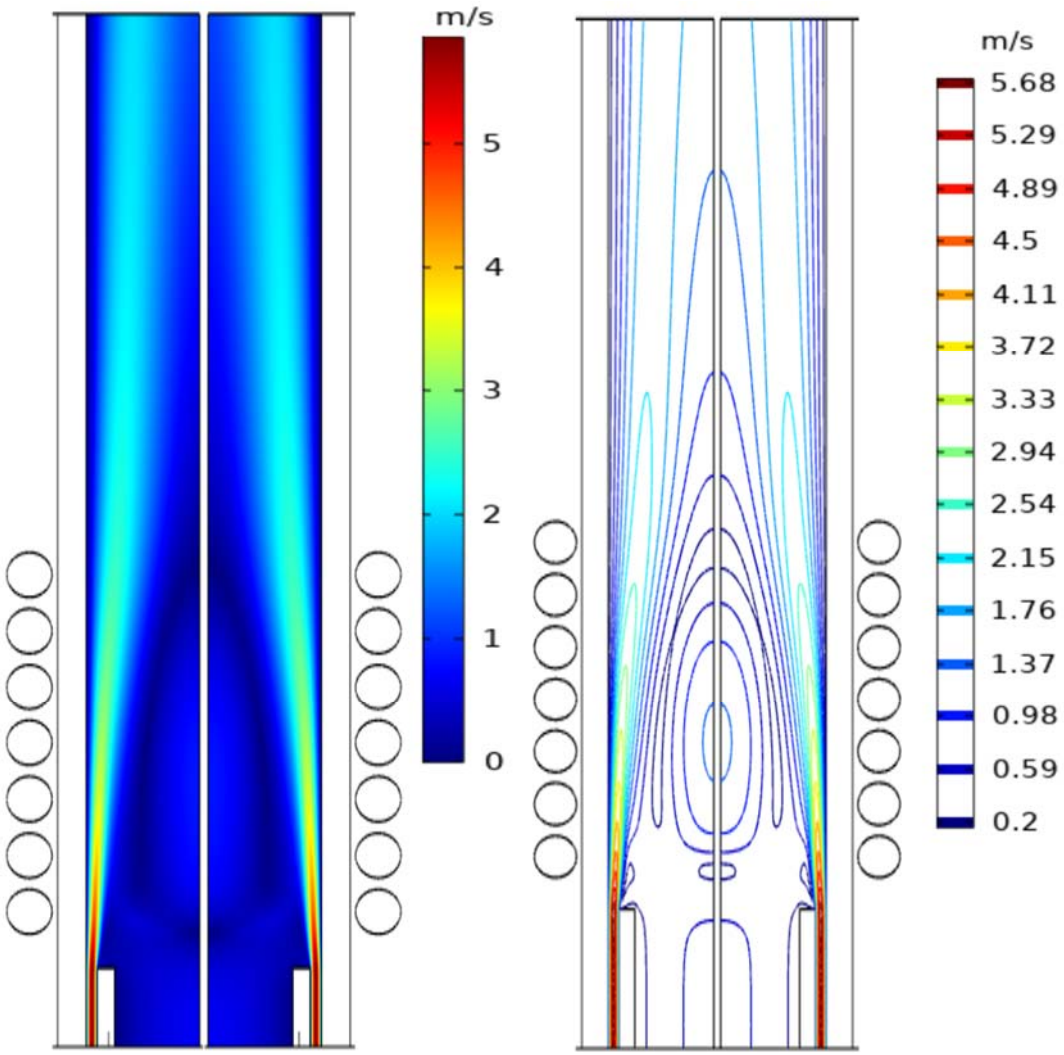

Figure 5.8 Plasma jet velocity profile. Magnitude to the left and contour to the right

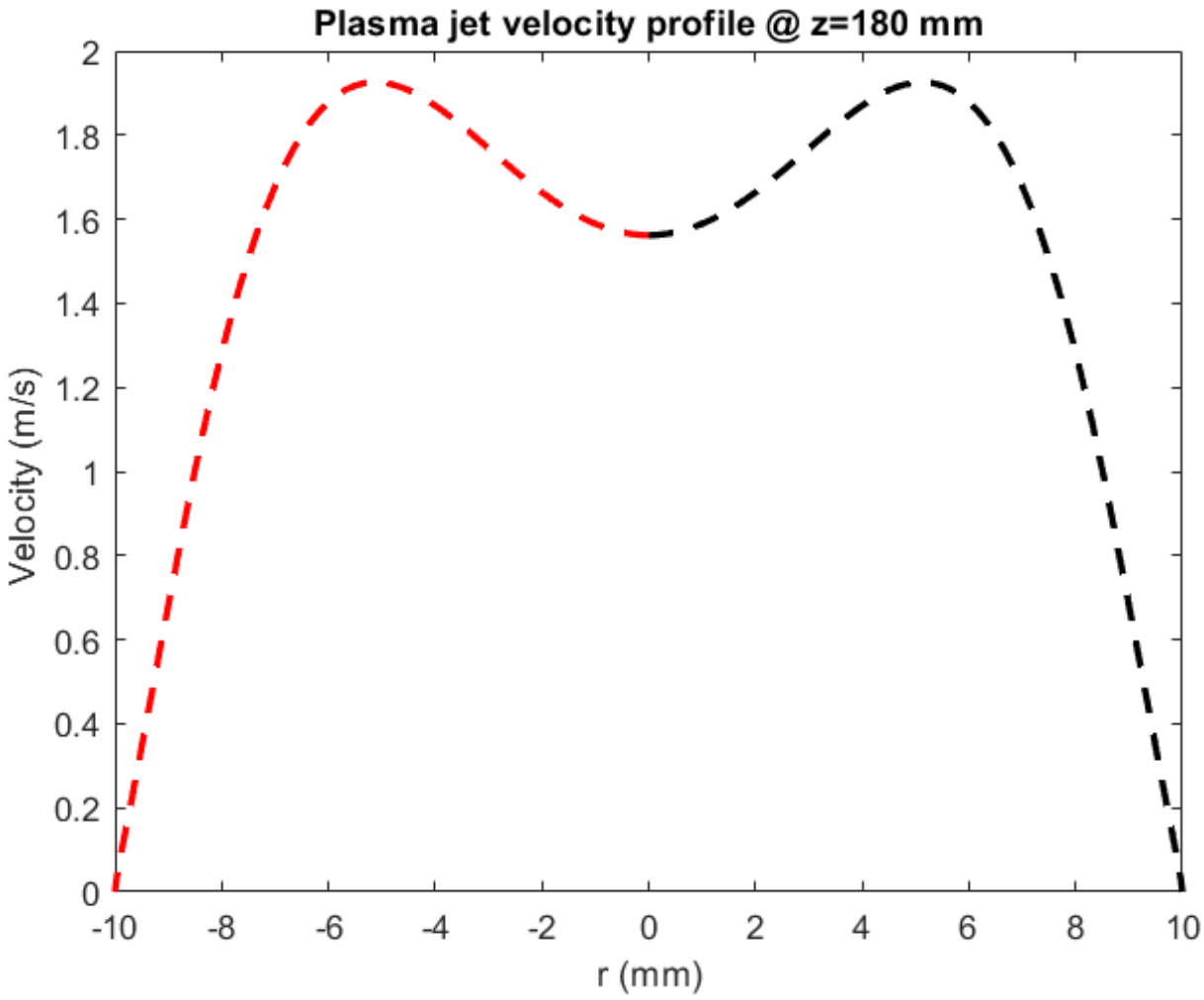

Figure 5.9 Plasma jet velocity vs arc length r, at exit of the torch (z=180)

5.4.2 Case 2. ICPT in chamber Simulation

In case 2, ICPT, with the same characteristics as in case 1 and operation condition as described from chapter 5.1 – 5.3, with the same parameter as in table 5.1 and domain and material as shown in figure 5.2, is simulated with its nozzle inside a chamber. The chamber has a length (height) of 10 cm (100 mm) and a radius of 5 cm (50 mm). Figure 5.8 shows the schematics of the ICPT in the chamber used in this simulation.

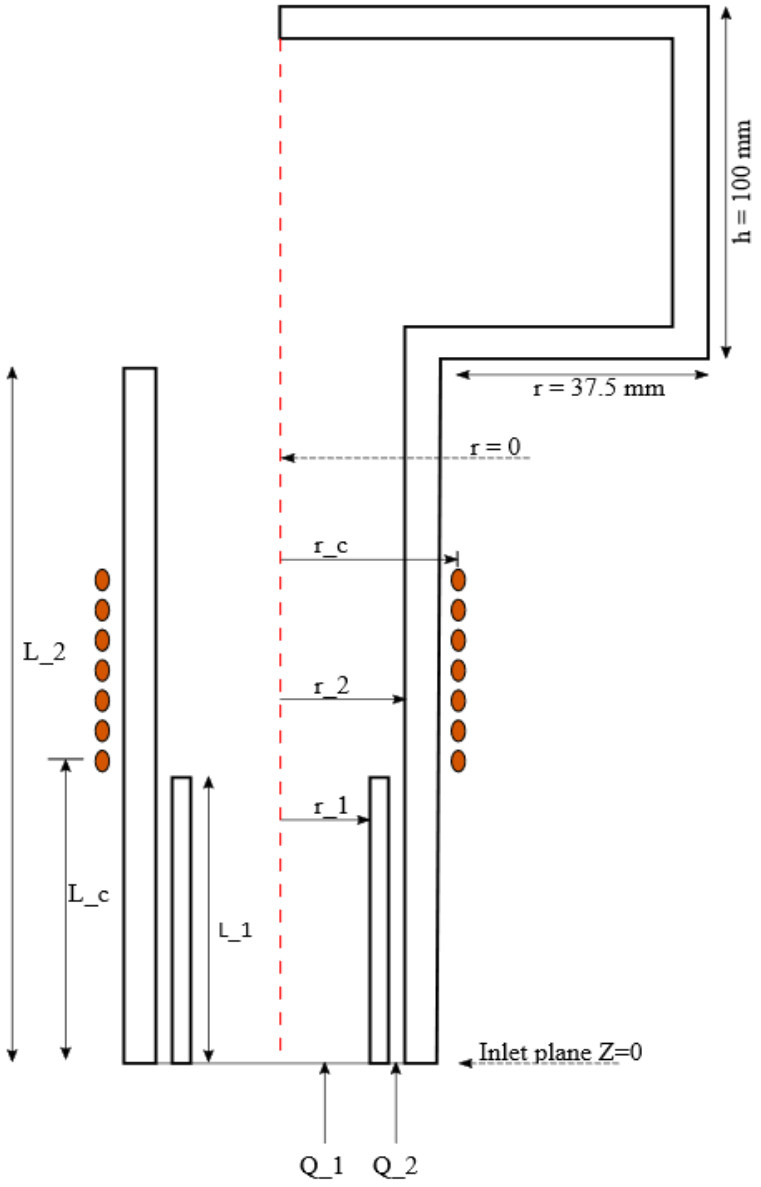

Figure 5.10 Schematics of ICPT and chamber used for the simulation.

5.4.2.1 Plasma jet temperature and velocity profile in ICPT and Chamber

Temperature

The temperature profile of the plasma jet inside the chamber is show in figure 5.11. The absolute maximum temperature of 1323 K is found at r, z coordinate (4.6, 104.3) mm. The z coordinate of the maximum temperature value corresponds to near the center line of the second coil. From the same figure, it can be observed that the plasma volume always shrinks radially as it propagates more in axial direction.

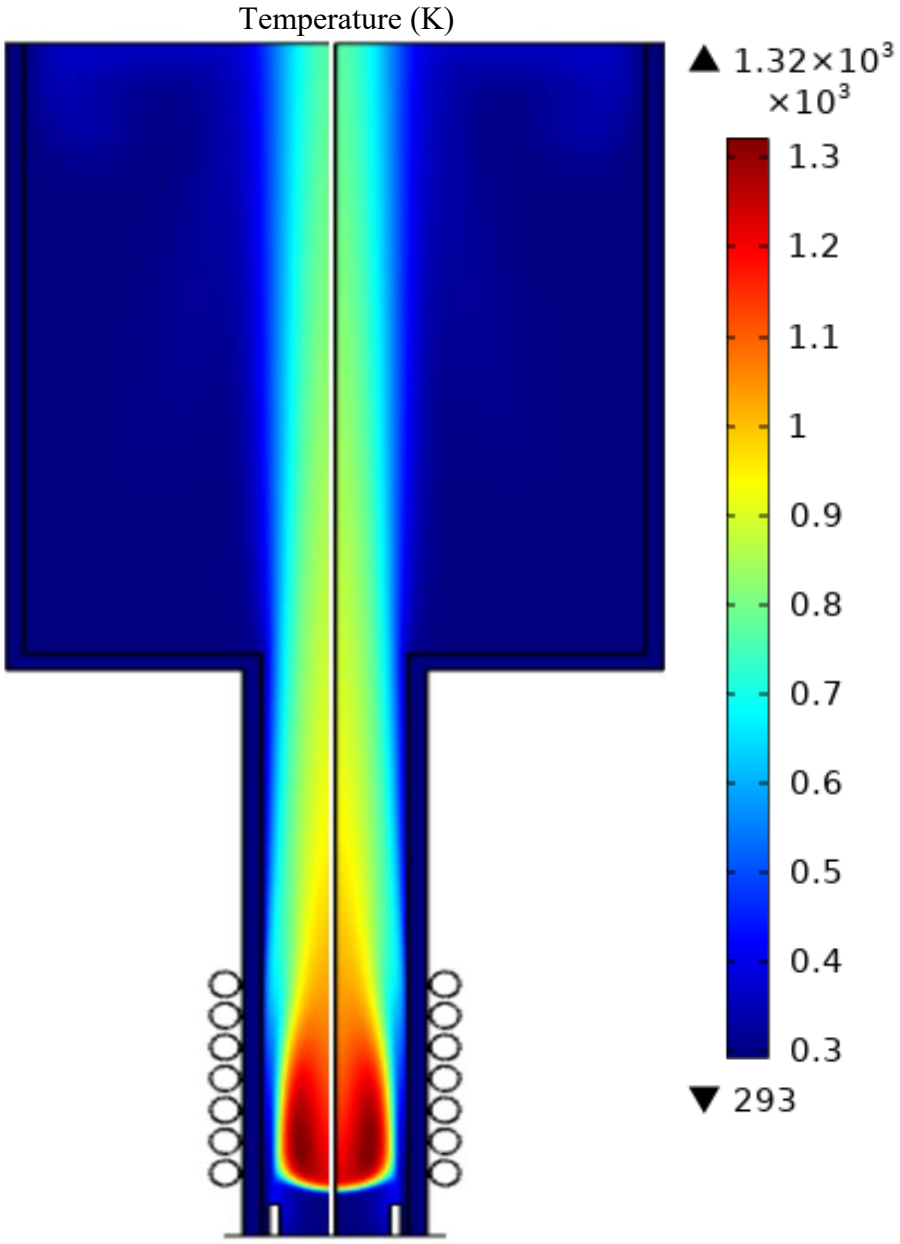

Figure 5.11 Temperature profile of ICPT in a chamber.

In the center line temperature profile as shown in figure 5.12, a local maximum temperature of 1240 K is reached at z = 99.6 m. This point is close to the center point of the first coil. As in figure 5.6, after reaching a peak, the temperature starts to drop along the axial direction. The local maximum temperature moves towards the center line r = 0, moving away from absolute maximum in the axial direction.

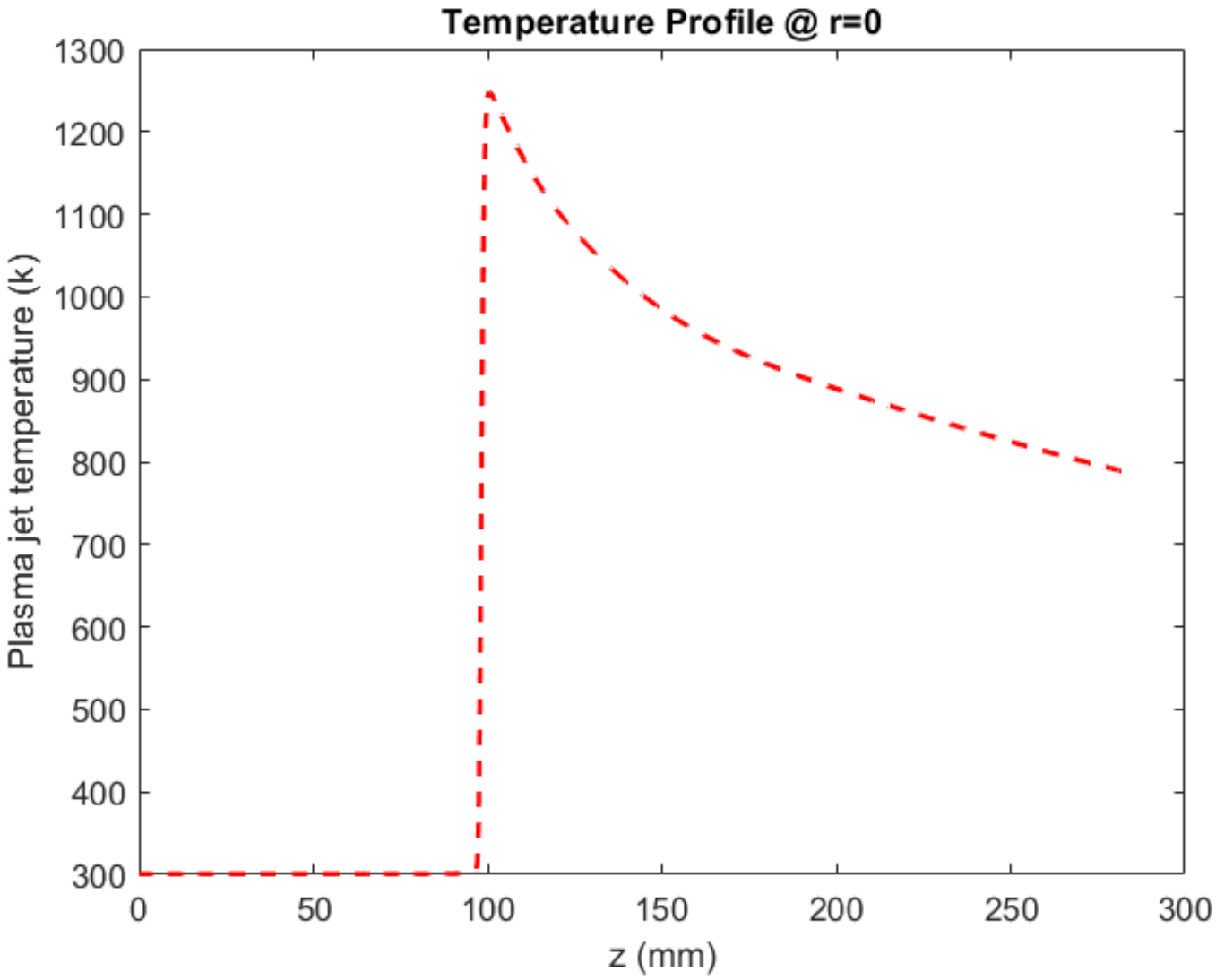

Figure 5.12 Temperature profile of plasma jet at center line r = 0 in a 100 mm long chamber

As shown in figure 5.11, the plasma jet is focused on a small surface cross-section. The part of the chamber that is exposed to high temperature plasma jet is in the vicinity of the center line – -9 < r < 9 mm. Figure 5.13 shows the plasma jet profile at the end of the chamber z = 280 mm, this length corresponds to 100 mm from the end of the plasma torch nozzle. A peak temperature of 771 K is reached at r = 0 at z = 280 mm. A drop-in temperature as we move farther from the center line in radial direction is observed as in figure 5.7.

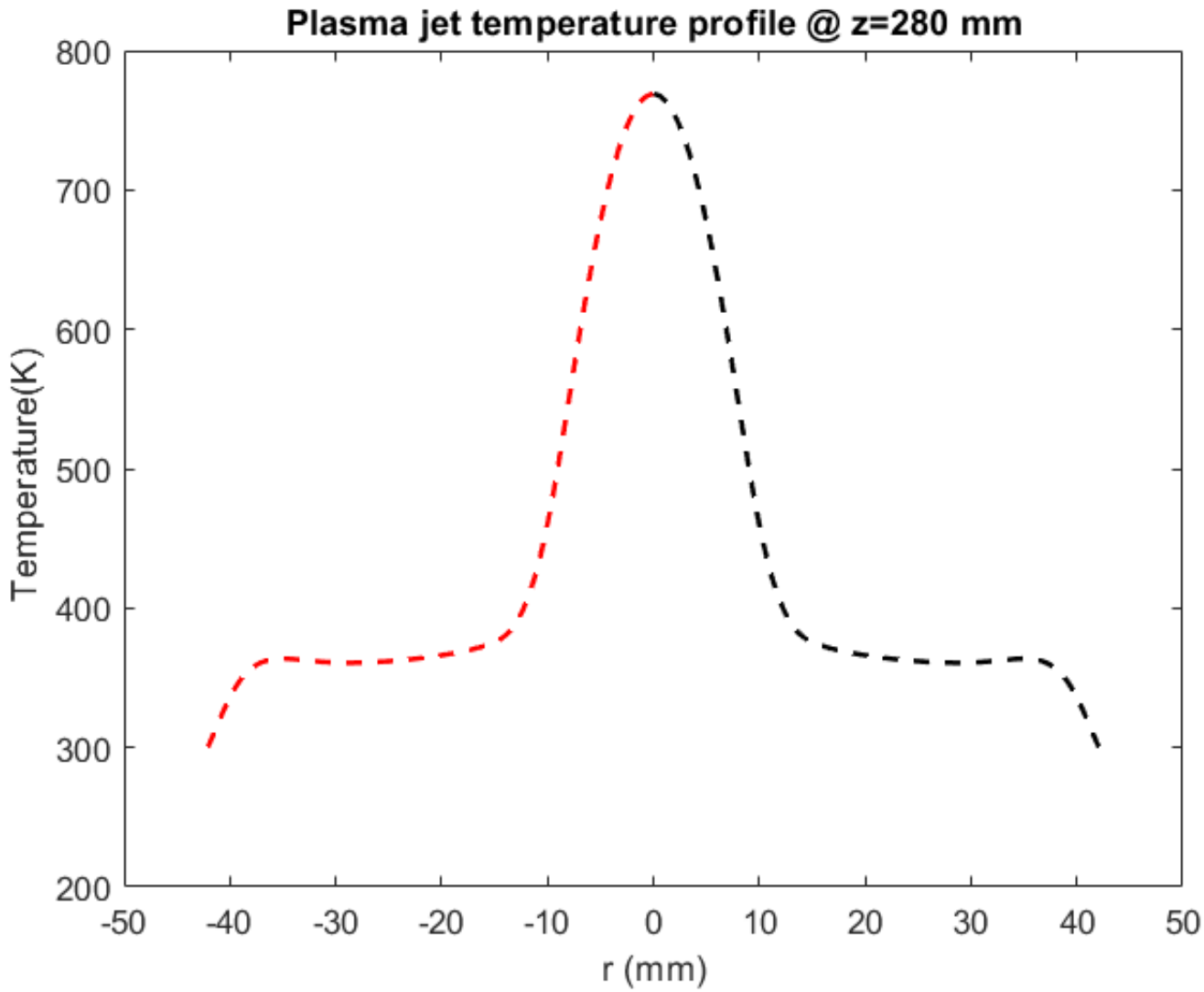

Figure 5.13 Radial temperature profile of plasma jet at the end of chamber (i.e., z = 280)

5.4.3 Case 1 vs 2. ICPT vs ICPT in chamber Simulation

A temperature profile comparison of the simulations of ICPT inside a chamber and without a chamber was computed. The result shows, despite similar parameters, there are some differences in magnitude and position of maximum temperatures. In case 1, the absolute maximum temperature of the plasma jet of 1407 K is found at r, z coordinate of (3.5, 107) mm, close to the top edge of the second coil. While in case 2, the absolute maximum temperature of the plasma jet of 1323 K is found at r, z coordinate (4.6, 104.3) mm, close to the center line of the second coil. T

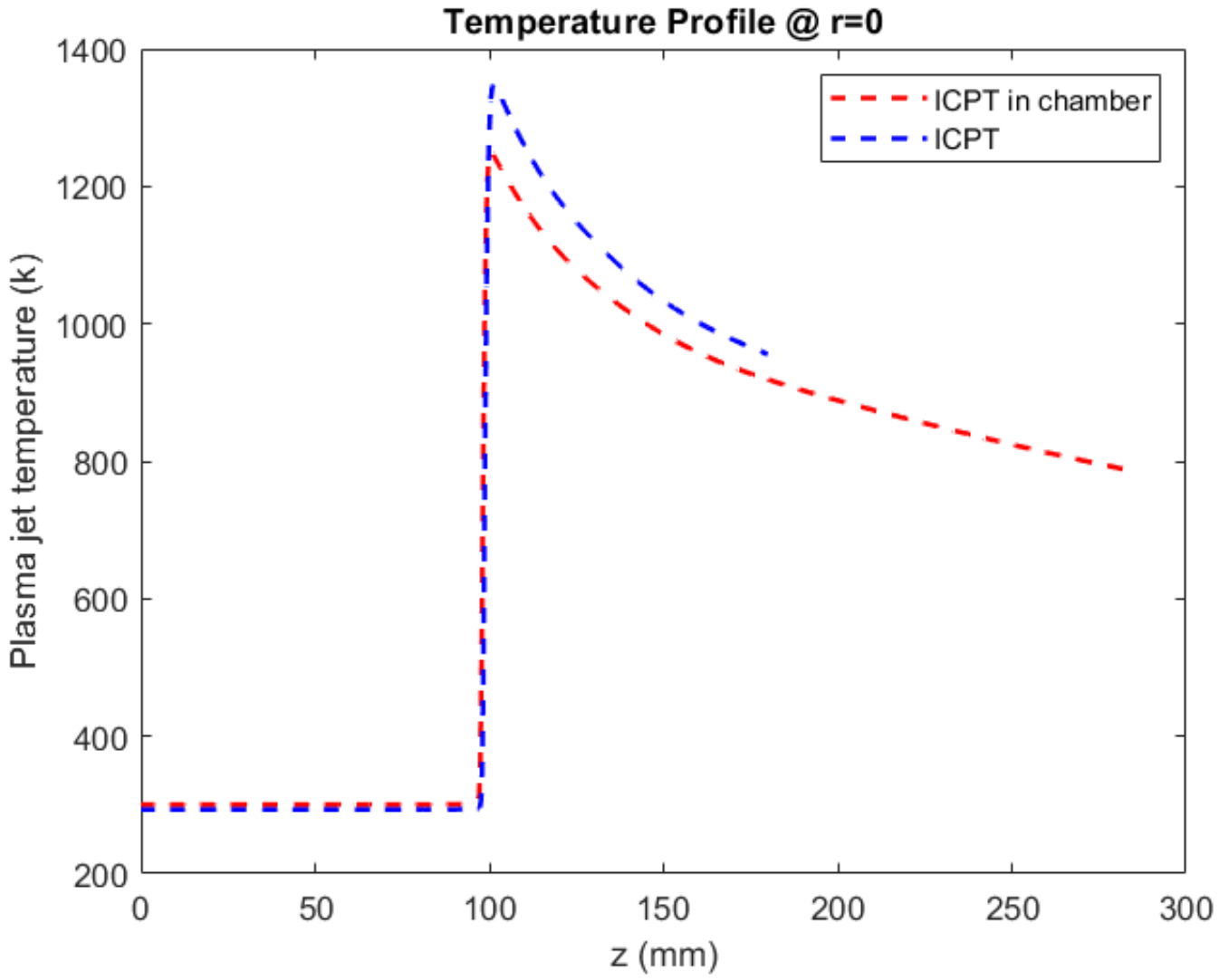

Figure 5.14 Comparison of center line plasma jet temperature profile with and without chamber of ICPT simulation

The difference in temperature is insignificant to have noticeable impact on the torch. It may be due to computational domain differences between case 1 and case 2. Figure 5.14 shows the plasma jet temperature profile in axial direction for both case 1 and case 2 at the center line. It can be observed that in case 2 (i.e., ICPT in chamber), the local maximum temperature is less than case 1 in magnitude. It also shows that the rise in temperature in case 2 comes a couple of mms earlier than that of case 1.

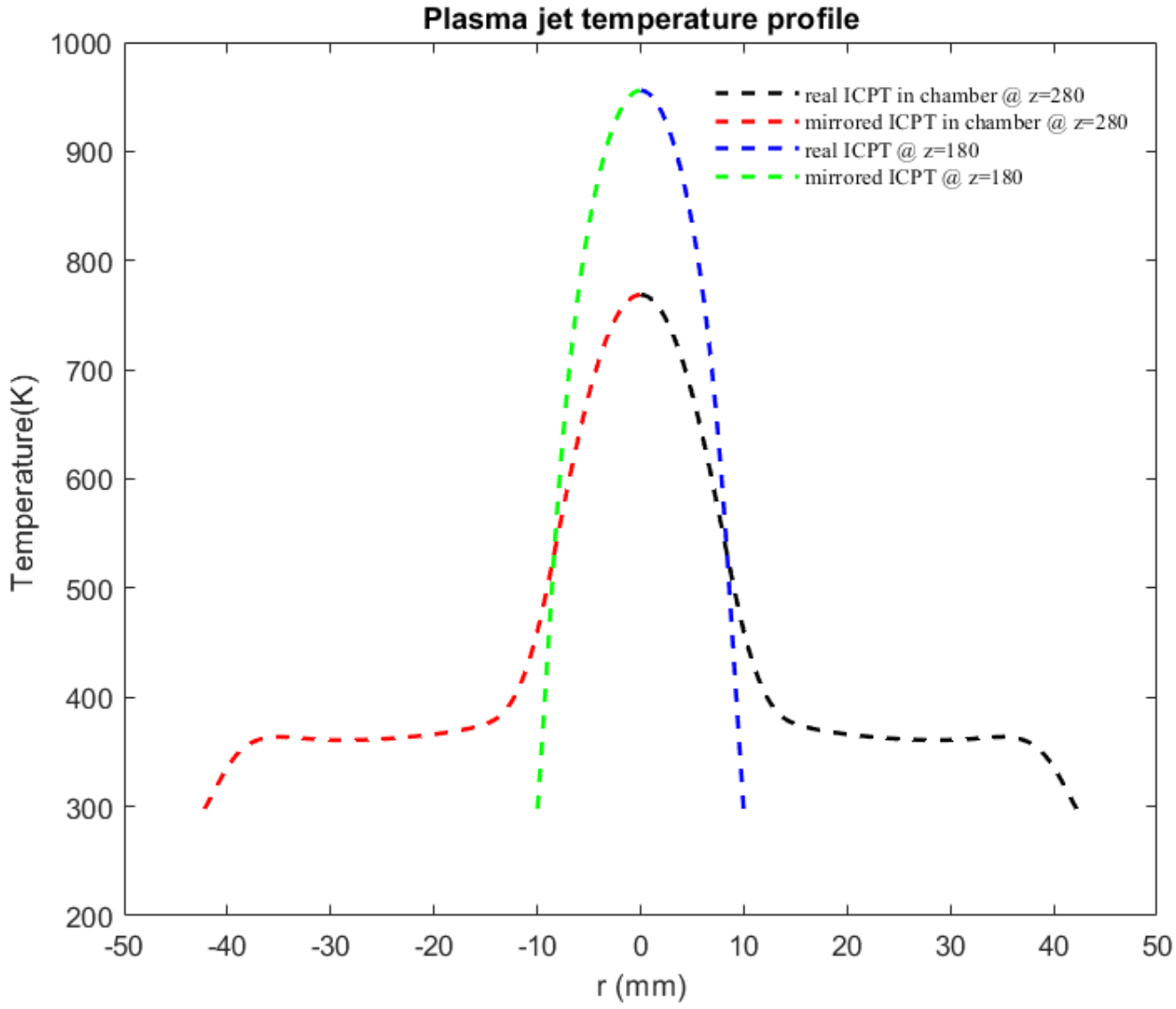

Figure 5.15 Radial plasma jet temperature profile of ICPT at z = 180 mm and ICPT inside a chamber at z = 280 mm

Figure 5.15 shows the ICPT (in blue and green) and ICPT in chamber (in black and red). The ICPT temperature profile is taken at z = 180 mm, while temperature profile in ICPT in chamber is taken at z = 280 mm. Temperature drop of about 150 – 200 K can be observed. This implies, the temperature drop from the exit of the torch to the bottom of the chamber is around 170 K.

Chapter 6: Preliminary Experiment of RF ICPT and Thermoplastic Behavior in High Temperature

In this chapter, a preliminary experiment of RF ICPT will be discussed. The experimental setup is shown in figure 6.1. Materials, procedures, safety and results of experiment will be presented.

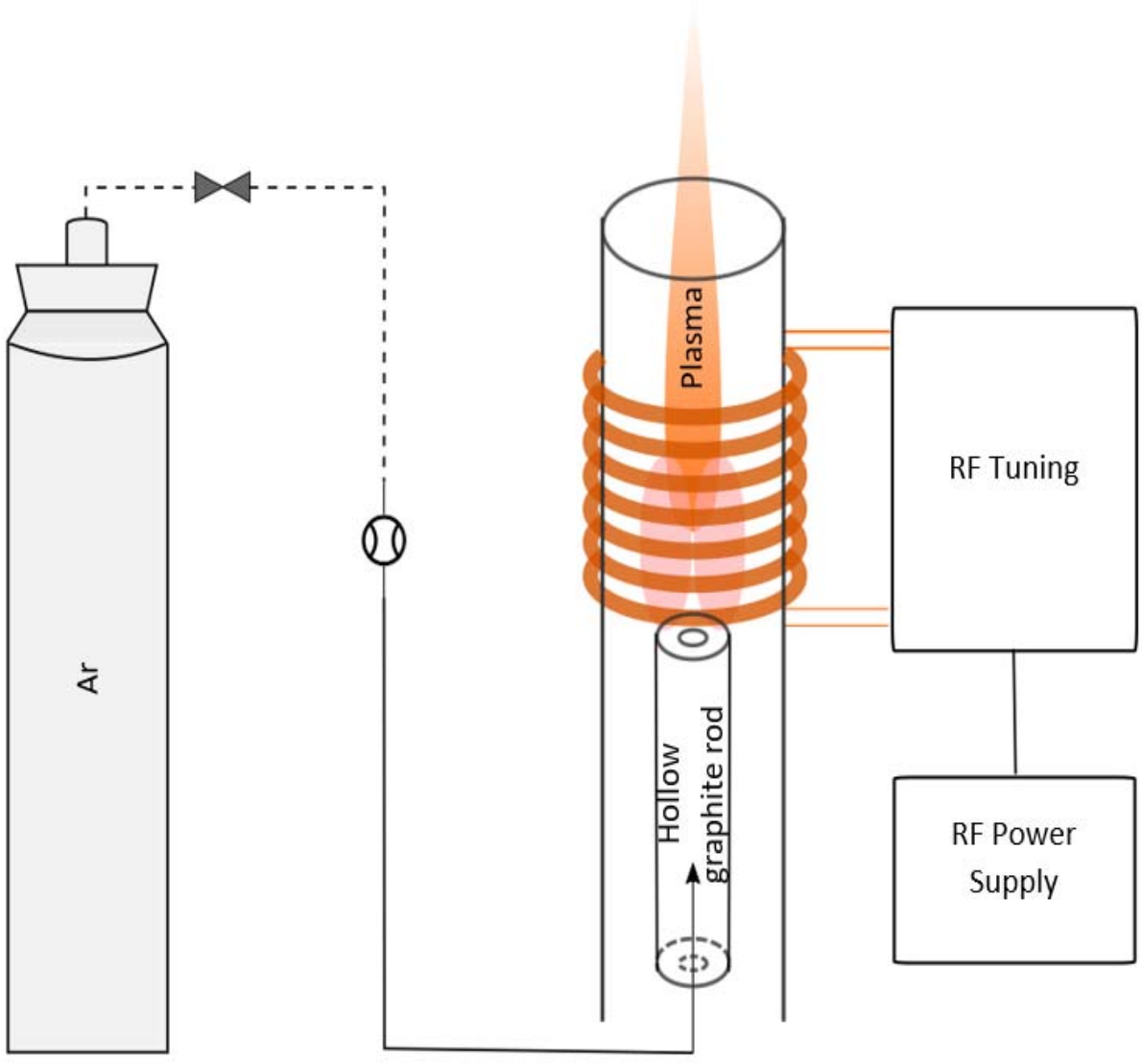

Figure 6.1 RF ICPT preliminary experimental setup

6.1 Materials

RF power supply

RF power supply is supplied by RF VII Inc, model # RF-10-XII, serial #: RF 1K-0228 1000 W at 13.56 MHz power generator. The RF generator is connected to an automatic matching (tuning) network.

RF Tuning/ Matching Network

The RF generator is connected to the matching network procured from Advanced Energy M/N 3155405-300 S/N 1370363 by a coaxial N-N 8 ft cable. This matching network has an impedance/ inductive reactance of 50 ohms.

Induction Coils

A refrigeration copper tubing of 4 mm and 3 mm outer and inner diameter respectively was procured. Based on the optimal value of the inductance, a certain length of the coil was cut to form N-turn (N = 7). As shown in figure (4.4), the induction coil is connected to the matching network, which in turn is connected to the RF power generator.

Gas Cylinder Tank

A stainless-steel gas cylinder tank with argon from Air Liquide.

The argon gas cylinder tank has a volume of 9.3 m^3, a pressure of 17820 KPa, with purity of argon gas > 99.999% O_2 < 2 part per million (ppm), H_2O < 3 ppm and THC < 0.5 ppm.

Flowmeter

Porter instrumental company model B-1187 and 1188

6.2 Safety Precautions

6.2.1 Hazards

Operation of ICPT, deals with high voltage and temperature. Thus, when operating the system, there are health hazards that needs to be listed. These hazards are:

- Electrical: ICP uses high power and high voltage sources; any improper or loose wire connection, pinched or pierced wire insulation may cause electric shock.

- Radiation: In ICPT, there are two types of radiation hazards: A) R.F radiation, which is the source of power for sustaining the torch. B) UV radiation, which is produced by the plasma jet at high temperature.

- Compressed Gas: One of the most important part of part of ICP is gas flow, this comes from a compressed gas tank. The hazard posed is due to airborne particles and dust.

- Hot surfaces: The torch components and interfaces such as coils, graphite rods and quartz tube remain at very elevated temperature even sometime after the plasma system is turned off.

6.2.2 Precautions

Prior to performing any operation that may cause risks to the safety and security of personnel and properties, there must be a risk assessment of the operation. One part of the risk assessment is taking precautions to prevent any undesired events from taking place – if they do take place to limit their consequences to the minimum as possible. Precaution for ICPT involves in three steps: A) preoperational safety checks, B) Operational safety check and C) Post-operational safety checks.

Prior to start any experiment with ICPT, some steps must be taken. These steps include:

- Personnel must be familiar with ICPT (i.e., proper training must be provided)
- Personnel must ensure proper connection of all electrical wires.
- All emergencies stop equipment must be readily available and accessible.
- Personnel must have all the necessary personal protective equipment (PPE) prior to start operating.
- Personnel must ensure no gas leakage from any of the pipes and gas tanks.

During operation of ICPT, the steps that need to be taken are:

- Fume-hood for fume extraction need to be turned on.
- Always there should be at least two personnel in the lab (never leave ICPT unattended)
- Mark all the hot and sharp materials

After the completion of the experiment:

- Turn off the fume-hood.
- Turn of the RF power source and matching/tuning network.
- Let all materials to cool before handling them.
- Detect and put aside any defective equipment.
- Ensure the workstation is safe and tidy.

6.2.3 Procedures

The steps to perform preliminary experimental run of plasma torch are as following:

1. Open the valve of the cylinder tank with argon gas. A gas flowing sound should be heard. Adjust the flow meter connected to the argon cylinder to the desired flow rate. Low flow rate to start the gas breakdown is recommended to then gradually increase the flow rate.

2. Plug the RF power supply, RF tuning.

3. Run cooling water to flow inside the induction coil.

4. Switched on RF power supply and increase the power level to the maximum turns 1000 W (1110 W when perfectly coupled).

6.3 Preliminary Experimental Results

The torch design in this thesis has taken as input the results from lab experimental trials conducted prior to the design work. In this chapter the experiments performed will be shown. Figure 6.2 and 6.3 shows the result of the preliminary experimental run of ICPT in atmospheric pressure at various flow rate. The experiment shown in figure 6.2 has a flow rate ranging from 15 – 20 SLPM in a single gas flow line. In figure 6.3, a lower gas flow rate was used, the flow was as low as 4 SLPM. As shown in figure 6.2, a stable plasma jet could be achieved when a graphite rod was inserted in the torch, however the maximum power of 1100 W could not be reached. The maximum power reached was 900 W and the power could not be increased any further. Due to relatively high flow rate, the plasma is stretched towards the z-direction and is not touching the wall. For this reason, the quartz wall was not damaged or over heated.

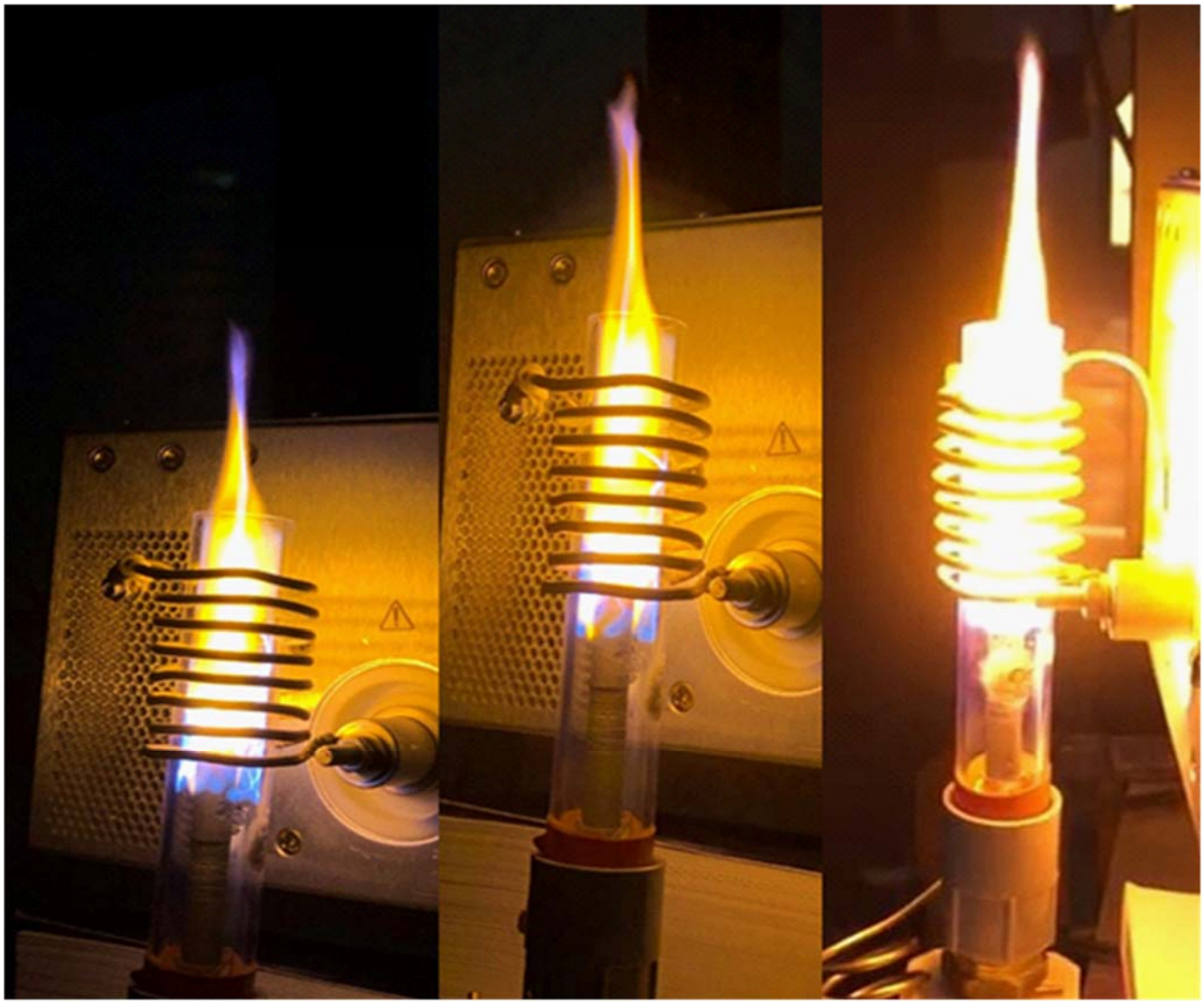

Figure 6.2 Preliminary experimental run of ICPT with graphite rod inside the torch

Figure 6.3 shows experimental result for low gas flow rate. At this gas flow rate, there is 0 reflected power, and maximum power of 1100 W was reached. The plasma is very dense, and the plasma jet does not go beyond the seventh turn copper coil. The heat from the plasma and the lack of cooling through high flow rate cause damage to the quartz tube. A temperature measurement of the plasma jet could not be performed, this is because the temperature of the jet is estimated to be beyond 5000 k at the core of the plasma and a spectrometer was not available to take the

measurement. There is no direct way of measuring such a high temperature plasma jet; a spectroscopic analysis is usually performed to estimate plasma temperature.

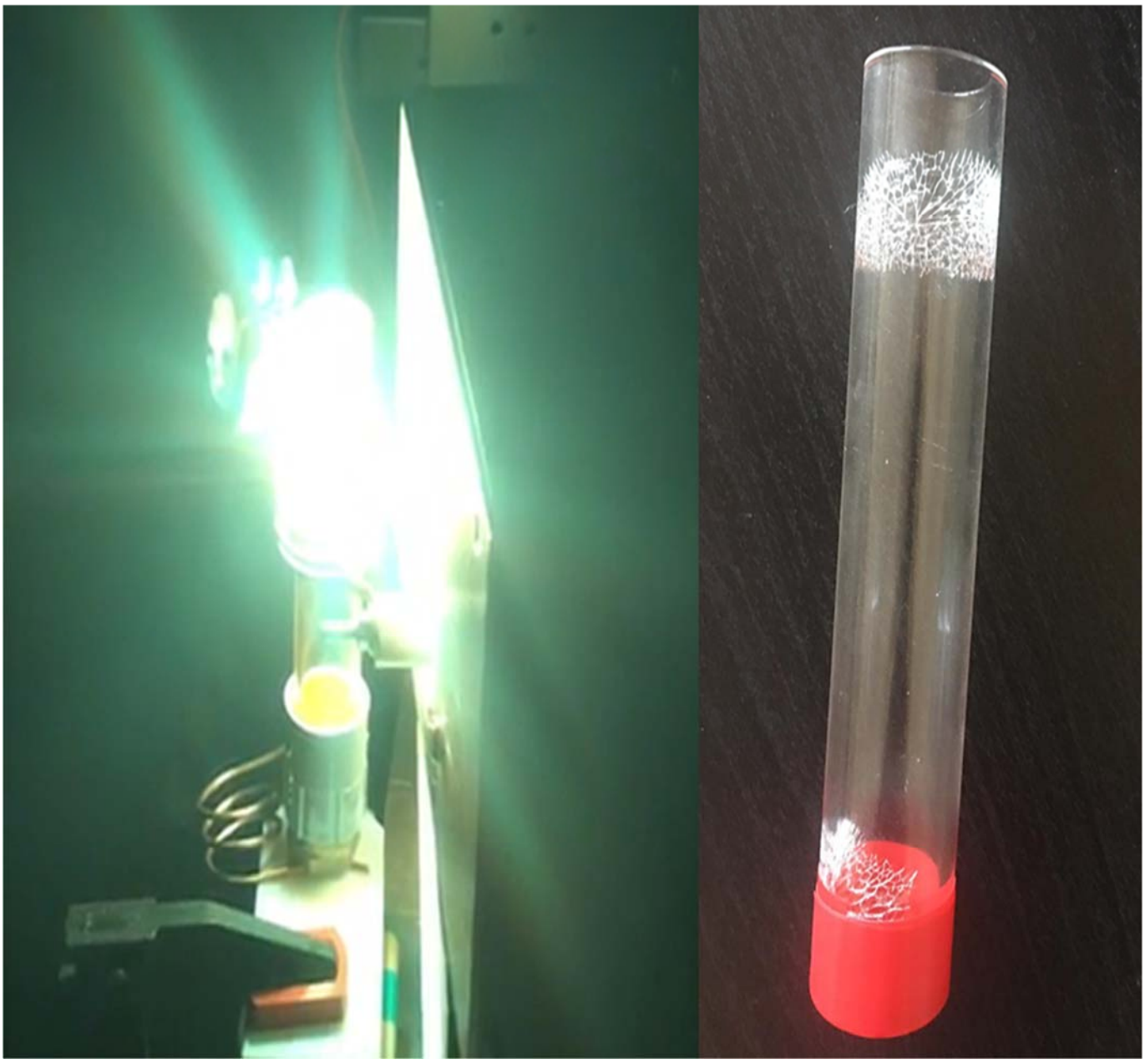

Figure 6.3 Experimental run of ICPT at low flow rate of 4 SLPM (left) and damaged quartz tube in the experiment (right)

Although temperature measurements were not taken for the experiments, the first experiment (figure 6.2) has similar plasma volume as in the simulation. In fact, the flow rate for this experiment and simulation are 19 slpm total.

As these experiments showed a high flow rate is necessary in order to push the plasma jet along the z-direction. For this reason, the ICPT is designed to have a high gas flow rate to cool the torch wall and carry the plasma jet axially.

Chapter 7: Conclusion Remarks

7.1 Conclusion

Objective 1 and 3. Design of a RF atmospheric pressure ICPT with key features and design of adaptor for reactor chamber, ICPT integration in the chamber

A detailed industrial 3D CAD of a RF ICPT, with novelty like RF/EMC shielding with water-cooling potential and 100% energy coupling between power supply and induction coil, was computed using SOLIDWORKS engineering software. A detailed engineering document describing dimensions and materials of each components were provided.

Objective 2 and 3. Evaluation of the designed ICPT through Multiphysics modelling and simulation and simulation of fluid heat transfer inside a chamber.

A Multiphysics modelling and simulation of the designed ICPT and ICPT inside a chamber were performed by using COMSOL Multiphysics software.

The results from modelling and simulation of the ICPT has demonstrated that the plasma jet can reach a temperature of up-to 1410 K in its core and can reach a temperature of up-to 771 K 100 mm inside the chamber. These temperatures are high enough to melt and/or gasify thermoplastics like polyethylene and PVC. The equilibrium melting temperature of polyethylene and PVC ranges from 160 – 245 $°C$ and at temperatures 350 – 500 $°C$ up to 70 % of their composition gasifies [10] [9]. This shows RF ICPT can be a potential technology source to treat thermoplastic RW.

7.1.1 Advantages and limitations of ICPT for treatment of thermoplastics RW

Advantages of ICPT for thermoplastic RW treatment include the capacity to reach temperature high enough to degrade the crystals of these materials in absence of oxygen. Shortcomings of ICPT are not technical rather, they are related to capital cost of the technology. ICPT are expensive to purchase, and the capital cost of such facility is very costly.

7.2 Future Work and Recommendations

This thesis focused on design of RF ICPT for thermoplastic RW treatment and on the study of modelling and simulation of the torch and its integration to the chamber. Future work should include construction and assembly of the torch and chamber adaptor. Once constructed and assembled, a series of investigation and experimental run should be done. After successful experimental runs, the torch can be applied for waste treatment application. Schematics of the recommended experimental runs are shown in figure 7.1 – 7.3.

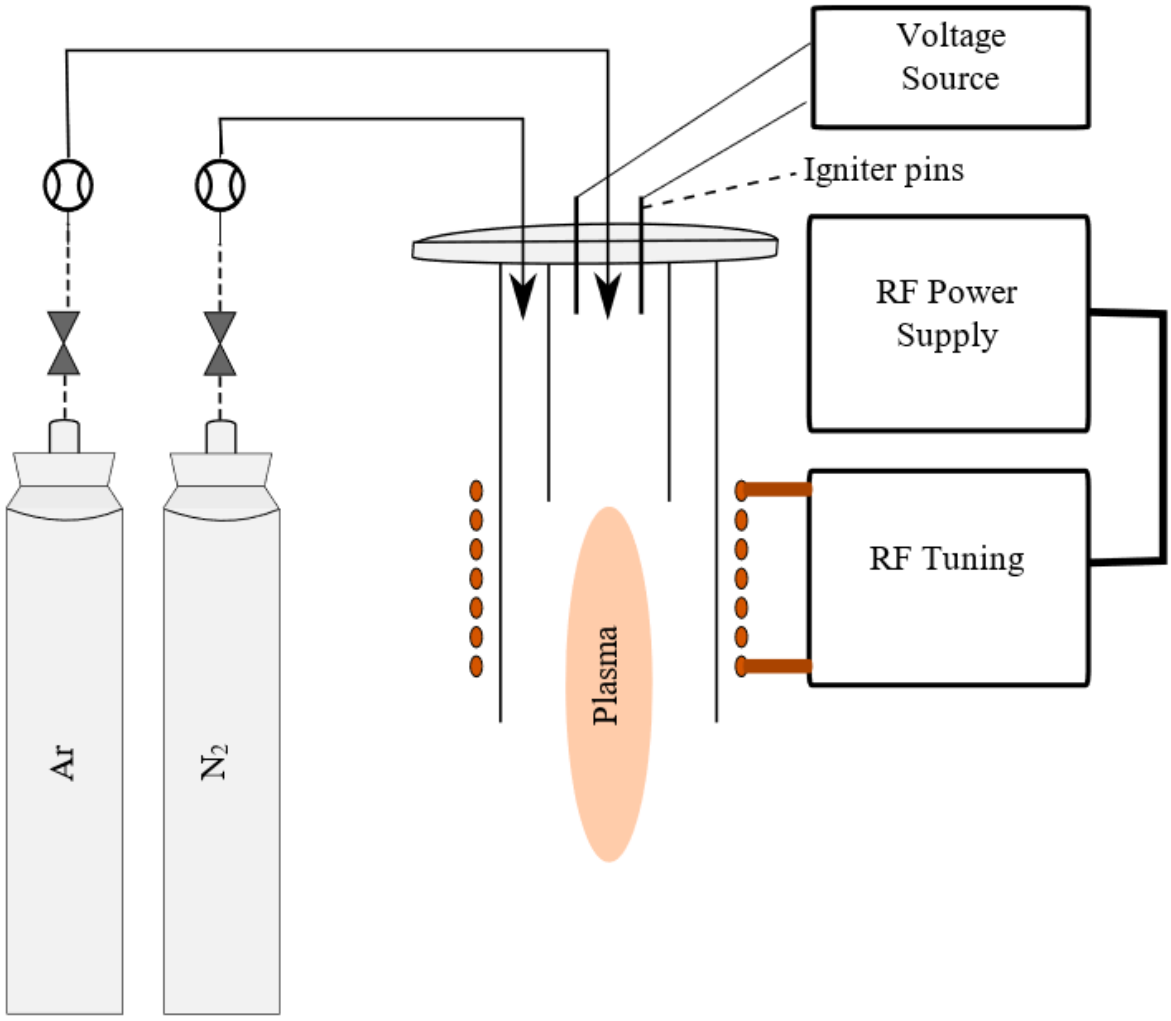

Figure 7.1 Recommended experimental setup of ICPT.

The first recommendation is to test the designed torch with a set up as shown in figure 7.1. If the first experiment is successful, a temperature analysis of the plasma jet from the torch can be done as shown in figure 7.2. A spectroscopic temperature measurement of the plasma core and, a temperature measurement of a solid (with high melting point) which is exposed to the end of the plasma jet can be done by using a pyrometer. Finally, the torch can be used for waste treatment application. Figure 7.3 demonstrates the setup recommended for the torch in waste treatment application.

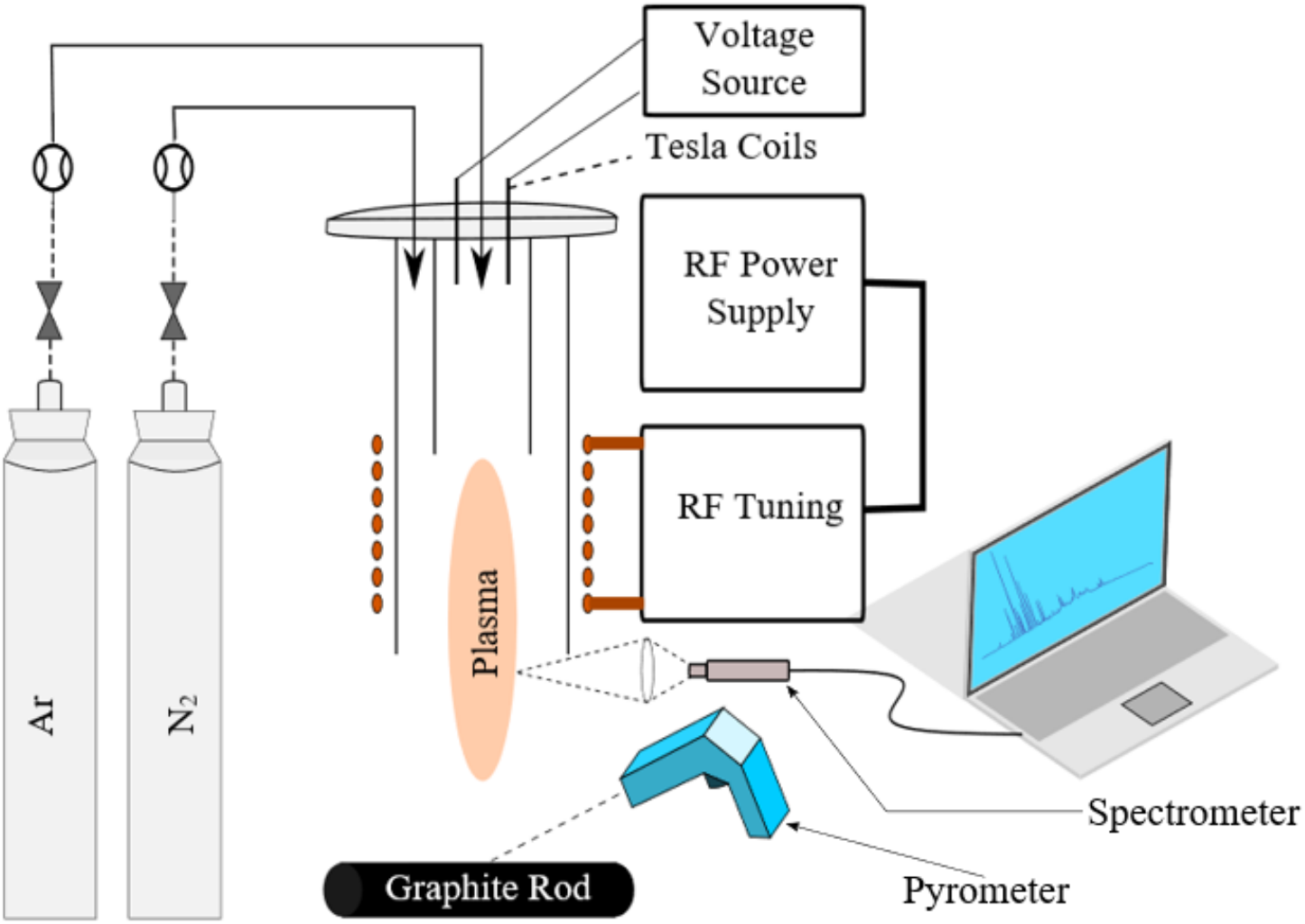

Figure 7.2 Experimental setup for temperature measurement of plasma jet

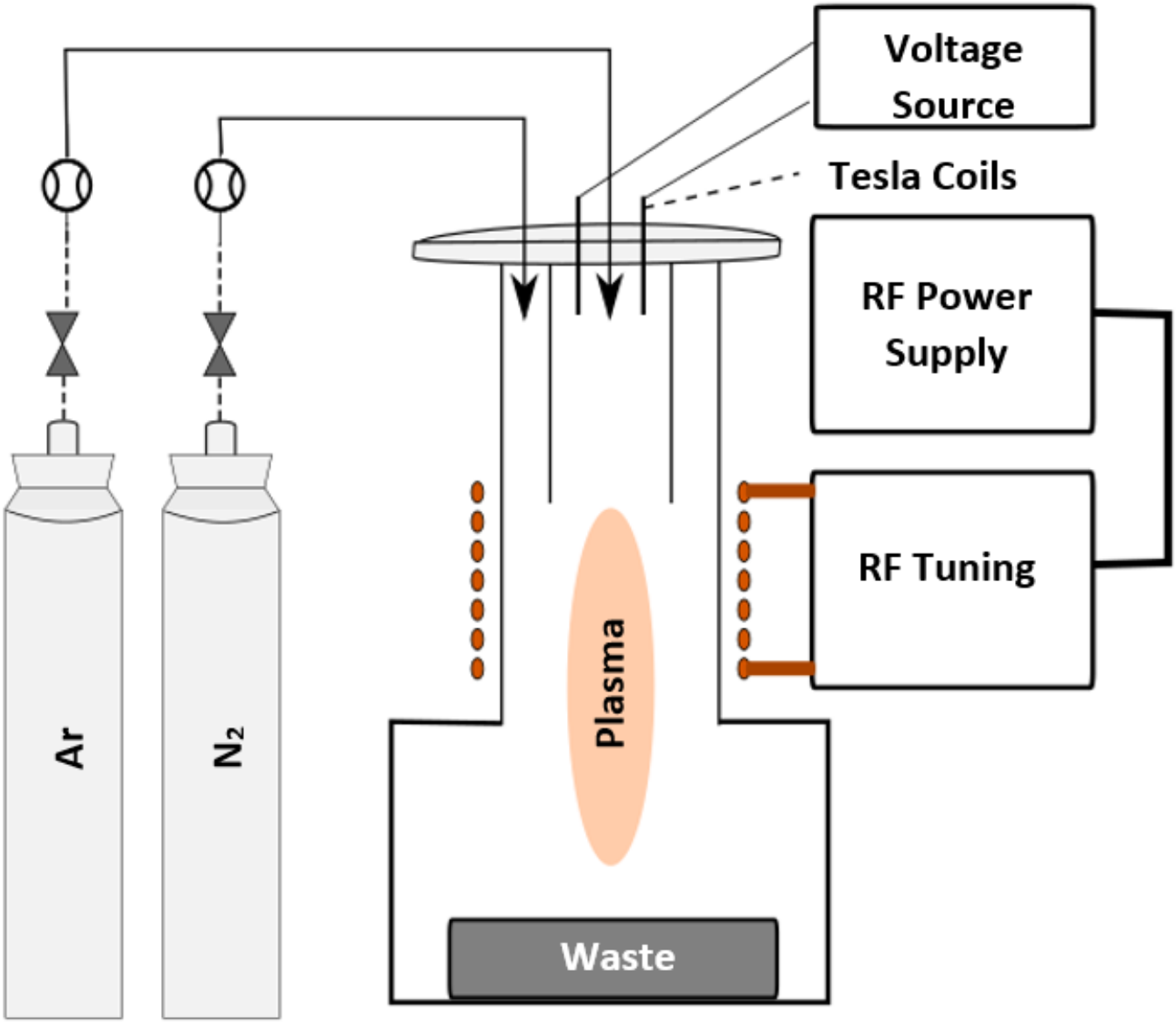

Figure 7.3 Experimental setup of ICPT for waste treatment application

REFERENCES

[1] B. W. Brook, A. Alonso, D. A. Meneley, J. Misak, T. Blees, and J. B. van Erp, "Why nuclear energy is sustainable and has to be part of the energy mix," *Sustain. Mater. Technol.*, 2014, doi: 10.1016/j.susmat.2014.11.001.

[2] A. Horvath and E. Rachlew, "Nuclear power in the 21st century: Challenges and possibilities," *Ambio*, 2016, doi: 10.1007/s13280-015-0732-y.

[3] J. E. Marra and R. A. Palmer, "Radioactive Waste Management," in *Waste*, 2011.

[4] J. Fried and J. Eyles, "Welcome waste - Interpreting narratives of radioactive waste disposal in two small towns in Ontario, Canada," *Journal of Risk Research*. 2011, doi: 10.1080/13669877.2011.571774.

[5] IAEA, "STATUS AND TRENDS IN SPENT FUEL AND RADIOACTIVE WASTE MANAGEMENT," *IAEA Nucl. ENERGY Ser.*, pp. 37–45, 2018.

[6] IAEA, "(NP-T-3.20) Buried and Underground Piping and Tank Ageing Management for Nuclear Power Plant," pp. 35–37, 2018, [Online]. Available: http://www.iaea.org/Publications/index.html.

[7] M. Sadat-Shojai and G. R. Bakhshandeh, "Recycling of PVC wastes," *Polymer Degradation and Stability*. 2011, doi: 10.1016/j.polymdegradstab.2010.12.001.

[8] H. Yu, J., Sun, L., Ma, C., Qiao, Y., & Yao, "Thermal degradation of PVC: A review," *Waste Manag.*, vol. 48, pp. 300–314, 2015.

[9] M. Sogancioglu, E. Yel, and G. Ahmetli, "Pyrolysis of waste high density polyethylene (HDPE) and low density polyethylene (LDPE) plastics and production of epoxy composites with their pyrolysis chars," *J. Clean. Prod.*, 2017, doi: 10.1016/j.jclepro.2017.07.157.

[10] Y. Q. Gill, J. Jin, and M. Song, "Melt flow behavior of high density polyethylene nanocomposites with 1D, 2D and 3D nanofillers," *Nanocomposites*, 2015, doi: 10.1179/2055033215Y.0000000012.

[11] A. Concetti, "Integrated approaches for designing and optimizing thermal plasma processing for metal cutting and material treatment," University of Bologna, 2011.

[12] T. H. Kim, J. H. Oh, M. Kim, S. H. Hong, and S. Choi, "Thermal plasma synthesis of ceramic nanomaterials," *Applied Science and Convergence Technology*. 2020, doi: 10.5757/ASCT.2020.29.5.117.

[13] J. L. Basdevant, J. Rich, and M. Spiro, *Fundamentals in nuclear physics: From nuclear structure to cosmology*. 2005.

[14] M. Pfützner, M. Karny, L. V. Grigorenko, and K. Riisager, "Radioactive decays at limits of nuclear stability," *Rev. Mod. Phys.*, 2012, doi: 10.1103/RevModPhys.84.567.

[15] J. E. Turner, *Atoms, Radiation, and Radiation Protection: Third Edition*. 2007.

[16] R. B. Hayes, “Applications of Radioisotopes,” in *Encyclopedia of Sustainability Science and Technology*, 2017.

[17] I. A. E. A. IAEA, “Radioactive Waste Managment Glossary,” *Acta Acust.*, p. 48, 2003.

[18] V. Valdovinos, F. Monroy-Guzman, and E. Bustos, “Treatment Methods for Radioactive Wastes and Its Electrochemical Applications,” in *Environmental Risk Assessment of Soil Contamination*, 2014.

[19] M. I. Ojovan, *Handbook of Advanced Radioactive Waste Conditioning Technologies*. 2011.

[20] The International Atomic Energy Agency (IAEA), *Application of the concepts of exclusion, exemption and clearance (IAEA RS-G-1.7)*. 2004.

[21] IAEA, “IAEA Safety Standards: Classification of Radioactive Waste - No. GSG-1,” *Gen. Saf. Guid. IAEA*, 2009.

[22] IAEA, “Application of Thermal Technologies for Processing of Radioactive Waste,” *IAEA-TECDOC-1527*, no. 1011–4289, pp. 1–15, 2006.

[23] E. S. P. Prado, F. S. Miranda, L. G. de Araujo, G. Petraconi, and M. R. Baldan, “Thermal plasma technology for radioactive waste treatment: a review,” *Journal of Radioanalytical and Nuclear Chemistry*. 2020, doi: 10.1007/s10967-020-07269-4.

[24] K. Wen *et al.*, “Numerical simulation and experimental study of Ar-H2 DC atmospheric plasma spraying,” *Surf. Coatings Technol.*, 2019, doi: 10.1016/j.surfcoat.2019.04.053.

[25] Y. Byun, M. Cho, S.-M. Hwang, and J. Chung, “Thermal Plasma Gasification of Municipal Solid Waste (MSW),” in *Gasification for Practical Applications*, 2012.

[26] X. Cai and C. Du, “Thermal Plasma Treatment of Medical Waste,” *Plasma Chemistry and Plasma Processing*. 2020, doi: 10.1007/s11090-020-10119-6.

[27] F. Fabry, C. Rehmet, V. Rohani, and L. Fulcheri, “Waste gasification by thermal plasma: A review,” *Waste and Biomass Valorization*. 2013, doi: 10.1007/s12649-013-9201-7.

[28] J. Zeng *et al.*, “Co-treatment of hazardous wastes by the thermal plasma to produce an effective catalyst,” *J. Clean. Prod.*, 2019, doi: 10.1016/j.jclepro.2018.10.069.

[29] J. Deckers, “Incineration and plasma processes and technology for treatment and conditioning of radioactive waste,” in *Handbook of Advanced Radioactive Waste Conditioning Technologies*, 2011.

[30] W. Heep, “The Zwilag plasma facility ‘five years of successful operation,’” 2010, doi: 10.1115/ICEM2010-40128.

[31] J. Deckers, “Plasma Technology to Recondition Radioactive Waste: Tests with Simulated Bitumen and Concrete in a Plasma Test Facility,” 2020, doi: 10.1088/1757-899X/818/1/012006.

[32] E. S. P. Prado, F. S. Miranda, G. Petraconi, and A. J. Potiens, “Use of plasma reactor to

viabilise the volumetric reduction of radioactive wastes," *Radiat. Phys. Chem.*, 2020, doi: 10.1016/j.radphyschem.2019.108625.

[33] T. W. Cheng, J. P. Chu, C. C. Tzeng, and Y. S. Chen, "Treatment and recycling of incinerated ash using thermal plasma technology," *Waste Manag.*, 2002, doi: 10.1016/S0956-053X(01)00043-5.

[34] J. Mostaghimi and M. I. Boulos, "Thermal Plasma Sources: How Well are They Adopted to Process Needs?," *Plasma Chem. Plasma Process.*, 2015, doi: 10.1007/s11090-015-9616-y.

[35] J. Winter, R. Brandenburg, and K. D. Weltmann, "Atmospheric pressure plasma jets: An overview of devices and new directions," *Plasma Sources Sci. Technol.*, 2015, doi: 10.1088/0963-0252/24/6/064001.

[36] J. Mostaghimi, L. Pershin, and S. Yugeswaran, "Heat transfer in DC and RF plasma torches," in *Handbook of Thermal Science and Engineering*, 2018, pp. 53–70.

[37] G. I. Babat, "Electrodeless discharges and some allied problems," *J. Inst. Electr. Eng. - Part III Radio Commun. Eng.*, 1947, doi: 10.1049/ji-3-2.1947.0005.

[38] T. B. Reed, "Induction-Coupled plasma torch," *J. Appl. Phys.*, 1961, doi: 10.1063/1.1736112.

[39] R. H. Wendt and V. A. Fassel, "Induction-Coupled Plasma Spectrometric Excitation Source," *Anal. Chem.*, 1965, doi: 10.1021/ac60226a003.

[40] C. M. Hollabaugh, D. E. Hull, L. R. Newkirk, and J. J. Petrovic, "R.F.-plasma system for the production of ultrafine, ultrapure silicon carbide powder," *J. Mater. Sci.*, 1983, doi: 10.1007/BF00544142.

[41] J. Mostaghimi, M. Dostie, and J. Jurewicz, "Analysis of an RF induction plasma torch with a permeable ceramic wall," *Can. J. Chem. Eng.*, 1989, doi: 10.1002/cjce.5450670610.

[42] T. Kameyama *et al.*, "Highly efficient and stable radio-frequency. Thermal plasma system for the production of ultrafine and ultrapure β-SiC powder," *J. Mater. Sci.*, 1990, doi: 10.1007/BF03372203.

[43] H. Yabuta, H. Miyahara, M. Watanabe, E. Hotta, and A. Okino, "Design and evaluation of dual inlet ICP torch for low gas consumption," 2002, doi: 10.1039/b202178a.

[44] S. Alavi, T. Khayamian, and J. Mostaghimi, "Conical Torch: The Next-Generation Inductively Coupled Plasma Source for Spectrochemical Analysis," *Anal. Chem.*, 2018, doi: 10.1021/acs.analchem.7b04356.

[45] M. P. Freeman and J. D. Chase, "Energy-transfer mechanism and typical operating characteristics for the thermal rf plasma generator," *J. Appl. Phys.*, 1968, doi: 10.1063/1.1655729.

[46] M. I. Boulos, P. L. Fauchais, E. Pfender, M. I. Boulos, P. Fauchais, and E. Pfender, "Inductively Coupled Radio Frequency Plasma Torches," in *Handbook of Thermal*

Plasmas, 2016.

[47] A. E. M. and L.R.Boedeker, "Theoretical Investigations of R-F Induction Heated Plasmas," *NASA/CR-1312,* 1969.

[48] M. I. Boulos, "The inductively coupled r.f. (radio frequency) plasma," *Pure Appl. Chem.*, 1985, doi: 10.1351/pac198557091321.

[49] L. G. Christophorou, *Nuclear Instruments and Methods in Physics Research*. 1988.

[50] M. Hoshino, T., Mito, K., Nagashima, A., & Miyata, "Determination of the thermal conductivity of argon and nitrogen over a wide temperature range through data evaluation and shock-tube experiments," *J. Thermophys.*, vol. 7(3), pp. 647–662, 1986, doi: 10.1007/BF00502397.

[51] C. Torres, P. G. Reyes, F. Castillo, and H. Martínez, "Paschen law for argon glow discharge," *J. Phys. Conf. Ser.*, vol. 370, p. 012067, Jun. 2012, doi: 10.1088/1742-6596/370/1/012067.

[52] V. Colombo, D. Bernardi, E. Ghedini, A. Mentrelli, and T. Trombetti, "Three dimensional modelling of inductively coupled plasma torches: Comparison with experiments and applications," *Czechoslov. J. Phys.*, 2004, doi: 10.1007/BF03166443.

[53] J. Mostaghimi, P. Proulx, and M. I. Boulos, "An analysis of the computer modeling of the flow and temperature fields in an inductively coupled plasma," *Numer. Heat Transf.*, 1985, doi: 10.1080/01495728508961849.

[54] J. Mostaghimi, P. Proulx, and M. I. Boulos, "Parametric study of the flow and temperature fields in an inductively coupled r.f. plasma torch," *Plasma Chem. Plasma Process.*, 1984, doi: 10.1007/BF00566841.

[55] P. Proulx, J. Mostaghimi, and M. I. Boulos, "Heating of powders in an r.f. inductively coupled plasma under dense loading conditions," *Plasma Chem. Plasma Process.*, 1987, doi: 10.1007/BF01015998.

[56] J. Mostaghimi, P. Proulx, and M. I. Boulos, "A two-temperature model of the inductively coupled rf plasma," *J. Appl. Phys.*, 1987, doi: 10.1063/1.338073.

[57] D. Bernardi, V. Colombo, E. Ghedini, and A. Mentrelli, "Three-dimensional effects in the modelling of ICPTs Part I: Fluid dynamics and electromagnetics," *Eur. Phys. J. D*, 2003, doi: 10.1140/epjd/e2003-00244-0.

[58] D. Bernardi, V. Colombo, E. Ghedini, and A. Mentrelli, "Three-dimensional modelling of inductively coupled plasma torches," *Eur. Phys. J. D*, 2003, doi: 10.1140/epjd/e2002-00233-9.

[59] D. Bernardi, V. Colombo, E. Ghedini, and A. Mentrelli, "Three-dimensional modeling of inductively coupled plasma torches," 2005, doi: 10.1351/pac200577020359.

[60] M. Aghaei, H. Lindner, and A. Bogaerts, "Effect of a mass spectrometer interface on inductively coupled plasma characteristics: A computational study," *J. Anal. At. Spectrom.*, 2012, doi: 10.1039/c2ja10341a.

[61] H. Lindner and A. Bogaerts, “Multi-element model for the simulation of inductively coupled plasmas: Effects of helium addition to the central gas stream,” *Spectrochim. Acta - Part B At. Spectrosc.*, 2011, doi: 10.1016/j.sab.2011.04.007.

[62] P. Yang, J. A. Horner, N. N. Sesi, and G. M. Hieftje, “Comparison of simulated and experimental fundamental ICP parameters,” *Spectrochim. acta, Part B At. Spectrosc.*, 2000, doi: 10.1016/S0584-8547(00)00274-3.

[63] S. Xue, P. Proulx, and M. I. Boulos, “Extended-field electromagnetic model for inductively coupled plasma,” *J. Phys. D. Appl. Phys.*, 2001, doi: 10.1088/0022-3727/34/12/321.

[64] Nist, “NIST reference fluid thermodynamic and transport properties-REFPROP,” … *Chem. Prop.* …, 2002.

[65] C. Multiphysics and C. Multiphysics, “COMSOL Multiphysics ® v.5.5,” *COMSOL Multiphysics ® 5.5*, 2020.

[66] S. B. Punjabi, N. K. Joshi, H. A. Mangalvedekar, B. K. Lande, A. K. Das, and D. C. Kothari, “A comprehensive study of different gases in inductively coupled plasma torch operating at one atmosphere,” *Phys. Plasmas*, 2012, doi: 10.1063/1.3676598.